LABORATORIO DE MICROSCOPÍAS AVANZADAS

ANNUAL REPORT 2017-2018

LMA
LABORATORIO
DE MICROSCOPÍAS
AVANZADAS

Laboratorio de Microscopías Avanzadas

Annual Report 2017-2018

LMA
LABORATORIO
DE MICROSCOPÍAS
AVANZADAS

EDITA
Laboratorio
de Microscopías Avanzadas
C/ Mariano Esquillor, s/n.
50018 Zaragoz (Spain)
Tel. +34 976 762 980
Fax +34 976 762 777
Email: lma@unizar.es
http://lma.unizar.es/

DISEÑO GRÁFICO
José Luis Lizano

Index

Introduction

Manuel Ricardo Ibarra García
Director

The Laboratory of Advanced Microscopies recognition is based in the top level infrastructures in different fields of microscopies, establishing the necessary instrumentation and expertise to attend the demand of scientists and companies to face new challenges in nanoscience and nanotechnology. Our mission is to attract world class science, creating a high research level atmosphere and based in the selective criteria of access and internalization of the laboratory. LMA has been one of the promoters of the new networks of ICTS for ELECtron MIcroscopy (ELECMI) that gives support to the Spanish scientific community.

Several international partnerships have promoted synergies which allowed raising cutting edge scientific and technological outputs. The international collaboration with Midi Pyrenees Region through the Associate Laboratory CNRS-UNIZAR "Microscopy and Materials cOnsortium ZARagoza Toulouse" (M2OZART"). The Transpyrenean Node for Scientific Instrumentation (TNSI) within the frame of European Interreg V-A program POCTEFA.

The recent created "Joint Laboratory on Environment" with Hong Kong University of Science and Technology (HKUST), constitutes a bridge between Europe and Asia scientific communities and this is enhanced by the participation of LMA in the European ESTEEM3 consortium which allows a fluent scientific exchange with top level researchers.

Our facilities have been completely settled and improved during this period and world-class groups are frequently using our laboratories. The combination of expertise in nanofabrication and nanocharacterization at the same facility constitutes one of the most valuable characteristic that envision a promising future for the LMA.

Our scientific and technical staff covers a wide range of experimental facilities in advanced microscopies. Our challenge for the next period is to become an international reference Laboratory to promote and to establish new bridges among scientists and companies

Foreword

Pilar Cea Mingueza
Scientific Coordinator

Since the first agreements for the creation of a singular laboratory in Aragón related to nanofabrication and materials characterization back in the year 2007, the scientists and technicians at the Laboratory for Advances Microscopies (LMA) have worked really hard to locate the city of Zaragoza in the map of national and international scientific facilities. In 2009, the I+D+I building at Campus Río Ebro was inaugurated with the installation of the most advanced infrastructures at that time in the field of materials characterization. In 2014 the LMA was recognized by the Ministry of Economy and Competitivity of Spain as a National Facility or, as they are called in Spain, a Singular Scientific and Technical Infrastructure (ICTS), and such recognition was renewed in 2018. ICTS' are defined as are large installations, resources, facilities and services, unique in its kind, that are dedicated to cutting edge and high quality research and technological development, as well as to promote exchange, transmission and preservation of knowledge, technology transfer and innovation. In this context, as the reader can verify throughout this biennial report, the LMA scientists, technicians and users have achieved an unprecedented research level and transfer of knowledge to the industrial sector. In the 2017-18 period, the LMA has consolidated its scientific excellence with more than 200 publications, 24 with an impact factor higher than 10, a remarkable international projection with 22 users from abroad institutions, participation in associated laboratories and international consortiums as well as the organization of international conferences and workshops. Importantly, the transfer of knowledge to industry as well as the innovation capabilities of our technicians and scientists is reflected by the registration of two patents and a relevant number of industrial users from local, national and international companies.

Reaching such an excellent scientific and transfer to industry level has been a challenging process that required from the collaboration of scientists, technicians and LMA managers but also from local and national authorities that provided LMA with the required infrastructure and funds. In particular, the local support from the Aragón Government, has been crucial for the maintainance and day-to-day running of the facility. In 2019 the LMA has reached a relevant level of maturity that paves the road to pursue new and even more challenging objectives, to be at the forefront of the scientific and technological vanguard in the field of materials characterization. In this scenario, the LMA needs more than ever the support from funding agencies at the Local, National and International level to upgrade the instruments, address the acquisition of the next generation of instruments required to overcome new scientific challenges, attract talented researchers to our laboratories, lead relevant international consortiums, etc.

The Laboratory for Advanced Microscopies: a National Facility

The Laboratory for Advanced Microscopies: a National Facility

The Council of Scientific, Technological and Innovation Policy (CPCTI) approved the current Map of Unique Scientific and Technical Infrastructures (ICTS) in Spain on 6th November 2018. The map is composed of 29 ICTS with a total of 62 infrastructures, organized in eight scientific fields. On that Map, the distributed ELECMI (Integrated Infrastructure of Electron Microscopy for Materials Characterization) was renewed as an ICTS (first recognition on 7th October 2014). ELECMI is currently composed of four nodes: (i) the Laboratory for Advanced Microscopies (LMA) that belongs to the University of Zaragoza, (ii) the National Center for Electron Microscopy (CNME) that belongs to the University Complutense of Madrid, (iii) the Division for Electron Microscopy from the University of Cádiz (DME-UCA) and (iv) the Unity for Electron Microscopy applied to Materials Characterization from the University of Barcelona (UMEAP-UB).

According to the CPCTI, a detailed process of analysis and assessment of the proposals presented by the candidate infrastructures was carried out by international experts using criteria of maximum scientific, technical and innovation quality. The presence of ELECMI in the map of ICTS in Spain has undoubtedly provided an effective answer to the need of different techniques for the characterization of materials. Proof of this is the high demand for the instruments offered by this ICTS by research centers and companies not only in Spain but also in the international arena.

Distribution of the nodes that compose ELECMI (Integrated Infrastructure of Electron Microscopy for Materials Characterization)

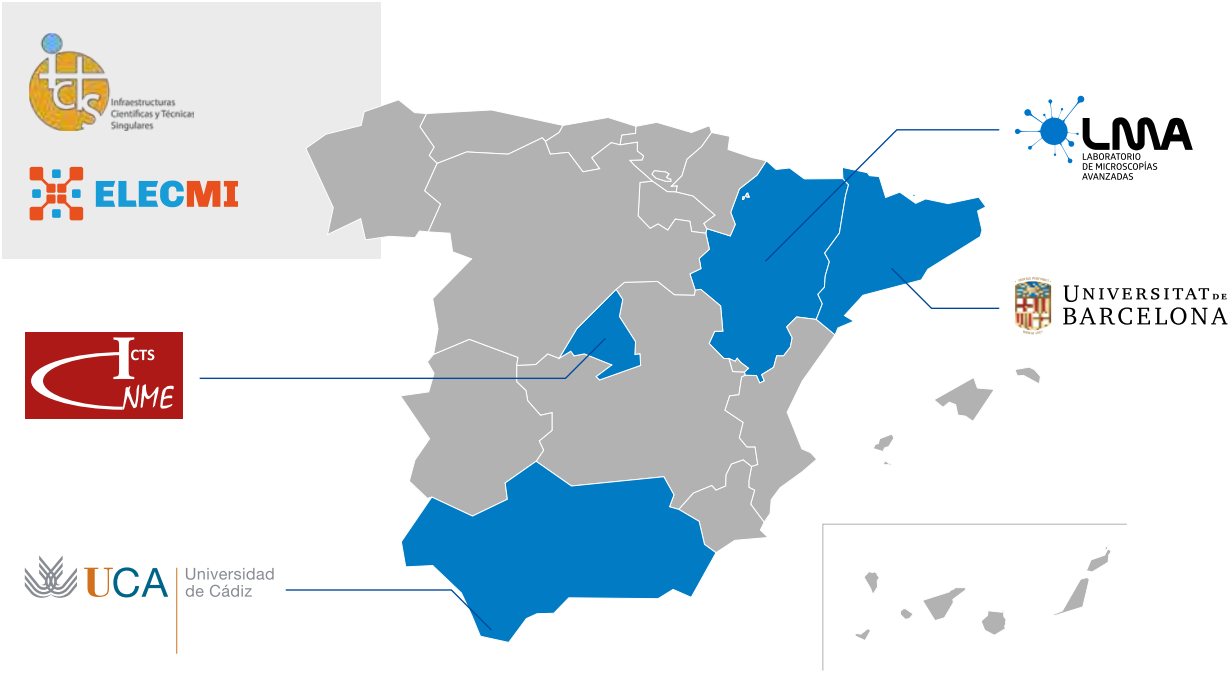

ELECMI emerged on the Spanish scientific scene as a result of the fruitful activity in the field of new materials both at a national and international level as well as the need to characterize these materials by means of singular techniques in the framework of costly infrastructures that only a few – or even a single – and very specialized centers in the technological vanguard can offer to the scientist and companies in the country. Over the years after its creation, such a need of a National Facility for the Materials Characterization through Electron Microscopy has not only grown but also evolved towards new requirements as scientific challenges appear opening new avenues for further technological developments.

The LMA has a wide range of top level equipment and know-how in Electron Microscopy. One of the most relevant distinguished characteristics of the LMA is that in addition to the singular infrastructures in the field of Electron Microscopy, it also offers a large number of other complementary nanofabrication and characterization techniques dedicated to the observation and analysis of materials at atomic and molecular scale. All these instruments are at the service of researchers, universities, research centers and Industry, with the ability to address the most relevant societal challenges in the field of advanced materials for applications in energy efficiency, data storage and transmission speed, new sensors generation, biomedical diagnosis, therapy and prosthetics, etc.

The LMA has coordinated ELECMI since its recognition as an ICTS in 2014. Prof. Ricardo M. Ibarra is the president of ELECMI and Prof. Pilar Cea is the coordinator of this ICTS. In this coordination role, the University of Zaragoza was awarded with two National grants from the Ministry of Economy and Competitiviness of Spain for the implementation, boosting and internationalization of ELECMI (MAT2015-70977-REDI and MAT2017-90779-REDI) with a total income of more than 250,000 €.

The above statements – in terms of uniqueness of the instruments available within the LMA, their outstanding character, expertise of the scientific and technical staff together with the completeness of the available techniques – reveal that the LMA possess a RELEVANT STRATEGIC CHARACTER in the field of MATERIALS CHARACTERIZATION not only at a National level but also in Europe where the LMA has participated in relevant consortiums and was awarded with relevant grants. The availability of these nanofabrication and characterization techniques to any researcher by a simple procedure (see below) together with a permanently open call for the use of this Aragonees infrastructure provides an added value to the Spanish RDI system and strongly contributes to the internationalization of Aragon. Thus, the LMA is a pole of attraction for international users and talented scientist who wish to make use of these infrastructures or even develop their research activities at the University of Zaragoza or other associated research centers due to the opportunities offered by these unique facilities.

Organization Chart

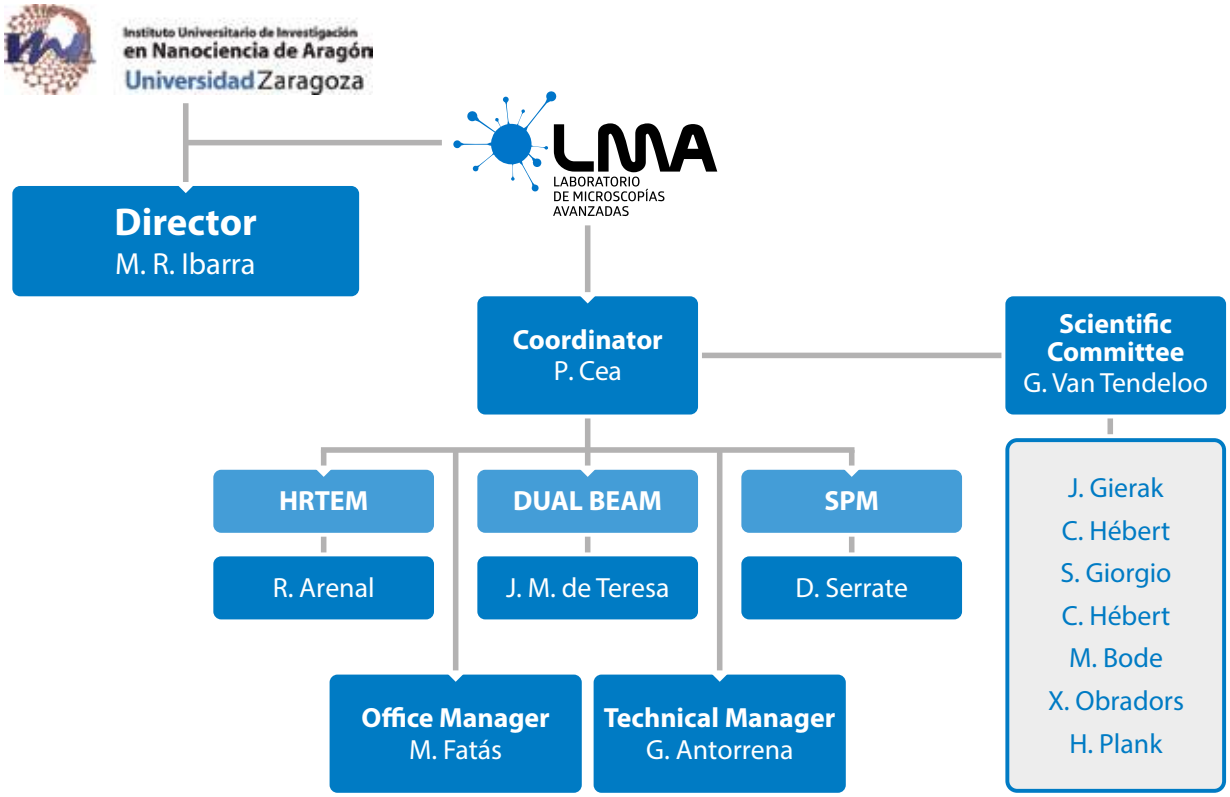

Human Resources

The LMA members in the 2017-2018 include:

Management

M. Ricardo Ibarra	**Director**
Pilar Cea	**Scientific Coordinator**
Guillermo Antorrena	*Technical Manager*
Mercedes Fatás	*Office Manager*
José Antonio Romero	*Technology Transfer Manager*
Miriam Santos	*Administrative Support*

LMA staff

Technical staff	12
Instrument responsible	1
Administration staff	2
Technology Transfer Manager	1

LMA Associated scientists

Scientific	29

List of LMA technicians an associated scientists

TEM

Arenal, Raúl	**Head of TEM Area**
Aguirre, Myriam	*Researcher*
Hettler, Simon	*Postdoctoral Researcher*
Fdez. Pacheco, Rodrigo	*TEM Technician*
Ibarra, Alfonso	*TEM Technician*
Magén, César	*Researcher*
Navarro, Marta	*Sample Preparation Technician*
Herguedas, Beatriz	*Researcher*
Hurtado, Ramón	*Researcher*
García Nafría, Javier	*Researcher*
Pablo, Javier	*PhD Student*
Peláez, Mario	*PhD Student*

DUAL BEAM

De Teresa, José Mª	**Head of DUAL BEAM Area**
Antorrena, Guillermo	*XPS Technician*
Barrado, Mariano	*Dual Beam Technician*
Casado, Laura	*Dual Beam Technician*
Goya, Gerardo	*Associate Professor*
Gracia Abad, Ruben	*PhD Student*
Irusta, Silvia	*Associate Research Professor*
López, Teobaldo	*Dual Beam Technician*
Orús, Pablo	*PhD Student*
Pardo, José Ángel	*Associate Professor*
Rivas, Isabel	*Dual Beam Technician*

Sangiao, Soraya	*Associate Professor*
Sesé, Javier	*Associate Research Professor*
Simón, Gala	*Clean Room Technician*
Valero, Rubén	*Clean Room Technician*

SPM

Serrate, David	**Head of SPM Area**
Arnaudas, José Ignacio	*Professor*
Cea, Pilar	*Professor*
Chiodini, Stefano	*Postdoctoral Researcher*
Díez, José Luís	*SPM Technician*
Domínguez, Amelia	*PhD Student*
Escorihuela, Enrique	*PhD Student*
García, Aitor	*PhD Student*
Gracia-Lostao, Ana Isabel	*Researcher, ARAID Foundation*
Herrer, Lucía	*Postdoctoral Researcher*
Martín, Carlos	*SPM Technician*
Martín, Santiago	*Associate Professor*
Moya, Alberto	*PhD Student*
Piantek, Marten	*Instrument responsible*
Ruiz, Silvia	*PhD Student*

The Scientific Committee

The Scientific Committee is in charge of providing scientific and advisory support to the Management Board. It is composed of internationally prominent scientists in the field of advanced microscopies, with outstanding professional and scientific track record in line with LMA objectives.

Members

President: Prof. G. Van Tendeloo (Chair)	**University of Antwerp (Belgium)**
Dr. Jacques Gierak	*LPN – CNRS (France)*
Prof. Suzanne Giorgio	*CINM – CNRS (France)*
Prof. Cecile Herbert	*EPFL (Switzerland)*
Dr. Matthias Bode	*Wuerzburg Univ. (Germany)*
Prof. Xavier Obradors	*ICMAB – CSIC (Spain)*
Dr. Harald Plank	*Graz Univ. of Technology (Austria)*

Functions

- Provide advice in relation with the scientific policy guidelines
- Evaluate and inform on the Annual Report of activities and on the proposals for the Annual Action Plans
- Provide feedback on the usefulness of programs, resources and capabilities of the different laboratories.
- Assess on the technology transfer strategy
- Assess on the recruitment policy for scientific personnel
- Inform on the creation of research programs

Access to LMA by the RDI Community

To achieve the goals of expanding the microscopy techniques both to industry and the scientific community we offer the use of our facilities to experienced users as well as novel users and groups not necessarily connected with microscopy methods. Users find at LMA a flexible and competent center to carry out their characterization and research studies with the support of specialized technical staff and scientists.

In accordance with the range of experimental tools and methods, we offer access to our facilities either as a service (carried out by our technical staff) or as project-oriented collaborations (demanding studies requiring the active participation of our scientific personnel). Our experience is that, depending on the user and the type of measurement, the support by the LMA staff varies.

LMA offers access to the following type of nanofabrication and characterization facilities:

- Structural and chemical High Resolution Transmission Electron Microscopy (HR-TEM) studies of materials and devices
- Studies of local magnetic configuration by electron holography and magnetic force microscopy
- Plasmon mapping
- Cryo-TEM studies of soft materials
- Nanostructuration by Focused Ion Beam
- Surface analysis by scanning probe microscopy, including atomic manipulation, follow-up of catalytic reactions and thin-film growth modes.
- Studies of single molecule configuration and spectroscopy by UHV Tunneling microscopy
- Magnetic microscopy under high magnetic fields in combination with electric transport measurements.

Three types of access can be distinguished depending on the applicant's degree of expertise, on the instrument, and on the challenge of the proposed measurements:

- **Service:** measurements are carried out by our technical staff. In general the attendance of the applicant is desired. This modality is applied to industrial partners, as well as to scientific users not directly working with similar instruments, who in general seek for a measurement complementary to their own techniques.
- **Scientific Use:** Some of our facilities are used by external experience users, who do not have at hand at their institutions of the specific tools like the ones available at LMA. In this case, users are advised by our technical staff about the use of the system and allowed to work independently.

> **Collaborative Use:** when challenging measurements are required, we offer the possibility to carry out collaborative projects with scientists of the LMA. In this case, our scientists get deeply involved in the measurements and analysis of the results.

Administrative and scientific and technical support to users

The LMA offers to potential users all types of local supports in terms of additional equipment for sample preparation and characterization, and technical, scientific and administrative staff.

Before the arrival: For each accepted project, a "local contact" is designated, who will organize with the external user(s) his/her visit (together with the administration staff) and experiment (together with the technical staff) at the infrastructure. The local contact is chosen among the respective local experts of the corresponding infrastructure, depending on their own expertise and on the equipment that has been requested. This local contact is also in charge of checking that the equipment and samples are ready for the experiment, the viability of the measurements, and of reserving enough time in advance for preparing the experiment.

During the measurement: All the instruments offered are continuously maintained by highly specialized technical operators, who support and/or train the user in their initial use, as well as in the preparation of samples for measurement. They consider each specific requirement to ensure the success of the measurement. For some specific measurements in which special sophisticated methods are needed, the local contact will be also available to assist the user(s) in performing measurements, as well as in the data analysis.

After the measurement: When leaving the infrastructure, the user(s) will take away all the raw images and spectra obtained with the LMA equipment and when carried out, the data that have been analyzed with the LMA researchers. In some special cases, LMA researches could offer subsequent support in terms of interpretation, and discussion of obtained results, especially in those cases when the local contacts were particularly involved in the scientific project.

The LMA offers open competitive access to its infrastructures. The University of Zaragoza guarantees that, at least, 30% of the time of use of the instruments is offered to external users. Two types of accesses can be distinguished. First, access to the singular instruments (HR-TEM and Dual Beam), which requires an application as described below. Second, access to complementary instruments through a simplified protocol.

Access protocol to the singular facilities

To gain access to the singular instruments of LMA, eligible users need to submit a research proposal describing their requirements. A standardized proposal form is available in the LMA website and can be filled on-line (lma.unizar.es)

The research proposal to gain access contains the administrative location of the requesting person or group leader and should also describe:

> The scientific aim of the project, including

- The state of the art and conceptual framework of the project
- The expected output of the project
- The potential industrial applications of the Project results

- Possible special requests (for example: use of particular stages, precautions, low temperature, gas atmosphere, low voltages…)

> The requested instrument(s) including measuring conditions and sample preparation facilities, if needed.

> The requested access time to the instrument and sample preparation time (if any)

> The preferred dates for the measurements.

> The requested time for computing / data treatment and analysis time (if any).

Currently there is a permanently open call for submission of proposals, which are evaluated by at least one member of the Access Committee. Successful proposals enjoy experimental time as soon as possible. The feedback time to the user is very fast, in the range of 1-2 weeks, warranting the timeliness of the experiment.

For every successful proposal, the area leader of the LMA selects a scientific in-house correspondent (local contact). The applicant is then notified of the acceptance of the proposal and invited to communicate details and dates of the experiment with the local contact at the LMA.

Access Committee

The evaluation of the proposals is performed by specialized committees in each of the three scientific divisions of the LMA. The committees are chaired by the corresponding responsible scientist of the TEM, SPM and Dual Beam areas and are formed by the following experienced external scientists.

> Prof. Odile Stéphan (LPS-UPS, Paris, France)

> Prof. J. Arbiol (ICMAB, Barcelona, Spain)

> Prof. Luca Ortolani (University of Bologna, Italy)

> Prof. Ana Belén Hungría Hernández (UCA, Spain)

> Prof. Sonia Estradé (UB, Spain)

> Prof. María Varela (UCM, Spain)

> Prof. Raul Arenal (Unizar, Spain)

> Prof. Etienne Snoeck (CEMES, Toulouse, France)

> Prof. Gianluigi Botton (McMaster University, Canada)

> Prof. Ivo Utke (EMPA, Switzerland)

> Prof. Bruno Humbel (University of Lausanne, Switzerland)

> Prof. Osamu Terasaki (University of Shangai)

> Prof. Ana Sánchez (University of Warwick, UK)

> Prof. Marta Rossel (EMPA, Switzerland)

> Prof. Ute Kolb (University of Mainz, Germany)

Description of the evaluation procedure

Each proposal is assessed by the Access Committee against the following selection criteria:

> **Technological or Scientific Merit of the proposal** (rank: weak: 0 – outstanding: 10)

> **Capabilities of the user team** (rank: weak: 0 – outstanding: 10)

> **Feasibility of the experiment:** the experiment must be feasible; this is discussed with the technicians and the scientists of the LMA.

Proposals are accepted provided that the threshold mark of 5 is reached in the first two criteria and the experiment is found to be feasible. Proposals with a total ranking less than 10 are rejected and the users are normally invited to resubmit their proposal following the advice of the reviewer report to improve their application. Accepted proposals designate a local person who is the contact for the user(s) to organize and perform the experiment.

Access to complementary facilities through a simplified protocol

Users willing to make use of other LMA facilities can apply through a simplified protocol. The LMA and ELECMI web sites include a list of the instruments offered to the scientific community and industrial sector. The applicant just have to fill some basic institutional information as well as a brief description of the experiment and technical requirements. The application is received by the technical staff at the LMA that, in a short period of time (often two or three working days) will provide specific feedback to the user and will open a direct cannal of communication to discuss the fine details of the experiment and the calendar.

The LMA in the International Arena

The facilities available within the LMA, the quality of the technical staff and world wide recognition of the LMA scientist have pave the road towards a relevant role of the LMA in the international scene. Below, some of the most relevant agreements of the LMA with international entities as well as participation of the LMA in relevant international consorptiums are described.

Technical Scientific University of Hong Kong (HKUST)-LMA

The University of Zaragoza and the Technical Scientific University of Hong Kong (HKUST) signed in 2018 a collaboration agreement in order to create an international laboratory in advanced microscopes and nanoscience research. The University of Zaragoza participates through the Advanced Microscopy Laboratory (LMA). Thanks to this agreement, researchers from both centers will be able to share resources and undertake joint projects for the study of new materials aimed at the manufacture of sensors and nanoparticles for different applications in nanobiomedicine, food or detection of pollutants in the environment, among others.

Transpyrenean Associated Laboratory for Electron Microscopy (TALEM)

The CEMES-INA collaboration started back in the year 2009 when the INA launched the LMA. The LMA has motivated different laboratories in Spain and France to start or intensify their collaborations with the INA-LMA researchers. In 2009, CEMES and INA submitted a project to create an European Associated Laboratory (LEA) "TALEM" (Transpyrenean Associated Laboratory for Electron Microscopy). The objective of TALEM was to establish a long-term partnership between CEMES and INA, focusing in particular on the development of new TEM techniques and on selected (nano) materials subjects requiring advanced TEM technics (mainly tomography, electron holography and Lorentz microscopy, Cs corrected STEM-HAADF and monochromated STEM-EELS Quantitatively, these various collaborations have resulted in:

30 joint publications, two chapters in books, and more than **70 invited lectures** given in conferences have resulted from this collaboration. Also, **three PhDs** were co-supervised by researchers of CEMES and INA and TALEM researchers participated to **seven thesis juries** in Toulouse and Saragossa.

Almost twenty permanent staff, 7 PhD students and 11 post-doctoral researchers were involved in TALEM, totalled more than **660 days of visit** between the 3 laboratories. In addition, the laboratories jointly organized **7 TALEM workshops** with an average of 26 participants.

These eight years of "TALEM" were particularly fruitful not only in scientific activities but also in structuring our joint activities and enhancing the synergy between the 3 laboratories.

Participation in the European ESTEEM3 consortium

On 21th August 2018, the ESTEEM3 project was accepted by the European Commission.

ESTEEM3 – **Enabling Science and Technology through European Electron Microscopy** – is an EU funded project for electron microscopy, which aims at **providing access to the leading European state-of-the-art electron microscopy research infrastructures**, facilitating and extending **transnational access services** of the most powerful **atomic scale characterization techniques** in advanced electron microscopy research to a wide range of academic and industrial research communities for the analysis and engineering of novel materials in physical, chemical and biological sciences.

The objective of the ESTEEM3 project is to **deliver access to users coming from a wide range of disciplines**. Transnational Access (TA) to ESTEEM3 centres is obtained through a transparent, simple peer review process based on merit and scientific priorities.

This project will receive funding from the European Union's Horizon 2020 research and innovation programme under grant agreement No. 823717 – ESTEEM3, the duration will be four years 2019-2022, the Budget is 10,000,000 €.

The LMA will receive € 446,000 over the next four years. This participation will allow a fluent scientific exchange with top level researches and the LMA will consolidate an international standing position.

LIA Microscopy and Materials cOnsortium ZARagoza Toulouse

M²OZART

A new International Associated Laboratory (LIA) was proposed between France and Spain, in 2018, focused on fundamental research for the next four years (2018-2022). This LIA **"M²OZART"** (Microscopy and Materials cOnsortium ZARagoza Toulouse) should allow us to set up new research lines on themes in intense development but also to support the recent scientific activities already existing. The composition is:

- Centre d'Elaboration de Matériaux et d'Etudes Structurales (CEMES), UPR 8011, CNRS, headed by Prof. Etienne Snoek.
- Laboratoire de Physique et Chimie des Nano-Objets (LPCNO), UMR 5215, (CNRS – UPS – INSA Toulouse), headed by Prof. Bruno Chaudret.
- Instituto de Ciencia de Materiales de Aragón (ICMA), headed by Prof. Javier Campo.
- Instituto de Nanociencia de Aragón (INA), directed by Prof. Ricardo Ibarra.

European Interreg V-A program POCTEFA through ERDF funds

Interreg POCTEFA

TNSI

The Transpyrenean Node for Scientific Instrumentation (TNSI) is a 1.9 M€ project conceived to enable cooperation in R&D and technology transfer between small and medium-sized enterprises (SMEs) and research centres based in the Spain-France border regions. The TNSI project is **65% cofunded by the European Interreg V-A program POCTEFA through ERDF funds.** TNSI is participated by 3 SMEs, 1 Spanish Singular Infraestructure (ALBA) and 5 word-class research centres. The activities of the consortium are focused on nanotechnologies, advanced materials and manufacturing processes. INA is one of the involved research centres, handling a budget of 218 k€. Its role within the project is to provide access and training to the unique techniques available at the Scanning Probe Methods area of the LMA. Thanks to their flexibility and top performance, LMA laboratories are ideally suited to test TNSI prototypes and the applications portfolio of new technologies. The LMA personnel participating in TNSi offers as well continuous R&D training in surface science methods to all partners.

Some Relevant Figures of the LMA (2017-2018)

17,4M€ Investment (2009-2018)	10 Technicians	1 Technology Transfer Manager
2 Staff Administration	15,200 Hours of work in the LMA instruments	110 Users
4,500 Hours of work from External Users	22 Users from Abroad Institutions	209 Scientific Publications
24 Publications with Impact Factor < 10	3 Patents	2 International Associated Laboratories
2 European Infraestructures Projects	2 ELECMI International Workshops	3 Conference Organized
1 Practical Course for Companies	5 Visibility Actions in Industry Forums	21 Companies Benefited from the LMA

The Laboratories

The Laboratories

Location

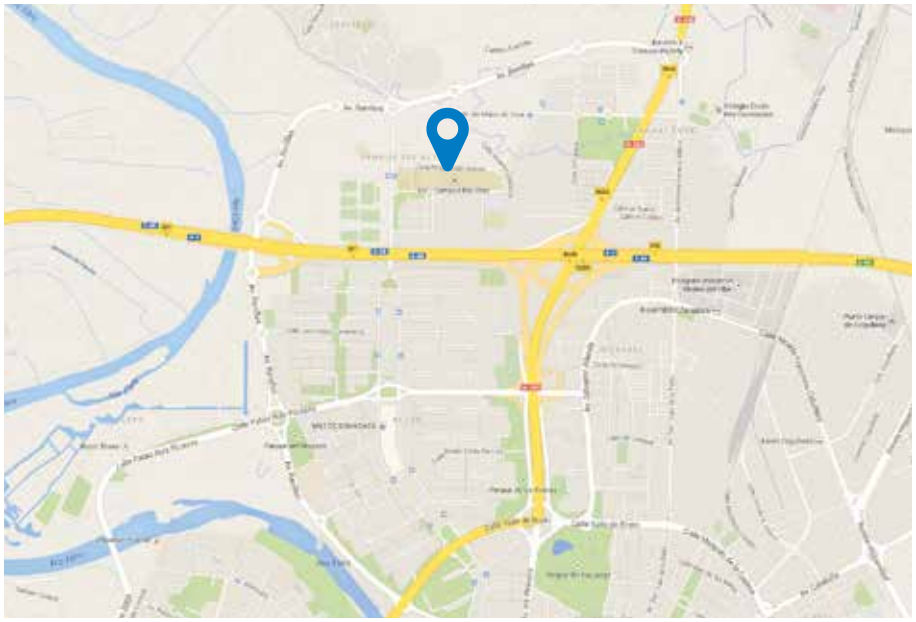

Campus Río Ebro – University of Zaragoza

Laboratorio de Microscopías Avanzadas (LMA)
***Advanced Microscopies Laboratory* (LMA)**
Edificio I+D
Campus Río Ebro
Universidad de Zaragoza
C/ Mariano Esquillor, s/n.
50012 Zaragoza (Spain)
Tel: +34 976 762 980
Fax: +34 976 762 776
Email: lma@unizar.es
http://lma.unizar.es/

University Research Institutes Building – Campus Río Ebro.

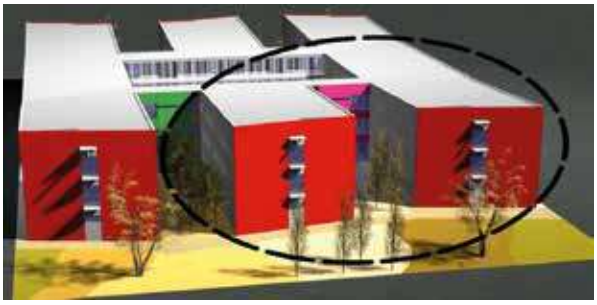

LMA Laboratories.

Transmission Electron Microscopy Laboratories

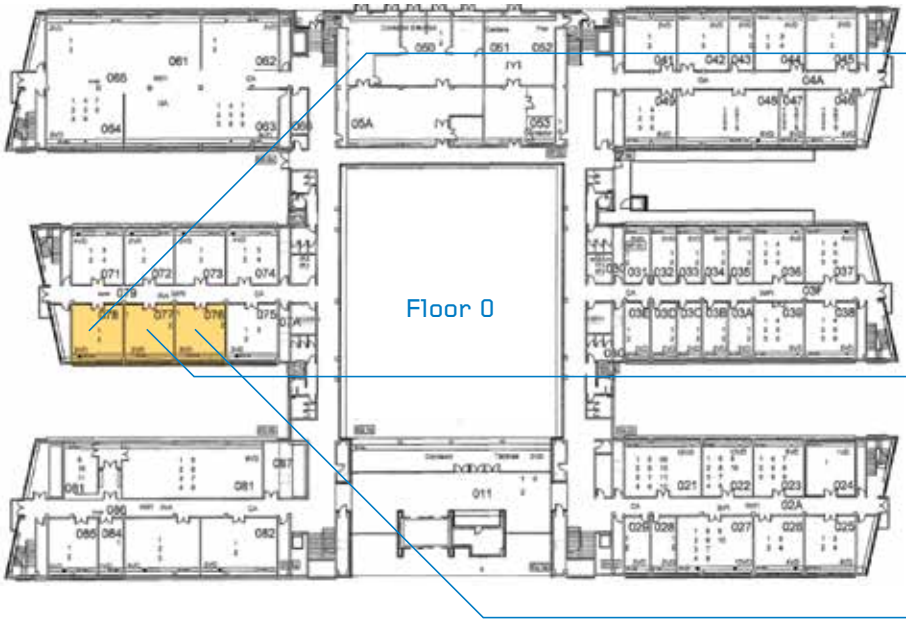

TITAN³

TITAN STEM

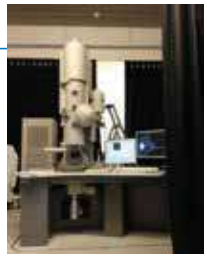

F30

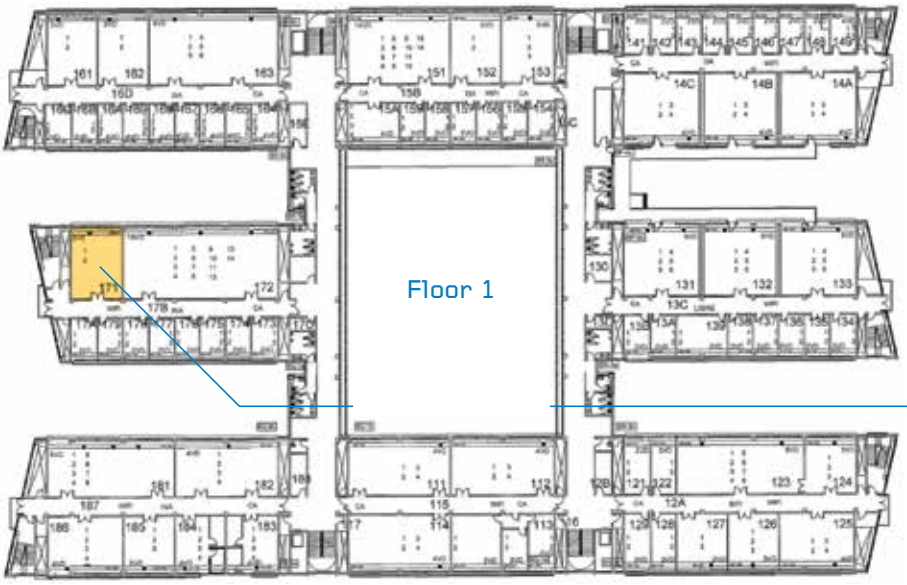

Sample Preparation

a) Transmission Electron Microscopy Laboratories (UHRTEM snd HRTEM) & Sample Preparation

There are three HRTEM instruments working up to 300 kV available: a F30 TEM and two TITAN Cs corrected microscopes of the very last generation.

a.1) High resolution transmission electron microscope (F30)

This 300 kV Field Emission Gun (FEG) TEM is fitted with a SuperTwin® lens allowing a point resolution of 1.9 Å. This TEM can work in TEM and STEM mode. For Z-contrast imaging in STEM mode, it is fitted with a High-Angle Annular Dark Field (HAADF) detector. This TEM is equipped for spectroscopy experiments performed either in EDS (X-Ray Microanalysis) or in Electron Energy Loss spectroscopy (EELS). For the latter, it is fitted with the "Tridiem" Gatan Energy Filter (GIF). This EELS set-up allows Energy Filtered TEM (EFTEM) images to be recorded as well as line spectra or spectrum imaging experiments to be performed. A 2K x 2K Ultrascan CCD camera (Gatan) is located before the GIF for TEM imaging. In addition to these capabilities the F30 TEM is also fitted with a Lorentz lens which permits the study of magnetic materials in an environment free of magnetic field (for magnetic domain imaging). Furthermore, the F30 allows tomography experiments to be performed both in TEM and STEM mode using a dedicated single tilt holder (+/- 70°) from Fischione.

a.2) Cs probe corrected STEM microscope (TITAN Low base) dedicated to EELS and STEM HAADF studies

This Scanning Transmission Electron Microscope works either in TEM or in STEM mode at voltages between 60 kV and 300 kV. It can be used at low voltage to analyse electron irradiation sensitive materials. It is fitted with the last generation of a high brightness Schotky emitter developed by FEI (the so called "X-FEG" gun) a monochromator and a Gatan 2k x 2k CCD camera.

STEM: As this microscope is devoted for STEM and EELS experiments, it is equipped with a CETCOR Cs-probe corrector from CEOS Company allowing for the formation of an electron probe of 0.08 nm mean size. The TEM is equipped with all the STEM facilities (BF, DF, ADF and HAADF detectors) and a 0.08 nm spatial resolution has indeed been achieved in STEM-HAADF mode.

EELS and EDS: For EELS experiments, the microscope is fitted with a Gatan Energy Filter Tridiem 866 ERS and a monochromator. An energy resolution of 0.14 eV has been recently achieved with this setup. In addition, an EDS (EDAX) detector allows performing EDX experiments in scanning mode with a spatial resolution of about ~0.2 nm.

Lorentz and holography: Beside these analytical capabilities, the Titan STEM corrected microscope is fitted with a Lorentz lens and an electrostatic biprism allowing Lorentz and medium resolution electron holography experiments to be carried out in a field-free environment (as needed for magnetic materials studies). Tomography: In addition, a tomography set-up with a +/- 70° single tilt stage permits to perform 3D analyses either in TEM or STEM modes.

a.3) Cs objective lens corrected microscope (TITAN3) dedicated to Ultra High Resolution TEM imaging

This TEM also works at voltages between 60 and 300 kV. It is located in a "box" (cube) to avoid mechanical and thermal perturbation (see figure). It contains a normal FEG (Shottky emitter) and a Gatan 2k x 2k CCD camera for (HR)TEM images acquisition.

HREM: As this microscope is devoted for High Resolution Transmission Electron Microscopy (HRTEM) studies, it is equipped with a SuperTwin® objective lens and a CETCOR Cs-objective corrector from CEOS Company allowing a point to point resolution of 0.08 nm.

STEM: In addition this Titan3 is equipped with the basic STEM facilities (BF, DF detectors) for STEM imaging at medium resolution

EELS: a Gatan Energy Filter Tridiem 863 allows Titan3 to perform EELS experiments in a standard and routine way (energy resolution of ~0.7 eV).

Lorentz and holography: As for the dedicated Titan STEM, beside these spectroscopy capabilities, the Titan3 corrected microscope is fitted with a Lorentz lens and an electrostatic biprism allowing Lorentz and medium resolution electron holography experiments to be carried on.

a.4) Sample Preparation Laboratory

The sample preparation laboratory carries out preparation of biological and synthetic samples to make them suitable for electron microscopes. The laboratory hosts all facilities necessary for adapting them to the dimensions of microscopes and for analyzing them by scanning (SEM) and transmission electron microscopy (TEM): cutting, ultrathin sectioning, polishing, ion milling, embedding, staining, coating, fixation/dehydration, vitrification, etc.

Sample Preparation Laboratory

Flat and smooth surfaces are required for good quality images and chemical contrast in SEM. LMA has tuned up the automated grinder-polisher Buehler Phoenix Beta, specially designed to polish multiple samples embedded in resin. Coating of samples by conducting materials is achieved by the vacuum coater Leica EM ACE200.

Mechanical thinning of materials in a highly controlled way in combination with low-angle and low-energy ion milling produces a flat specimen of a few microns in thickness, with defect-free surfaces ready for TEM observation. Ultramicrotomy is another technique to produce 50-70 nm thick slices of soft (biological and synthetic) materials. Depending on the specific features of materials, samples can be sectioned between -180 °C (cryo-ultramicrotomy) and room temperature. In the case of biological samples, a previous treatment is necessary in which samples are fixed, dehydrated and embedded in epoxy resin before cutting.

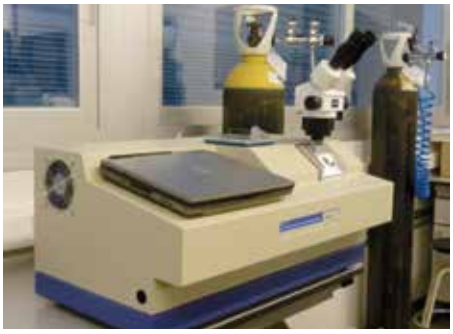

Ion mill equipment to obtain electron transparent areas in the samples for the TEM observation.

Vitrification of samples and their analysis in cryogenic conditions are other outstanding techniques available in LMA. The vacuum coater LEICA EM ACE200 is eqquiped with a glow discharge option to make grids temporarily hydrophilic and allow aqueous solutions to spread easily.

DUAL BEAM Laboratories

µ-structural chacterization & Spectroscopy

Life Sciences

Dual Beam in Clean Room

b) Dual Beam Laboratorie & Microcharacterization

b.1) Dual Beams Laboratory in Clean Room

In the Clean Room facilities of the institute, several lithography facilities permit to pattern structures at the micro- and nano-meter scale and to create devices. There are two dual beam equipment (Helios 600 and Helios 650), located on two concrete platforms inside the 125 m2 10,000-class Clean Room.

The dual beam equipment consists of a 30 kV field-emission scanning electron column and a 30 kV Ga focused ion beam placed at 52º one from each other. The ion column is able to work properly at low voltage (5 kV and lower).

Both instruments are routinely used for the following tasks: lamellae preparation (in combination with the Omniprobe nanomanipulator), cross-section imaging, nanolithography based on ion patterning, ion irradiation, ion/electron nanodeposition, electronic transport measurements (Kleindiek) and electron beam lithography (Raith® software/hardware).

Helios 600 dual beam equipment installed inside the Clean Room of the INA building.

The Helios 650 model is an improved version of the Helios 600 one. Thus, the SEM column bears a monochromator and beam deceleration. The FIB column is differentially vacuum-pumped at the lowest part, allowing a well-defined beam profile impacting on the sample surface and higher currents in order to mill hard materials and large areas.

The internal and external users come from multidisciplinary knowledge areas: physics, chemistry, geology, engineering…

Every year, the LMA technical staff prepares more than 200 lamellae with high-enough quality for atomic-resolution TEM imaging.

Thanks to five gas injectors installed on the Dual Beams, growth of nanodeposits with high resolution is performed. It is possible to grow W-based superconducting nanodeposits with lateral size of 40 nm and Co-based ferromagnetic nanodeposits with lateral size of 30 nm, these ultranarrow dimensions being at the forefront of the research on these nanomaterials.

Helios 600 dual beam equipment installed inside the Clean Room of the INA building.

Helios 650 equipment installed inside the Clean Room of the INA building.

Nova 200 dual beam equipment and the cryo-transfer setup, installed at INA building .

b.2) Cryogenic Dual Beam

The third dual beam equipment is used for electron sensitive materials and life sciences and has been installed in the same room as the environmental SEM and the field-emission SEM. This instrument is based on the Nova 200 model (existing in our laboratory since November 2006) but upgraded with a cryo-transfer chamber. This equipment has worked properly since 2007 and in combination with the cryo-transfer set-up is being used to produce series of ion-cuts of cells embedded in resin or frozen with the help of liquid nitrogen. These images will be used to produce three dimensional (3D) reconstructions. Appropriate software for 3D compositional reconstructions based on energy-dispersive x-ray micro-analysis is also included in this equipment. If needed, the equipment also holds an Omniprobe nanomanipulator for lamellae preparation as well as 5 gas injectors.

b.3) Other facilities for micro and surface characterization

Environmental SEM-FEG

An environmental SEM, model Quanta 250, is installed in the same room as the Nova 200 dual beam. The SEM column allows beam deceleration, which permits to keep resolution of 1.4 nm even at 1 kV electron landing voltage. The Quanta equipment can work under three different pressure ranges, the maximum pressure being 4,000 Pa, thus close to ambient pressure. This allows observation of life-sciences samples without previous metallic coating. The equipment allows the use of a Wet-STEM, which permits to inspect samples with controlled humidity, this being crucial in life-science samples in order to maintain the same conditions as hold when functional. The equipment can also use a heater to perform observation on samples heated up to 1,000º C.

Environmental SEM, Quanta FEG 250 equipment, installed at the INA building.

Field-emission SEM, INSPECT equipment, installed at the INA building.

SEM-FEG

The last SEM equipment, the Inspect model, is a general-purpose field-emission SEM for high-resolution imaging and composition analysis by energy-dispersive x-ray microanalysis.

Laboratory of Microstructural Characterization and Spectroscopy

The XRD and the XPS-AES equipments are installed in the room devoted to microstructural and spectroscopy sample analysis. Those equipments have been working since 2006providing a great variety of useful results for most of the research groups at INA and other centres and companies. In the following paragraphs, the main characteristics of these equipments are described:

XRD diffractometers

1. Bruker D8 Advance High resolution Diffractometer: The equipment configuration is optimized for high-resolution X-ray diffraction (HR-XRD) and reflectivity (XRR) studies in nanostructured thin films and superlattices. For this purpose it includes parallel beam optics, monochromator, collimators, soller slits, attenuators and eulerian cradle. It also allows the local mapping of flat samples through motorized lateral displacements. The equipment is completed with an analysis software pack and database.

2. PANalytical Empyream Multipurpose Diffractometer: Multipurpose diffractometer prepared for transmission and reflection XRD, equipped with parallel and focused beam optics and solid state 1D detector and Multiple interchangeable optics and platforms for Non-ambient XRD up to 1200 K, GIXRD, SAXS and SA-XRD

XPS Photoelectronc Spectrometers

1. Kratos AXIS UltraDLD Photoelectron Spectrometer: XPS spectrometer equipped with Al-Mono and Mg/Al dual anodes, multidetector energy analyzer and 2D detector for parallel imaging. Automatic stage with sample holder for 4-axis high-precision displacements. Ar+ ion gun for cleaning and depth profile analysis. Electron gun for AES spectroscopy.

2. Kratos AXIS Supra Photoelectron Spectrometer: XPS spectrometer equipped with dual Al/Ag-Mono anode, multidetector energy analyzer and 2D detector for parallel imaging. Automatic stage with sample holder for 5-axis high-precision displacements. UV discharge lamp for HeI/HeII UPS spectroscopy. GCIB with cluster and mono ion modes for depth profiling of organic/sensitive and inorganic materials.

XRD (left image) and the XPS-AES (right image) equipment, installed at LMA

Laboratories for Local Probe Microscopy

High Magnetic Field

UHV-LT (II)

Environmental

UHV-LT (I)

c) Laboratories for Local Probe Microscopy

The available facilities in the area of Scanning Probe Microscopy (SPM) section of the LMA are composed by three focused laboratories hosting up to six different SPM heads:

Low-temperature, ultra high vacuum scanning probe microscopy Laboratory

The laboratory of UHV-LT is specifically designed for surface science microscopy and spectroscopy methods. The aim is to cover a wide variety of problems in surface science, from molecular chemistry to atomic magnetism. Two independent UHV systems are equipped with different preparation techniques, as well as with large variety of epitaxial growth facilities. Force- and Tunnel-based methodologies can be combined, allowing the investigation of samples with different electronic properties. The accessible temperature range for experiments is from 0.5 K to 1300 K. The laboratory by the following microscopes:

c.1) SPECS JT-STM

This equipment is specifically oriented to investigate atomic scale magnetism and to high resolution spectroscopy of molecules and atoms. It features a base temperature of 1.1 K (0.5 K using 3He). In 2018, this facility has provided the scientific community with spin-polarized STM on a regular basis, being the only laboratory offering worldwide this technique via a competitive proposal scheme. The details of the equipment are the following:

SPECS JT-STM

Joule Thomson cryostat (1K-10K) UHV-STM; 3 T axial B field; energy resolution 0.15 meV; Metal and organic epitaxy in situ.

Attached UHV facilities

Surface conditioning, LEED/Auger characterization; 6 Molecular Beam Epitaxy pockets (all with fast reload option), 1 crucible evaporator for organic materials, 3 gats inlets. Homemade accessories for the preparation of tips to perform spin-polarized STM.

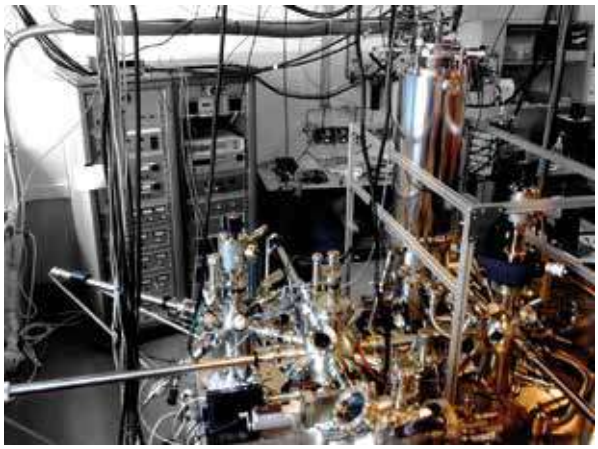

c.2) AAHRUS VT-AFM/STM

This microscope is applied to the study surface dynamics and chemistry with atomic resolution as a function of temperature and gas partial pressure. It is a variable temperature STM/AFM (from 100 K to 1300 K), with a fast and flexible measurement approach. Technical specifications:

AAHRUS VT-STM/AFM:

Aarhus variable temperature (100 K-1300 K) STM, Non-contact-AFM, in-situ evaporation

Attached UHV facilities:

Surface conditioning, 2 Molecular Beam Epitaxy pockets (1 with fast reload option), 3 crucible evaporators for organic materials. 5 gas inlets. Mass spectrometer.

c.3) OMICROM LT-qPlus

This set up includes the last development in UHV non-contact AFM. Working at a base temperature of 5 K, the use of a qPlus sensor allows to simultaneously acquire local tunneling spectroscopy and forces spectroscopy. Measurement of both forces and conductance is especially interesting in the field of molecular physics on surfaces.

Force microscopy is also especially suitable to work on insulating surfaces. This experimental set up has been equipped with various methods to deposit organic materials on inorganic surfaces. The research lines are oriented to molecular interactions, self-assembly and magnetic, electronic and structural properties of hybrid metal-organic films.

OMICROM LT-aPlus: Low temperature (4.3 K-40 K) UHV STM equipped with a qPlus sensor allows users to correlate resonance frequency shifts of a quartz tuning forlk with the gradient of forces beween tip and sample.

Preparation: Surface conditioning, LEED/Auger, metal epitaxy, and sublimation of organic materials by one K-cell and two crucible evaporators.

Laboratory of SPM under high magnetic field

c.4) High field SPM

The laboratory of high magnetic fields offers the possibility of combining probe measurements (AFM, MFM, STM) with ultra-low temperatures and a high vector magnetic field. It is especially suitable for combination of local probe and magneto-transport measurements as, for example, scanning gate microscopy. Therefore, it runs research lines oriented towards low temperature magnetism, transport through nanodevices, spintronics and superconductivity.

ATTOCUBE AFM/STM: STM/AFM/MFM head inserted into a large bore superconducting magnet reaching 8T/2T vector magnetic field. The equipment has a quick load facility, allowing an easy sample replacement and measurements. A variable temperature module allows one to continuously change the temperature from 2 K up to 300 K. Further characteristics include: in-situ optical access, compatible chip carrier with dual-beam facilities.

Laboratory AFM/STM in ambient conditions

c.5) Near ambient SPM heads

The biology, chemistry and physics community are all of them potential users of these facilities. They demand a set of microscopy tools with large versatility and able of working under different environments close to ambient conditions. The laboratory contains both force and tunnel scanning microscopes that allow users the characterization of samples in liquid or air environments with controlled humidity and/or temperature.

Atomic Force Microscopy

AFM is a key technique in Nanoscience, supporting multidisciplinary activities. Hence it is a central facility in the LMA. Highly specialized researchers working regularly with LMA facilities offer training to other users and newcomers to the laboratory. Sub-angstrom topographic resolution in contact or dynamic modes can be routinely achieved, as well as imaging of magnetic forces and dedicated force spectroscopy sessions.

Equipment:

1) Nanotec: Cervantes Fullmode SPM from Nanotec Electrónica S.L. AFM/MFM/STM equipped with variable magnetic field and liquid cell.

2) Veeco: Multimode 8 from Bruker. SPM equipped with KPM, conductive AFM, liquid and electrochemistry cells, PicoForce module for force spectroscopy measures, and variable temperature (-40 ºC to 100 ºC), environmental cell to vary humidity or partial pressure of varius gases.

CervFullmode SPM from Nanotec Electronics

Multimode 8 from Veeco-Bruker

Scientific Activity

List of Publications

IF=impact factor

1. **Self-Assembled Core-Shell CdTe/Poly(3-hexylthiophene) Nanoensembles as Novel Donor-Acceptor Light-Harvesting Systems**
Istif, E., Kagkoura, A., Hernandez-Ferrer, J., Stergiou, A., Skaltsas, T., Arenal, R., Benito, A.M., Maser, W.K., Tagmatarchis, N.
2017 *ACS Applied Materials and Interfaces* 9 (51), pp 44695-44703
DOI: 10.1021/acsami.7b13506
IF: 8.097

2. **Functionalization of MoS2 with 1,2-dithiolanes: toward donor-acceptor nanohybrids for energy conversion**
Canton-Vitoria, R., Sayed-Ahmad-Baraza, Y., Pelaez-Fernandez, M., Arenal, R., Bittencourt, C., Ewels, C.P., Tagmatarchis, N.
2017 *npj 2D Materials and Applications* 1 (1) 13
DOI: 10.1038/s41699-017-0012-8
IF: no Impact Factor assigned in 2017

3. **A building blocks strategy for preparing photocatalytically active anatase TiO2/rutile SnO2 heterostructures by hydrothermal annealing**
de Mendonça, V.R., Avansi, W., Arenal, R., Ribeiro, C.
2017 *Journal of Colloid and Interface Science* 505, pp 454.459
DOI: 10.1016/j.jcis.2017.06.024
IF: 5.091

4. **Design and development of multi-walled carbon nanotube-liposome drug delivery platforms**
Pippa, N., Chronopoulos, D.D., Stellas, D., Fernández-Pacheco, R., Arenal, R., Demetzos, C., Tagmatarchis, N.
2017 *International Journal of Pharmaceutics* 528, pp 429-439
DOI: 10.1016/j.ijpharm.2017.06.043
IF: 3.862

5. **Enhancement of the spin Peltier effect in multilayers**
Uchida, K., Iguchi, R., Daimon, S., Ramos, R., Anadón, A., Lucas, I., Algarabel, P.A., Morellón, L., Aguirre, M.H., Ibarra, M.R., Saitoh, E.
2017 *Physical Review B* 95 (18) 184437
DOI: 10.1103/PhysRevB.95.184437
IF: 3.813

6. **Controlling the Electrical and Magnetoelectric Properties of Epitaxially Strained Sr1−xBaxMnO3 Thin Films**
Langenberg, E., Maurel, L., Marcano, N., Guzmán, R., Štrichovanec, P., Prokscha, T., Magén, C., Algarabel, P.A., Pardo, J.A.
2017 *Advanced Materials Interfaces* 4 (9) 1601040
DOI: 10.1002/admi.201601040
IF: 4.834

7. **Quantum interference effects on the intensity of the G modes in double-walled carbon nanotubes**
Tran, H.N., Blancon, J.-C., Arenal, R., Parret, R., Zahab, A.A., Ayari, A., Vallée, F., Del Fatti, N., Sauvajol, J.-L., Paillet, M.
2017 *Physical Review B* 95 (20) 205411
DOI: 10.1103/PhysRevB.95.205411
IF: 3.813

8. **Microcystin-LR Binds Iron, and Iron Promotes Self-Assembly**
Ceballos-Laita, L., Marcuello, C., Lostao, A., Calvo-Begueria, L., Velazquez-Campoy, A., Bes, M.T., Fillat, M.F., Peleato, M.-L.
2017 *Environmental Science and Technology* 51 (9), pp 4841-4850
DOI: 10.1021/acs.est.6b05939
IF: 6.653

9. **Temperature dependence of the spin Seebeck effect in [Fe3O4/Pt]n multilayers**
Ramos, R., Kikkawa, T., Anadón, A., Lucas, I., Uchida, K., Algarabel, P.A., Morellón, L., Aguirre, M.H., Saitoh, E., Ibarra, M.R.
2017 *AIP Advances* 7 (5) 55915
DOI: 10.1063/1.4974060
IF: 1.653

10. **Investigation of the Optical and Excitonic Properties of the Visible Light-Driven Photocatalytic BiVO4 Material**
Das, T., Rocquefelte, X., Laskowski, R., Lajaunie, L., Jobic, S., Blaha, P., Schwarz, K.
2017 *Chemistry of Materials* 29 (8), pp 3380-3386
DOI: 10.1021/acs.chemmater.6b02261
IF: 9.890

11. **Sustainable Preparation of MIL-100(Fe) and Its Photocatalytic Behavior in the Degradation of Methyl Orange in Water**
Guesh, K., Caiuby, C.A.D., Mayoral, Á., Díaz-García, M., Díaz, I., Sanchez-Sanchez, M.
2017 *Crystal Growth and Design* 17 (4), pp 1806.1813
DOI: 10.1021/acs.cgd.6b01776
IF: 3.972

12. Accurate determination of the chiral indices of individual carbon nanotubes by combining electron diffraction and Resonant Raman spectroscopy
Levshov, D.I., Tran, H.N., Paillet, M., Arenal, R., Than, X.T., Zahab, A.A., Yuzyuk, Y.I., Sauvajol, J.-L., Michel, T.
2017 *Carbon* 114, pp 141-159
DOI: 10.1016/j.carbon.2016.11.076
IF: 7.082

13. Intrinsic phonon properties of double-walled carbon nanotubes
Tran, H.N., Levshov, D.I., Nguyen, V.C., Paillet, M., Arenal, R., Than, X.T., Zahab, A.A., Yuzyuk, Y.I., Phan, N.M., Sauvajol, J.-L., Michel, T.
2017 *Advances in Natural Sciences: Nanoscience and Nanotechnology* 8 (1) 15018
DOI: 10.1088/2043-6254/aa5957
IF: no Impact Factor assigned in 2017

14. Spin-phonon coupling in epitaxial S r0.6 B a0.4Mn O3 thin films
Goian, V., Langenberg, E., Marcano, N., Bovtun, V., Maurel, L., Kempa, M., Prokscha, T., Kroupa, J., Algarabel, P.A., Pardo, J.A., Kamba, S.
2017 *Physical Review B* 95 (7) 75126
DOI: 10.1103/PhysRevB.95.075126
IF: 3.813

15. Titania-coated gold nanorods with expanded photocatalytic response. Enzyme-like glucose oxidation under near-infrared illumination
Ortega-Liebana, M.C., Hueso, J.L., Arenal, R., Santamaria, J.
2017 *Nanoscale* 9 (5), pp 1787-1792
DOI: 10.1039/c6nr06300d
IF: 7.233

16. Spin Seebeck effect in insulating epitaxial γ–Fe2O3 thin films
Jiménez-Cavero, P., Lucas, I., Anadón, A., Ramos, R., Niizeki, T., Aguirre, M.H., Algarabel, P.A., Uchida, K., Ibarra, M.R., Saitoh, E., Morellón, L.
2017 *APL Materials* 5 (2) 26103
DOI: 10.1063/1.4975618
IF: 4.127

17. Structuring of Alkyl-Triazole Bridged Silsesquioxanes
Nunes, S.C., Toquer, G., Cardoso, M.A., Mayoral, A., Ferreira, R.A.S., Carlos, L.D., Ferreira, P., Almeida, P., Cattoën, X., Wong Chi Man, M., de Zea Bermudez, V.
2017 *ChemistrySelect* 2 (1), pp 432-442
DOI: 10.1002/slct.201601806
IF: 1.505

18. Nanostructured carbon-metal hybrid aerogels from bacterial cellulose
Wicklein, B., Arranz, J., Mayoral, A., Aranda, P., Huttel, Y., Ruiz-Hitzky, E.
2017 *RSC Advances* 7 (67), pp 42203-42210
DOI: 10.1039/c7ra07534k
IF: 2.936

19. Monitoring in real-time focal adhesion protein dynamics in response to a discrete mechanical stimulus
Von Bilderling, C., Caldarola, M., Masip, M.E., Bragas, A.V., Pietrasanta, L.I.
2017 *Review of Scientific Instruments* 88 (1) 13703
DOI: 10.1063/1.4973664
IF: 1.428

20. A physical picture for mechanical dissociation of biological complexes: From forces to free energies
Tapia-Rojo, R., Marcuello, C., Lostao, A., Gómez-Moreno, C., Mazo, J.J., Falo, F.
2017 *Physical Chemistry Chemical Physics* 19 (6), pp 4567-4575
DOI: 10.1039/c6cp07508h
IF: 3.906

21. Graphene oxide-carbon nanotube hybrid assemblies: Cooperatively strengthened OH···O=C hydrogen bonds and the removal of chemisorbed water
Núñez, J.D., Benito, A.M., Rouzière, S., Launois, P., Arenal, R., Ajayan, P.M., Maser, W.K.
2017 *Chemical Science* 8 (7), pp 4987-4995
DOI: 10.1039/c7sc00223h
IF: 9.063

22. Modification of anatase using noble-metals (Au, Pt, Ag): Toward a nanoheterojunction exhibiting simultaneously photocatalytic activity and plasmonic gas sensing
Karmaoui, M., Lajaunie, L., Tobaldi, D.M., Leonardi, G., Benbayer, C., Arenal, R., Labrincha, J.A., Neri, G.
2017 *Applied Catalysis B: Environmental* 218, pp 370-384
DOI: 10.1016/j.apcatb.2017.06.010
IF: 11.698

23. Extraordinary sensitizing effect of co-doped carbon nanodots derived from mate herb: Application to enhanced photocatalytic degradation of chlorinated wastewater compounds under visible light
Ortega-Liebana, M.C., Hueso, J.L., Ferdousi, S., Arenal, R., Irusta, S., Yeung, K.L., Santamaria, J.
2017 *Applied Catalysis B: Environmental* 218, pp 68-79
DOI: 10.1016/j.apcatb.2017.06.021
IF: 11.698

24. MoS2–Carbon Nanotube Hybrid Material Growth and Gas Sensing
Deokar G., Vancsó P., Arenal R., Ravaux F., Casanova-Cháfer J., Llobet E., Makarova A., Vyalikh D., Struzzi C., Lambin P., Jouiad M., Colomer J.-F.
2017 *Advanced Materials Interface*s 4 (24), 1700801
DOI: 10.1002/admi.201700801
IF: 4.834

25. Stability Assessment of Regenerated Hierarchical ZSM-48 Zeolite Designed by Post-Synthesis Treatment for Catalytic Cracking of Light Naphtha
Ahmed M.H.M., Muraza O., Nakaoka S., Jamil A.K., Mayoral A., Sebastian V., Yamani Z.H., Masuda T.
2017 *Energy and Fuels* 31 (12), pp 14097-14103
DOI: 10.1021/acs.energyfuels.7b02796
IF: 3.024

26. Chemical solution synthesis and ferromagnetic resonance of epitaxial thin films of yttrium iron garnet
Lucas I., Jiménez-Cavero P., Vila-Fungueiriño J.M., Magén C., Sangiao S., De Teresa J.M., Morellón L., Rivadulla F.
2017 *Physical Review Materials* 1 (7), 74407
DOI: 10.1103/PhysRevMaterials.1.074407
IF: no Impact Factor assigned in 2017

27. Structurally oriented nano-sheets in co thin films: Changing their anisotropic physical properties by thermally-induced relaxation
Vergara J., Favieres C., Magén C., de Teresa J.M., Ibarra M.R., Madurga V.
2017 *Materials* 10 (12) 1390
DOI: 10.3390/ma10121390
IF: 2.467

28. Cell damage produced by magnetic fluid hyperthermia on microglial BV2 cells
Calatayud M.P., Soler E., Torres T.E., Campos-Gonzalez E., Junquera C., Ibarra M.R., Goya G.F.
2017 *Scientific Reports* 7 (1), 8627
DOI: 10.1038/s41598-017-09059-7
IF: 4.122

29. Controlled growth of nano-hydroxyapatite on stilbite: Defluoridation performance
Sani T., Gómez-Hortigüela L., Mayoral Á., Chebude Y., Pérez-Pariente J., Díaz I.
2017 *Microporous and Mesoporous Materials* 254, pp 86-95
DOI: 10.1016/j.micromeso.2017.04.036
IF: 3.649

30. The FAD synthetase from the human pathogen Streptococcus pneumoniae: A bifunctional enzyme exhibiting activity-dependent redox requirements
Sebastián M., Lira-Navarrete E., Serrano A., Marcuello C., Velázquez-Campoy A., Lostao A., Hurtado-Guerrero R., Medina M., Martínez-Júlvez M.
2017 *Scientific Reports* 7 (1) 7609
DOI: 10.1038/s41598-017-07716-5
IF: 4.122

31. Competition between Superconductor-Ferromagnetic stray magnetic fields in YBa2Cu3O7-x films pierced with Co nano-rods
Rouco V., Córdoba R., De Teresa J.M., Rodríguez L.A., Navau C., Del-Valle N., Via G., Sánchez A., Monton C., Kronast F., Obradors X., Puig T., Palau A.
2017 *Scientific Reports* 7 (1) 5663
DOI: 10.1038/s41598-017-05909-6
IF: 4.122

32. Pumping Metallic Nanoparticles with Spatial Precision within Magnetic Mesoporous Platforms: 3D Characterization and Catalytic Application
Miguel-Sancho N., Martinez G., Sebastian V., Malumbres A., Florea I., Arenal R., Ortega-Liebana M.C., Hueso J.L., Santamaria J.
2017 *ACS Applied Materials and Interfaces* 9 (47), pp 41529-41536
DOI: 10.1021/acsami.7b11482
IF: 8.097

33. Functionalized Akiyama tips for magnetic force microscopy measurements
Stiller M., Barzola-Quiquia J., Esquinazi P.D., Sangiao S., De Teresa J.M., Meijer J., Abel B.
2017 *Measurement Science and Technology* 28 (12), 125401
DOI: 10.1088/1361-6501/aa925e
IF: 1.685

34 Platinum tripods as nanometric frequency multiplexing devices
Camargo B.C., Lassagne B., Arenal R., Gatel C., Blon T., Viau G., Lacroix L.-M., Escoffier W.
2017 *Nanoscale* 9 (38), pp 14635-14640
DOI: 10.1039/c7nr04544a
IF: 7.233

35. Suspended tungsten-based nanowires with enhanced mechanical properties grown by focused ion beam induced deposition
Córdoba R., Lorenzoni M., Pablo-Navarro J., Magén C., Pérez-Murano F., De Teresa J.M.
2017 *Nanotechnology* 28 (44), 445301
DOI: 10.1088/1361-6528/aa873c
IF: 3.404

36. Cs-Corrected STEM Imaging of both Pure and Silver-Supported Metal-Organic Framework MIL-100(Fe)
Mayoral A., Mahugo R., Sánchez-Sánchez M., Díaz I.
2017 *ChemCatChem* 9 (18), pp 3497-3502
DOI: 10.1002/cctc.201700519
IF: 4.674

37. High surface coverage of a self-assembled monolayer by: In situ synthesis of palladium nanodeposits
Herrer L., Sebastian V., Martín S., González-Orive A., Pérez-Murano F., Low P.J., Serrano J.L., Santamaría J., Cea P.
2017 *Nanoscale* 9 (35), pp 13281-13290
DOI: 10.1039/c7nr03365f
IF: 7.233

38. Structural and magnetic properties of [001] CoC r2 O4 thin films
Guzman R., Heuver J., Matzen S., Magén C., Noheda B.
2017 *Physical Review B* 96 (10) 104105
DOI: 10.1103/PhysRevB.96.104105
IF: 3.813

39. Noncovalent Stable Functionalization Makes Carbon Nanotubes Hydrophilic and Biocompatible
Ernst F., Gao Z., Arenal R., Heek T., Setaro A., Fernandez-Pacheco R., Haag R., Cognet L., Reich S.
2017 *Journal of Physical Chemistry C* 121 (34), pp 18887-18891
DOI: 10.1021/acs.jpcc.7b03062
IF: 4.484

40. Reversible Monolayer-Bilayer Transition in Supported Phospholipid LB Films under the Presence of Water: Morphological and Nanomechanical Behavior
Ruiz-Rincón S., González-Orive A., De La Fuente J.M., Cea P.
2017 *Langmuir* 33 (30), pp 7538-7547
DOI: 10.1021/acs.langmuir.7b01268
IF: 3.789

41. Chemical Disorder in Topological Insulators: A Route to Magnetism Tolerant Topological Surface States
Martínez-Velarte M.C., Kretz B., Moro-Lagares M., Aguirre M.H., Riedemann T.M., Lograsso T.A., Morellón L., Ibarra M.R., Garcia-Lekue A., Serrate D.
2017 *Nano Letters* 17 (7), pp 4047-4054
DOI: 10.1021/acs.nanolett.7b00311
IF: 12.080

42. Assembly-Disassembly-Organization-Reassembly Synthesis of Zeolites Based on cfi-Type Layers

Firth D.S., Morris S.A., Wheatley P.S., Russell S.E., Slawin A.M.Z., Dawson D.M., Mayoral A., Opanasenko M., Položij M., Čejka J., Nachtigall P., Morris R.E.

2017 *Chemistry of Materials* 29 (13), pp 5605-5611

DOI: 10.1021/acs.chemmater.7b01181

IF: 9.890

43. Hybrid YBa2Cu3O7 Superconducting–Ferromagnetic Nanocomposite Thin Films Prepared from Colloidal Chemical Solutions

Bartolomé E., Cayado P., Solano E., Mocuta C., Ricart S., Mundet B., Coll M., Gázquez J., Meledin A., van Tendeloo G., Valvidares S.M., Herrero-Martín J., Gargiani P., Pellegrin E., Magén C., Puig T., Obradors X.

2017 *Advanced Electronic Materials* 3 (7), 1700037

DOI: 10.1002/aelm.201700037

IF: 5.466

44. 55Mn NMR observation of colossal magnetoresistance effect in Sm0.55Sr0.45MnO3

Michalik J.M., Rybicki D., Tarnawski Z., Sikora M., De Teresa J.M., Ibarra M.R., Kapusta Cz.

2017 *Journal of Physics Condensed Matter* 29 (26), 265802

DOI: 10.1088/1361-648X/aa72c5

IF: 2.617

45. Core@shell, Au@TiOx nanoparticles by gas phase synthesis

Martínez L., Mayoral A., Espiñeira M., Roman E., Palomares F.J., Huttel Y.

2017 *Nanoscale* 9 (19), pp 6463-6470

DOI: 10.1039/c7nr01148b

IF: 7.233

46. Systematic Study of Oxygen Vacancy Tunable Transport Properties of Few-Layer MoO3– x Enabled by Vapor-Based Synthesis

Hanson E.D., Lajaunie L., Hao S., Myers B.D., Shi F., Murthy A.A., Wolverton C., Arenal R., Dravid V.P.

2017 *Advanced Functional Materials* 27 (17), 1605380

DOI: 10.1002/adfm.201605380

IF: 13.325

47. Simulation of STEM-HAADF Image Contrast of Ruddlesden-Popper Faulted LaNiO3 Thin Films
Coll C., López-Conesa L., Rebled J.M., Magén C., Sánchez F., Fontcuberta J., Estradé S., Peiró F.
2017 *Journal of Physical Chemistry C* 121 (17), pp 9300-9304
DOI: 10.1021/acs.jpcc.6b12484
IF: 4.484

48. Oxygen vacancies in strained SrTiO3 thin films: Formation enthalpy and manipulation
Iglesias L., Sarantopoulos A., Magén C., Rivadulla F.
2017 *Physical Review B* 95 (16), 165138
DOI: 10.1103/PhysRevB.95.165138
IF: 3.813

49. In situ lorentz microscopy and electron holography magnetization studies of ferromagnetic focused electron beam induced nanodeposits
Magén C., Rodríguez L.A., Serrano-Ramón L.E., Gatel C., Snoeck E., De Teresa J.M.
2017 *Magnetic Characterization Techniques for Nanomaterials* 305 (338)
DOI: 10.1007/978-3-662-52780-1_9
IF: no Impact Factor assigned in 2017

50. Tuning shape, composition and magnetization of 3D cobalt nanowires grown by focused electron beam induced deposition (FEBID)
Pablo-Navarro J., Sanz-Hernández D., Magén C., Fernández-Pacheco A., De Teresa J.M.
2017 *Journal of Physics D: Applied Physics* 50 (18) 18LT01
DOI: 10.1088/1361-6463/aa63b4
IF: 2.373

51. Co-sputtered PtMnSb thin films and PtMnSb/Pt bilayers for spin–orbit torque investigations
Krieft J., Mendil J., Aguirre M.H., Avci C.O., Klewe C., Rott K., Schmalhorst J.-M., Reiss G., Gambardella P., Kuschel T.
2017 *Physica Status Solidi - Rapid Research Letters* 11 (4) 1600439
DOI: 10.1002/pssr.201600439
IF: 3.721

52. STA-20: An ABC-6 Zeotype Structure Prepared by Co-Templating and Solved via a Hypothetical Structure Database and STEM-ADF Imaging
Turrina A., Garcia R., Watts A.E., Greer H.F., Bradley J., Zhou W., Cox P.A., Shannon M.D., Mayoral A., Casci J.L., Wright P.A.
2017 *Chemistry of Materials* 29 (5), pp 2180-2190
DOI: 10.1021/acs.chemmater.6b04892
IF: 9.890

53. Proximity-induced superconductivity in bismuth nanostripes
Sangiao S., Casado L., Morellón L., Ibarra M.R., De Teresa J.M.
2017 *Journal of Physics D: Applied Physics* 50 (12) 12LT02
DOI: 10.1088/1361-6463/aa5d31
IF: 2.373

54. All-Carbon Electrode Molecular Electronic Devices Based on Langmuir–Blodgett Monolayers
Sangiao S., Martín S., González-Orive A., Magén C., Low P.J., De Teresa J.M., Cea P.
2017 *Small* 13 (7) 1603207
DOI: 10.1002/smll.201603207
IF: 9.598

55. Anisotropic Self-Assembly of Supramolecular Polymers and Plasmonic Nanoparticles at the Liquid-Liquid Interface
Armao IV J.J., Nyrkova I., Fuks G., Osypenko A., Maaloum M., Moulin E., Arenal R., Gavat O., Semenov A., Giuseppone N.
2017 *Journal of the American Chemical Society* 139 (6), pp 2345-2350
DOI: 10.1021/jacs.6b11179
IF: 14.357

56. On the advantages of spring magnets compared to pure FePt: Strategy for rare-earth free permanent magnets following a bottom-up approach
Pousthomis M., Garnero C., Marcelot C.G., Blon T., Cayez S., Cassignol C., Du V.A., Krispin M., Arenal R., Soulantica K., Viau G., Lacroix L.-M.
2017 *Journal of Magnetism and Magnetic Materials* 424, pp 304-313
DOI: 10.1016/j.jmmm.2016.10.071
IF: 3.046

57. NanoSQUID magnetometry of individual cobalt nanoparticles grown by focused electron beam induced deposition
Martinez-Pérez M.J., Müller B., Schwebius D., Korinski D., Kleiner R., Sesé J., Koelle D.
2017 *Superconductor Science and Technology* 30 (2) 24003
DOI: 10.1088/0953-2048/30/2/024003
IF: 2.861

58. Nano-crystalline titanium(IV) tungstomolybdate cation exchanger: Synthesis, characterization and ion exchange properties
Kelta B., Taddesse A.M., Yadav O.P., Diaz I., Mayoral Á.
2017 *Journal of Environmental Chemical Engineering* 5 (1), pp 1004-1014
DOI: 10.1016/j.jece.2017.01.018
IF: no Impact Factor assigned in 2017

59. Advanced spectroscopic analyses on a:C-H materials: Revisiting the EELS characterization and its coupling with multi-wavelength Raman spectroscopy
Lajaunie L., Pardanaud C., Martin C., Puech P., Hu C., Biggs M.J., Arenal R.
2017 *Carbon* 112, pp 149-161
DOI: 10.1016/j.carbon.2016.10.092
IF: 7.082

60. Preserving π-conjugation in covalently functionalized carbon nanotubes for optoelectronic applications
Setaro A., Adeli M., Glaeske M., Przyrembel D., Bisswanger T., Gordeev G., Maschietto F., Faghani A., Paulus B., Weinelt M., Arenal R., Haag R., Reich S.
2017 *Nature Communication*s 8, 14281
DOI: 10.1038/ncomms14281
IF: 12.353

61. Nano-structured magneto-responsive membranes from block copolymers and iron oxide nanoparticles
Upadhyaya L., Semsarilar M., Fernández-Pacheco R., Martinez G., Mallada R., Coelhoso I.M., Portugal C.A.M., Crespo J.G., Deratani A., Quemener D.
2017 *Polymer Chemistry* 8 (3), pp 605-614
DOI: 10.1039/c6py01870j
IF: 4.927

62. Active magnetoplasmonic split-ring/ring nanoantennas
Feng H.Y., Luo F., Arenal R., Henrard L., García F., Armelles G., Cebollada A.
2017 *Nanoscale* 9 (1), pp 37-44
DOI: 10.1039/c6nr07864h
IF: 7.233

63. Magnetic hyperthermia enhances cell toxicity with respect to exogenous heating
Sanz B., Calatayud M.P., Torres T.E., Fanarraga M.L., Ibarra M.R., Goya G.F.
2017 *Biomaterials* 114, pp 62-70
DOI: 10.1016/j.biomaterials.2016.11.008
IF: 8.806

64. Magnetic properties of optimized cobalt nanospheres grown by focused electron beam induced deposition (FEBID) on cantilever tips
Sangiao S., Magén C., Mofakhami D., de Loubens G., De Teresa J.M.
2017 *Beilstein Journal of Nanotechnology* 8 (1), pp 2106-2115
DOI: 10.3762/bjnano.8.210
IF: 2.968

65. Thermoelectric Skutterudite/oxide nanocomposites: Effective decoupling of electrical and thermal conductivity by functional interfaces
Moure A., Rull-Bravo M., Abad B., Del Campo A., Rojo M.M., Aguirre M.H., Jacquot A., Fernandez J.F., Martin-Gonzalez M.
2017 *Nano Energy* 31, pp 393-402
DOI: 10.1016/j.nanoen.2016.11.041
IF: 13.120

66. Magnetite as a platform material in the detection of glucose, ethanol and cholesterol Jaime J., Rangel G., Muñoz-Bonilla A., Mayoral A., Herrasti P.
2017 *Sensors and Actuators, B: Chemica*l 238, pp 693-701
DOI: 10.1016/j.snb.2016.07.059
IF: 5.667

67. In-situ preparation of ultra-small Pt nanoparticles within rod-shaped mesoporous silica particles: 3-D tomography and catalytic oxidation of n-hexane
Uson L., Hueso J.L., Sebastian V., Irusta S., Arruebo M., Santamaria J., Arenal R., Florea I.
2017 *Catalysis Communications* 100, pp 93-97
DOI: 10.1016/j.catcom.2017.06.022
IF: 3.463

68. Influence of surface coverage on the formation of 4,4'-bipyridinium (viologen) single molecular junctions
Osorio H.M., Martín S., Milan D.C., González-Orive A., Gluyas J.B.G., Higgins S.J., Low P.J., Nichols R.J., Cea P.
2017 *Journal of Materials Chemistry C* 5 (45), pp 11717-11723
DOI: 10.1039/c7tc03624h
IF: 5.976

69. On the Porous Silicate HPM-5
Jo D., Mayoral A., Hong S.B., Camblor M.A.
2017 *European Journal of Inorganic Chemistry* 2017 (19), pp 2525-2531
DOI: 10.1002/ejic.201700023
IF: 2.507

70. Single-Molecule Conductance Studies of Organometallic Complexes Bearing 3-Thienyl Contacting Groups
Bock S., Al-Owaedi O.A., Eaves S.G., Milan D.C., Lemmer M., Skelton B.W., Osorio H.M., Nichols R.J., Higgins S.J., Cea P., Long N.J., Albrecht T., Martín S., Lambert C.J., Low P.J.
2017 *Chemistry - A European Journal* 23 (9), pp 2133-2143
DOI: 10.1002/chem.201604565
IF: 5.160

71. Control of reactivity through chemical order in very small RuRe nanoparticles
Ayvali T., Fazzini P.-F., Lecante P., Mayoral A., Philippot K., Chaudret B.
2017 *Dalton Transactions* 46 (43), pp 15070-5079
DOI: 10.1039/c7dt02287e
IF: 4.099

72. Evidence of a minority monoclinic LaNiO2.5 phase in lanthanum nickelate thin films
López-Conesa L., Rebled J.M., Pesquera D., Dix N., Sánchez F., Herranz G., Fontcuberta J., Magén C., Casanove M.J., Estradé S., Peiró F.
2017 *Physical Chemistry Chemical Physics* 19 (13), pp 9137-9142
DOI: 10.1039/c7cp00902j
IF: 3.906

73. Microwave heating and the fast ADOR process for preparing zeolites
Navarro M., Morris S.A., Mayoral Á., Čejka J., Morris R.E.
2017 *Journal of Materials Chemistry* A 5 (17), pp 8037-8043
DOI: 10.1039/c7ta02344h
IF: 9.931

74. Expansion of the ADOR Strategy for the Synthesis of Zeolites: The Synthesis of IPC-12 from Zeolite UOV
Kasneryk V., Shamzhy M., Opanasenko M., Wheatley P.S., Morris S.A., Russell S.E., Mayoral A., Trachta M., Čejka J., Morris R.E.
2017 *Angewandte Chemie - International Edition* 56 (15), pp 4324-4327
DOI: 10.1002/anie.201700590
IF: 12.102

75. Tuning the separation properties of zeolitic imidazolate framework core-shell structures via post-synthetic modification
Sanchez-Lainez, J; Veiga, A; Zornoza, B; Balestra, SRG; Hamad, S; Ruiz-Salvador, AR; Calero, S; Tellez, C; Coronas, J
2017 *Journal of Materials Chemistry A* 5 (48), pp 25601-25608
DOI: 10.1039/c7ta08778k
IF: 9.931

76. A new zeolitic hydroxymethylimidazolate material and its use in mixed matrix membranes based on 6FDA-DAM for gas separation
Perea-Cachero, A; Sanchez-Lainez, J; Berenguer-Murcia, A; Cazorla-Amoros, D; Tellez, C; Coronas, J
2017 *Journal of Membrane Science* 544, pp 88-97
DOI: 10.1016/j.memsci.2017.09.009
IF: 6.578

77. Light-Emitting Photon-Upconversion Nanoparticles in the Generation of Transdermal Reactive-Oxygen Species
Prieto, M; Rwei, AY; Alejo, T; Wei, T; Lopez-Franco, MT; Mendoza, G; Sebastian, V; Kohane, DS; Arruebo, M
2017 *ACS Applied Materials & Interfaces*. 9 (48), pp 41737-41747
DOI: 10.1021/acsami.7b14812
IF: 8.097

78. Unzipping of multi-wall carbon nanotubes with different diameter distributions: Effect on few-layer graphene oxide obtention
Torres, D; Pinilla, JL; Suelves, I
2017 *Applied Surface Science* 424 (1), pp 101-110
DOI: 10.1016/j.apsusc.2017.01.273
IF: 4.439

79. Magnetically responsive biopolymeric multilayer films for local hyperthermia
Criado, M; Sanz, B; Goya, GF; Mijangos, C; Hernandez, R
2017 *Journal of Materials Chemistry B*, 5 (43), pp 8570-8578
DOI: 10.1039/c7tb02361h
IF: 4.776

80. TEMPO-oxidized cellulose nanofibers as interfacial strengthener in continuous-fiber reinforced polymer composites
Uribe, BEB; Chiromito, EMS; Carvalho, AJF; Arenal, R; Tarpani, JR
2017 *Materials & Design* 133, pp 340-348
DOI: 10.1016/j.matdes.2017.08.004
IF: 4.525

81. Effect of an active label based on benzyl isothiocyanate on the morphology and ochratoxins production of Aspergillus ochraceus
Clemente, I; Aznar, M; Nerin, C
2017 *Food Research International* 101, pp 61-72
DOI: 10.1016/j.foodres.2017.08.060
IF: 3.520

82. Ultrathin Composite Polymeric Membranes for CO2/N-2 Separation with Minimum Thickness and High CO2 Permeance
Benito, J; Sanchez-Lainez, J; Zornoza, B; Martin, S; Carta, M; Malpass-Evans, R; Tellez, C; McKeown, NB; Coronas, J; Gascon, I
2017 *Chemsuschem* 10 (20), pp 4014-4017
DOI: 10.1002/cssc.201701139
IF: 7.411

83. Covalent immobilisation of magnetic nanoparticles on surfaces via strain-promoted azide-alkyne click chemistry
Fratila, RM; Navascuez, M; Idiago-Lopez, J; Eceiza, M; Miranda, JI; Aizpurua, JM; de la Fuente, JM
2017 *New Journal of Chemistry* 41 (19), pp 10835-10840
DOI: 10.1039/c7nj01822c
IF: 3.201

84. Easy Preparation of Tannin-Based Ag Catalysts for Ethylene Epoxidation
Schaefer, S; Ramirez, A; Mallada, R; Izquierdo, MT; Santamaria, J; Celzard, A; Fierro, V
2017 *Chemistryselect* 2 (27), pp 8509-8516
DOI: 10.1002/slct.201701548
IF: 1.505

85. Positive zeta potential of nanodiamonds
Gines, L; Mandal, S; Ashek-I-Ahmed; Cheng, CL; Sow, M; Williams, OA
2017 *Nanoscale* 9 (34), pp 12549-12555
DOI: 10.1039/c7nr03200e
IF: 7.233

86. The effect of graphene nanoplatelets on the thermal and electrical properties of aluminum nitride ceramics
Simsek, ING; Nistal, A; Garcia, E; Perez-Coll, D; Miranzo, P; Osendi, MI
2017 *Journal of The European Ceramic Society* 37 (12), pp 3721-3729
DOI: 10.1016/j.jeurceramsoc.2016.12.044
IF: 3.794

87. A non-invasive optical method for mapping temperature polarization in direct contact membrane distillation
Santoro, S; Vidorreta, IM; Sebastian, V; Moro, A; Coelhoso, IM; Portugal, CAM; Lima, JC; Desiderio, G; Lombardo, G; Drioli, E; Mallada, R; Crespo, JG; Criscuoli, A; Figoli, A
2017 *Journal of Membrane Science* 536, pp 156-166
DOI: 10.1016/j.memsci.2017.05.001
IF: 6.578

88. The effect of PEGylated hollow gold nanoparticles on stem cell migration: potential application in tissue regeneration
Encabo-Berzosa, MD; Sancho-Albero, M; Crespo, A; Andreu, V; Sebastian, V; Irusta, S; Arruebo, M; Martin-Duque, P; Santamaria, J
2017 *Nanoscale* 9 (28), pp 9848-9858
DOI: 10.1039/c7nr01853c
IF: 7.233

89. Probing localized strain in solution-derived YBa2Cu3O7-delta nanocomposite thin films
Guzman, R; Gazquez, J; Mundet, B; Coll, M; Obradors, X; Puig, T
2017 *Physical Review Materials* 1 (2)
DOI: 10.1103/PhysRevMaterials.1.024801
IF: no Impact Factor assigned in 2017

90. Selective liquid-phase hydrogenation of fructose to D-mannitol over copper-supported metallic nanoparticles
Zelin, J; Meyer, CI; Regenhardt, SA; Sebastian, V; Garetto, TF; Marchi, AJ
2017 *Chemical Engineering Journal* 319, pp 48-56
DOI: 10.1016/j.cej.2017.02.127
IF: 6.735

91. Surface/interface phenomena in nano-multilayer coating under severing tribological conditions
Fox-Rabinovich, GS; Gershman, IS; Yamamoto, K; Aguirre, MH; Covelli, D; Arif, T; Aramesh, M; Shalaby, MA; Veldhuis, S
2017 *Surface and Interface Analysis* 49 (7), pp 584-593
DOI: 10.1002/sia.6196
IF: 1.263

92. Structural Contraction of Zeolitic Imidazolate Frameworks: Membrane Application on Porous Metallic Hollow Fibers for Gas Separation
Cacho-Bailo, F; Etxeberria-Benavides, M; David, O; Tellez, C; Coronas, J
2017 ACS *Applied Materials & Interfaces* 9 (24), pp 20787-20796
DOI: 10.1021/acsami.7b05497
IF: 8.097

93. Multifunctional, biocompatible and pH-responsive carbon nanotube- and graphene oxide/tectomer hybrid composites and coatings
Garriga, R; Jurewicz, I; Seyedin, S; Bardi, N; Totti, S; Matta-Domjan, B; Velliou, EG; Alkhorayef, MA; Cebolla, VL; Razal, JM; Dalton, AB; Munoz, E
2017 *Nanoscale* 9 (239), pp 7791-7804
DOI: 10.1039/c6nr09482a
IF: 7.233

94. Chiral supramolecular organization from a sheet-like achiral gel: a study of chiral photoinduction
Royes, J; Polo, V; Uriel, S; Oriol, L; Pinol, M; Tejedor, RM
2017 *Physical Chemistry Chemical Physics* 19 (21), pp 13622-13628
DOI: 10.1039/c7cp01739a
IF: 3.906

95. Bactericidal Effect of Gold-Chitosan Nanocomposites in Coculture Models of Pathogenic Bacteria and Human Macrophages
Mendoza, G; Regiel-Futyra, A; Andreu, V; Sebastian, V; Kyziol, A; Stochel, G; Arruebo, M
2017 ACS *Applied Materials & Interfaces* 9 (21), pp 17693-17701
DOI: 10.1021/acsami.6b15123
IF: 8.097

96. Simultaneous use of MOFs MIL-101(Cr) and ZIF-11 in thin film nanocomposite membranes for organic solvent nanofiltration
Echaide-Gorriz, C; Navarro, M; Tellez, C; Coronas, J
2017 *Dalton Transactions* 46 (19), pp 6244-6252
DOI: 10.1039/c7dt00197e
IF: 4.099

97. Enhancement of Growth of MOF MIL-68(Al) Thin Films on Porous Alumina Tubes Using Different Linking Agents
Perea-Cachero, A; Calvo, P; Romero, E; Tellez, C; Coronas, J
2017 *European Journal of Inorganic Chemistry* 19, pp 2532-2540
DOI: 10.1002/ejic.201700302
IF: 2.507

98. In situ temperature measurements in microwave-heated gas-solid catalytic systems. Detection of hot spots and solid-fluid temperature gradients in the ethylene epoxidation reaction
Ramirez, A; Hueso, JL; Mallada, R; Santamaria, J
2017 *Chemical Engineering Journal* 316, pp 50-60
DOI: 10.1016/j.cej.2017.01.077
IF: 6.735

99. Hierarchical Porous Polybenzimidazole Microsieves: An Efficient Architecture for Anhydrous Proton Transport via Polyionic Liquids
Kallem, P; Drobek, M; Jube, A; Vriezekolk, EJ; Mallada, R; Pina, MP
2017 ACS *Applied Materials & Interfaces* 9 (17), pp 14844-14857
DOI: 10.1021/acsami.7b01916
IF: 8.097

100. Nanostructures based on ammonium-terminated amphiphilic Janus dendrimers as camptothecin carriers with antiviral activity
Lancelot, A; Claveria-Gimeno, R; Velazquez-Campoy, A; Abian, O; Serrano, JL; Sierra, T
2017 *European Polymer Journal* 90, pp 136-149
DOI: 10.1016/j.eurpolymj.2017.03.012
IF: 3.741

101. A magnetocaloric composite based on molecular coolers and carbon nanotubes with enhanced thermal conductivity
Roubeau, O; Natividad, E; Evangelisti, M; Lorusso, G; Palacios, E
2017 *Materials Horizons* 4 (3), pp 464-476
DOI: 10.1039/c6mh00533k
IF: 13.183

102. Strong Quantum Confinement and Fast Photoemission Activation in CH3NH3PbI3 Perovskite Nanocrystals Grown within Periodically Mesostructured Films
Anaya, M; Rubino, A; Rojas, TC; Galisteo-Lopez, JF; Calvo, ME; Miguez, H
2017 *Advanced Optical Materials* 5 (8)
DOI: 10.1002/adom.201601087
IF: 7.430

103. DNA Transfection to Mesenchymal Stem Cells Using a Novel Type of Pseudodendrimer Based on 2,2-Bis(hydroxymethyl)propionic Acid
Lancelot, A; Gonzalez-Pastor, R; Concellon, A; Sierra, T; Martin-Duque, P; Serrano, JL
2017 *Bioconjugate Chemistry* 28 (4), pp 1135-1150
DOI: 10.1021/acs.bioconjchem.7b00037
IF: 4.485

104. Sequential amine functionalization inducing structural transition in an aldehyde-containing zeolitic imidazolate framework: application to gas separation membranes
Cacho-Bailo, F; Etxeberria-Benavides, M; Karvan, O; Tellez, C; Coronas, J
2017 *Crystengcomm* 19 (11), pp 1545-1554
DOI: 10.1039/c7ce00086c
IF: 3.304

105. Interplay between epitaxial strain and low dimensionality effects in a ferrimagnetic oxide
Popova, E; Deb, M; Bocher, L; Gloter, A; Stephan, O; Warot-Fonrose, B; Berini, B; Dumont, Y; Keller, N
2017 *Journal of Applied Physics* 121 (11)
DOI: 10.1063/1.4978508
IF: 2.176

106. Gas separation with mixed matrix membranes obtained from MOF UiO-66-graphite oxide hybrids
Castarlenas, S; Tellez, C; Coronas, J
2017 *Journal of Membrane Science* 526, pp 205-211
DOI: 10.1016/j.memsci.2016.12.041
IF: 6.578

107. Designing strontium titanate-based thermoelectrics: insight into defect chemistry mechanisms
Kovalevsky, AV; Aguirre, MH; Populoh, S; Patricio, SG; Ferreira, NM; Mikhalev, SM; Fagg, DP; Weidenkaff, A; Frade, JR
2017 *Journal of Materials Chemistry A*, 5 (8), pp 3909-3922
DOI: 10.1039/c6ta09860f
IF: 9.931

108. Raman spectroscopy, electronic microscopy and SPME-GC-MS to elucidate the mode of action of a new antimicrobial food packaging material
Clemente, I; Aznar, M; Salafranca, J; Nerin, C
2017 *Analytical and Bioanalytical Chemistry* 409 (4), pp 1037-1048
DOI: 10.1007/s00216-016-0022-y
IF: 3.307

109. On the molecular mechanisms for the H-2/CO2 separation performance of zeolite imidazolate framework two-layered membranes
Cacho-Bailo, F; Matito-Martos, I; Perez-Carbajo, J; Etxeberria-Benavides, M; Karvan, O; Sebastian, V; Calero, S; Tellez, C; Coronas, J
2017 *Chemical Science* 8 (1), pp 325-333
DOI: 10.1039/c6sc02411d
IF: 9.063

110. Instantaneous formation of polyoxometalate-based cerium vanadium oxide gels
Seliverstov, A; Rangus, M; Hartmann, M; Mitchell, SG; Streb, C
2017 *Inorganic Chemistry Frontiers* 4 (1), pp 160-164
DOI: 10.1039/c6qi00457a
IF: 5.106

111. Generation of subnanometric platinum with high stability during transformation of a 2D zeolite into 3D
Liu, LC; Diaz, U; Arenal, R; Agostini, G; Concepcion, P; Corma, A
2017 *Nature Materials* 16 (1), pp 132-138
DOI: 10.1038/NMAT4757
IF: 39.235

112. Solid lubricant behavior of MoS2 and WSe2-based nanocomposite coatings
Dominguez-Meister, S; Rojas, TC; Brizuela, M; Sanchez-Lopez, JC
2017 *Science and Technology of Advanced Materials* 18 (1), pp 122-133
DOI: 10.1080/14686996.2016.1275784
IF: 4.787

113. Tm on W(110): A growth study by Scanning Tunneling Microscopy.
D. Coffey, J.I. Arnaudas, D. Serrate, M. Ciria
2017 *Epitaxy*, ISBN:978-953-51-5251-4 (book chapter)

114. Nanotubes from the Misfit Compound Alloy LaS-NbxTa(1–x)S2
Stolovas, D., Serra, M., Popovitz-Biro, R., Pinkas, I., Houben, L., Calvino, J.J., Joselevich, E., Tenne, R., Arenal, R., Lajaunie, L.
2018 *Chemistry of Materials* 30 (24), pp8829-8842
DOI: 10.1021/acs.chemmater.8b03632
IF: 10.159

115. Reversible magnetic switching of high-spin molecules on a giant Rashba surface
Kügel, J., Karolak, M., Krönlein, A., Serrate, D., Bode, M., Sangiovanni, G.
2018 *npj Quantum Materials* 3 (1) 53
DOI: 10.1038/s41535-018-0126-z
IF: no Impact Factor assigned in 2018

116. Jahn-Teller Splitting in Single Adsorbed Molecules Revealed by Isospin-Flip Excitations
Kügel, J., Hsu, P.-J., Böhme, M., Schneider, K., Senkpiel, J., Serrate, D., Bode, M., Lorente, N.
2018 *Physical Review Letters* 121 (22) 226402
DOI: 10.1103/PhysRevLett.121.226402
IF: 9.227

117. Interfacing Transition Metal Dichalcogenides with Carbon Nanodots for Managing Photoinduced Energy and Charge-Transfer Processes
Vallan, L., Canton-Vitoria, R., Gobeze, H.B., Jang, Y., Arenal, R., Benito, A.M., Maser, W.K., D'Souza, F., Tagmatarchis, N.
2018 *Journal of the American Chemical Society* 140 (41), pp 13488-13496
DOI: 10.1021/jacs.8b09204
IF: 14.695

118. Three-Dimensional Branched and Faceted Gold–Ruthenium Nanoparticles: Using Nanostructure to Improve Stability in Oxygen Evolution Electrocatalysis
Gloag, L., Benedetti, T.M., Cheong, S., Li, Y., Chan, X.-H., Lacroix, L.-M., Chang, S.L.Y., Arenal, R., Florea, I., Barron, H., Barnard, A.S., Henning, A.M., Zhao, C., Schuhmann, W., Gooding, J.J., Tilley, R.D.
2018 *Angewandte Chemie - International Edition* 57 (32), pp 10241-10245
DOI: 10.1002/anie.201806300
IF: 12.257

119. Optoelectronic properties of calcium cobalt oxide misfit nanotubes
Lajaunie, L., Ramasubramaniam, A., Panchakarla, L.S., Arenal, R.
2018 *Applied Physics Letters* 113 (3) 31102
DOI: 10.1063/1.5043544
IF: 3.521

120. Functional Hybrid Nanopaper by Assembling Nanofibers of Cellulose and Sepiolite
González del Campo, M.M., Darder, M., Aranda, P., Akkari, M., Huttel, Y., Mayoral, A., Bettini, J., Ruiz-Hitzky, E.
2018 *Advanced Functional Materials* 2 (27) 1703048
DOI: 10.1002/adfm.201703048
IF: 15.621

121. Quantifying the leading role of the surface state in the Kondo effect of Co/Ag(111)
Moro-Lagares, M., Fernández, J., Roura-Bas, P., Ibarra, M.R., Aligia, A.A., Serrate, D.
2018 *Physical Review B* 97 (23) 235442
DOI: 10.1103/PhysRevB.97.235442
IF: 3.736

122. Enhanced thermo-spin effects in iron-oxide/metal multilayers
Ramos, R., Lucas, I., Algarabel, P.A., Morellón, L., Uchida, K., Saitoh, E., Ibarra, M.R.
2018 *Journal of Physics D: Applied Physics* 51 (22) 224003
DOI: 10.1088/1361-6463/aabedb
IF: 2.829

123. Evidence of the spin Seebeck effect in Ni-Zn ferrites polycrystalline slabs
Arboleda, J.D., Arnache, O., Aguirre, M.H., Ramos, R., Anadón, A., Ibarra, M.R.
2018 *Solid State Communications* 270 (140) 146
DOI: 10.1016/j.ssc.2017.12.002
IF: 1.433

124. Purified and Crystalline Three-Dimensional Electron-Beam-Induced Deposits: The Successful Case of Cobalt for High-Performance Magnetic Nanowires
Pablo-Navarro, J., Magén, C., De Teresa, J.M.
2018 *ACS Applied Nano Materials* 1 (1), pp 38-46
DOI: 10.1021/acsanm.7b00016
IF: no Impact Factor assigned in 2018

125. Quaternary Chalcogenide-Based Misfit Nanotubes LnS(Se)-TaS(Se)2 (Ln = La, Ce, Nd, and Ho): Synthesis and Atomic Structural Studies
Lajaunie, L., Radovsky, G., Tenne, R., Arenal, R.
2018 *Inorganic Chemistry* 57 (2), pp 747-753
DOI: 10.1021/acs.inorgchem.7b02680
IF: 4.850

126. Tuning the interfacial charge, orbital, and spin polarization properties in La0.67Sr0.33MnO3/La1−xSrxMnO3 bilayers
Carreira, S.J., Aguirre, M.H., Briatico, J., Weschke, E., Steren, L.B.
2018 *Applied Physics Letters* 112 (3) 32401
DOI: 10.1063/1.5011172
IF: 3.521

127. Molecular basis for the integration of environmental signals by furb from anabaena sp. PCC 7120
Sein-Echaluce, V.C., Pallarés, M.C., Lostao, A., Yruela, I., Velázquez-Campoy, A., Luisa Peleato, M., Fillat, M.F.
2018 *Biochemical Journal* 475 (1), pp 151-168
DOI: 10.1042/BCJ20170692
IF: 4.331

128. Growth and structural characterization of strained epitaxial H f0.5 Z r0.5 O2 thin films
Torrejón, L., Langenberg, E., Magén, C., Larrea, Á., Blasco, J., Santiso, J., Algarabel, P.A., Pardo, J.A.
2018 *Physical Review Materials* 2 (1) 13401
DOI: 10.1103/PhysRevMaterials.2.013401
IF: 2.926

129. Effect of the paramagnetic to spin-glass phase transition on the fundamental absorption edge of MnIn2Se4magnetic semiconducting compound
Sagredo, V., Torres, T.E., Delgado, G.E., Rincón, C.
2018 *Revista Mexicana de Física* 65 (1), pp 14-19
DOI: 10.31349/REVMEXFIS.65.14
IF: no Impact Factor assigned in 2018

130. Electric polarization switching in an atomically thin binary rock salt structure
Martinez-Castro, J., Piantek, M., Schubert, S., Persson, M., Serrate, D., Hirjibehedin, C.F.
2018 *Nature Nanotechnology* 13 (1), pp 19-23
DOI: 10.1038/s41565-017-0001-2
IF: 33.407

131. Plasmonic properties of an Ag@Ag2Mo2O7 hybrid nanostructure easily designed by solid-state photodeposition from very thin Ag2Mo2O7 nanowires
Hakouk, K., Lajaunie, L., El Bekkachi, H., Serier-Brault, H., Humbert, B., Arenal, R., Dessapt, R.
2018 *Journal of Materials Chemistry C* 6 (41), pp 11086-11095
DOI: 10.1039/c8tc03170c
IF: 6.641

132. Epitaxial La 0.7 Sr 0.3 MnO 3 thin films on silicon with excellent magnetic and electric properties by combining physical and chemical methods
Vila-Fungueiriño J.M., Gázquez J., Magén C., Saint-Girons G., Bachelet R., Carretero-Genevrier A.
2018 *Science and Technology of Advanced Materials* 19 (1). pp 702-710
DOI: 10.1080/14686996.2018.1520590
IF: 3.585

133. NanoSQUID Magnetometry on Individual As-grown and Annealed Co Nanowires at Variable Temperature
Martínez-Pérez M.J., Pablo-Navarro J., Müller B., Kleiner R., Magén C., Koelle D., De Teresa J.M., Sesé J.
2018 *Nano Letters* 18 (12), pp 7674-7682
DOI: 10.1021/acs.nanolett.8b03329
IF: 12.279

134. Magnetic Shape Memory Turns to Nano: Microstructure Controlled Actuation of Free-Standing Nanodisks
Campanini M., Nasi L., Fabbrici S., Casoli F., Celegato F., Barrera G., Chiesi V., Bedogni E., Magén C., Grillo V., Bertoni G., Righi L., Tiberto P., Albertini F.
2018 *Small* 14 (49), 1803027
DOI: 10.1002/smll.201803027
IF: 10.856

135. Complex behavior of nano-scale tribo-ceramic films in adaptive PVD coatings under extreme tribological conditions
Fox-Rabinovich G., Kovalev A., Gershman I., Wainstein D., Aguirre M.H., Covelli D., Paiva J., Yamamoto K., Veldhuis S
2018 *Entropy* 20 (12), 989
DOI: 10.3390/e20120989
IF: 2.419

136. Direct and converse piezoelectric responses at the nanoscale from epitaxial BiFeO 3 thin films grown by polymer assisted deposition

Vila-Fungueiriño J.M., Gómez A., Antoja-Lleonart J., Gázquez J., Magén C., Noheda B., Carretero-Genevrier A.

2018 *Nanoscale* 10 (43), pp 20155-20161

DOI: 10.1039/c8nr05737k

IF: 6.970

137. Stabilization of Nanoparticles Produced by Hydrogenation of Palladium-N-Heterocyclic Carbene Complexes on the Surface of Graphene and Implications in Catalysis

Mollar-Cuni A., Ventura-Espinosa D., Martín S., Mayoral Á., Borja P., Mata J.A.

2018 *ACS Omega* 3 (811), pp 15217-15228

DOI: 10.1021/acsomega.8b02193

IF: 2.584

138. Zeolite framework functionalisation by tuneable incorporation of various metals into the IPC-2 zeolite

Mazur M., Kasneryk V., Přech J., Brivio F., Ochoa-Hernández C., Mayoral A., Kubu M., Čejka J.

2018 *Inorganic Chemistry Frontiers* 5 (11), pp 2746-2755

DOI: 10.1039/c8qi00732b

IF: 5.934

139. Crystal structure and local ordering in epitaxial Fe100−xGax/MgO(001) films

Ciria M., Proietti M.G., Corredor E.C., Coffey D., Begué A., Fuente C.D.L., Arnaudas J.I., Ibarra A.

2018 *Journal of Alloys and Compounds* 767, pp 905-914

DOI: 10.1039/c8qi00732b

IF: 4.175

140. Ultrathin Gold Nanowires with the Polytetrahedral Structure of Bulk Manganese

Vargas J.A., Petkov V., Nouh E.S.A., Ramamoorthy R.K., Lacroix L.-M., Poteau R., Viau G., Lecante P., Arenal R.

2018 *ACS Nano* 12 (9), pp 9521-9531

DOI: 10.1021/acsnano.8b05036

IF: 13.903

141. Unconventional Single-Molecule Conductance Behavior for a New Heterocyclic Anchoring Group: Pyrazolyl
Herrer I.L., Ismael A.K., Milán D.C., Vezzoli A., Martín S., González-Orive A., Grace I., Lambert C., Serrano J.L., Nichols R.J., Cea P.
2018 *Journal of Physical Chemistry Letters* 9 (1)8, pp5364-5372
DOI: 10.1021/acs.jpclett.8b02051
IF: 7.329

142. Selective catalytic cracking of n-hexane to olefins over SSZ-54 fabricated by facile and novel dual templating method
Lateef S.A., Bakare I.A., Mayoral A., Sebastian V., Muraza O.
2018 *Fuel* 227, pp 48- 58
DOI: 10.1016/j.fuel.2018.03.161
IF: 5.128

143. Hybrid TiO2-Graphene nanoribbon photoanodes to improve the photoconversion efficiency of dye sensitized solar cells
Akilimali R., Selopal G.S., Benetti D., Serrano-Esparza I., Algarabel P.A., De Teresa J.M., Wang Z.M., Stansfield B., Zhao H., Rosei F.
2018 *Journal of Power Sources* 396, pp 566-573
DOI: 10.1016/j.jpowsour.2018.06.044
IF: 7.467

144. Towards molecular electronic devices based on 'all-carbon' wires
Moneo A., González-Orive A., Bock S., Fenero M., Herrer I.L., Milan D.C., Lorenzoni M., Nichols R.J., Cea P., Perez-Murano F., Low P.J., Martin S.
2018 *Nanoscale* 10 (29), pp 14128-14138
DOI: 10.1039/c8nr02347f
IF: 6.970

145. Development and properties of high thermal conductivity molybdenum carbide - graphite composites
Guardia-Valenzuela J., Bertarelli A., Carra F., Mariani N., Bizzaro S., Arenal R.
2018 *Carbon* 135, pp 72-84
DOI: 10.1016/j.carbon.2018.04.010
IF: 7.466

146. M-SrFe12O19 and ferrihydrite-like ultrathin nanoplatelets as building blocks for permanent magnets: HAADF-STEM study and magnetic properties
Grindi B., BenAli A., Magen C., Viau G.
2018 *Journal of Solid State Chemistry* (264), pp 124-133
DOI: 10.1016/j.jssc.2018.05.015
IF: 2.291

147. Breaking the Nd3+-sensitized upconversion nanoparticles myth about the need of onion-layered structures
Estebanez N., Ferrera-González J., Francés-Soriano L., Arenal R., González-Béjar M., Pérez-Prieto J.
2018 *Nanoscale* 10 (26,) pp 12297-12301
DOI: 10.1039/c8nr00871j
IF: 6.970

148. Fluorescent Polymer—Single-Walled Carbon Nanotube Complexes with Charged and Noncharged Dendronized Perylene Bisimides for Bioimaging Studies
Huth K., Glaeske M., Achazi K., Gordeev G., Kumar S., Arenal R., Sharma S.K., Adeli M., Setaro A., Reich S., Haag R.
2018 *Small* 14 (28), 1800796
DOI: 10.1002/smll.201800796
IF: 10.856

149. Gold nanoclusters prepared from an eighteenth century two-phases procedure supported on thiol-containing SBA-15 for liquid phase oxidation of cyclohexene with molecular oxygen
Agundez J., Martin L., Mayoral A., Pérez-Pariente J.
2018 *Catalysis Today* 304, pp 172-180
DOI: 10.1016/j.cattod.2017.09.045
IF: 4.888

150. Chemical and structural analysis of sub-20 nm graphene patterns generated by scanning probe lithography
Dago A.I., Sangiao S., Fernández-Pacheco R., De Teresa J.M., Garcia R.
2018 *Carbon* 129, pp 281-285
DOI: 10.1016/j.carbon.2017.12.033
IF: 7.466

151. Understanding the role of Ti-rich domains in the stabilization of gold nanoparticles on mesoporous silica-based catalysts
Moragues A., Puértolas B., Mayoral Á., Arenal R., Hungría A.B., Murcia-Mascarós S., Taylor S.H., Solsona B., García T., Amorós P.
2018 Journal of Catalysis 360, pp 187-200
DOI: 10.1016/j.jcat.2018.02.003
IF: 7.723

152. Block copolymer based novel magnetic mixed matrix membranes-magnetic modulation of water permeation by irreversible structural changes
Upadhyaya L., Semsarilar M., Quémener D., Fernández-Pacheco R., Martinez G., Mallada R., Coelhoso I.M., Portugal C.A.M., Crespo J.G.
2018 *Journal of Membrane Science* 551, pp273-282
DOI: 10.1016/j.memsci.2018.01.032
IF: 7.015

153. Air-Stable Anisotropic Monocrystalline Nickel Nanowires Characterized Using Electron Holography
Drisko G.L., Gatel C., Fazzini P.-F., Ibarra A., Mourdikoudis S., Bley V., Fajerwerg K., Fau P., Kahn M.
2018 *Nano Letters* 18 (3), pp 1733-1738
DOI: 10.1021/acs.nanolett.7b04791
IF: 12.279

154. Vertical Growth of Superconducting Crystalline Hollow Nanowires by He+ Focused Ion Beam Induced Deposition
Córdoba R., Ibarra A., Mailly D., De Teresa J.M.
2018 *Nano Letters* 18 (2), pp 1379-13869
DOI: 10.1021/acs.nanolett.7b05103
IF: 12.279

155. Improvement of wear performance of nano-multilayer PVD coatings under dry hard end milling conditions based on their architectural development
Chowdhury S., Beake B.D., Yamamoto K., Bose B., Aguirre M., Fox-Rabinovich G.S., Veldhuis S.C.
2018 *Coatings* 8 (2) 59
DOI: 10.3390/coatings8020059
IF: 2.330

156. Synthesis of hybrid magneto-plasmonic nanoparticles with potential use in photoacoustic detection of circulating tumor cells
Ovejero J.G., Yoon S.J., Li J., Mayoral A., Gao X., O'Donnell M., García M.A., Herrasti P., Hernando A.
2018 *Microchimica Acta* 185 (2) 130
DOI: 10.1007/s00604-017-2637-x
IF: 5.479

157. Transmission XMCD-PEEM imaging of an engineered vertical FEBID cobalt nanowire with a domain wall
Wartelle A., Pablo-Navarro J., Staňo M., Bochmann S., Pairis S., Rioult M., Thirion C., Belkhou R., Teresa J.M.D., Magén C., Fruchart O.
2018 *Nanotechnology* 29 (4) 45704
DOI: 10.1088/1361-6528/aa9eff
IF: 3.399

158. 2D magnetic domain wall ratchet: The limit of submicrometric holes
Herrero-Albillos J., Castán-Guerrero C., Valdés-Bango F., Bartolomé J., Bartolomé F., Kronast F., Hierro-Rodriguez A., Álvarez Prado L.M., Martín J.I., Vélez M., Alameda J.M., Sesé J., García L.M.
2018 *Materials and Design* 138, pp 111-118
DOI: 10.1016/j.matdes.2017.09.060
IF: 5.770

159. Base-free selective oxidation of pectin derived galacturonic acid to galactaric acid using supported gold catalysts
Pazhavelikkakath Purushothaman R.K., Klis F.V.D., Frissen A.E., Haveren J.V., Mayoral A., Van Der Bent A., Van Es D.S.
2018 *Green Chemistry* 20 (12), pp 2763-2774
DOI: 10.1039/c8gc00103k
IF: 9.405

160. Luminescent mesoporous nanorods as photocatalytic enzyme-like peroxidase surrogates
Ortega-Liebana M.C., Hueso J., Fernandez-Pacheco R., Irusta S., Santamaria J.
2018 *Chemical Science* 9 (40), pp 7766-7778
DOI: 10.1039/c8sc03112f
IF: 9.556

161. Synthesis of zeolite A using raw kaolin from Ethiopia and its application in removal of Cr(III) from tannery wastewater
Ayele L., Pérez E., Mayoral Á., Chebude Y., Díaz I.
2018 *Journal of Chemical Technology and Biotechnology* 93 (1), pp 146-154
DOI: 10.1002/jctb.5334
IF: 2.659

162. Pillaring of layered zeolite precursors with ferrierite topology leading to unusual molecular sieves on the micro/mesoporous border
Roth W.J., Gil B., Mayoral A., Grzybek J., Korzeniowska A., Kubu M., Makowski W., Čejka J., Olejniczak Z., Mazur M.
2018 *Dalton Transactions* 47 (9), pp 3029-3037
DOI: 10.1039/c7dt03718j
IF: 4.052

163. Carbon nanofiber supported Mo2C catalysts for hydrodeoxygenation of guaiacol: The importance of the carburization process
Ochoa, E; Torres, D; Moreira, R; Pinilla, JL; Suelves, I
2018 *Applied Catalysis B-Environmental* 239, pp 463- 474
DOI: 10.1016/j.apcatb.2018.08.043
IF: 14.229

164. Hydrogen Separation at High Temperature with Dense and Asymmetric Membranes Based on PIM-EA(H-2)-TB/PBI Blends
Sanchez-Lainez, J; Zornoza, B; Carta, M; Malpass-Evans, R; McKeown, NB; Tellez, C; Coronas, J
2018 Industrial & Engineering Chemistry Research 57 (49), pp 16909-16916
DOI: 10.1021/acs.iecr.8b04209
IF: 3.375

165. Creation of Superhydrophobic and Superhydrophilic Surfaces on ABS Employing a Nanosecond Laser
Lavieja, C; Oriol, L; Pena, JI
2018 *Materials* 11 (12) 2547
DOI: 10.3390/ma11122547
IF: 2.972

166. Polymeric electrospun scaffolds for bone morphogenetic protein 2 delivery in bone tissue engineering
Aragon, J; Salerno, S; De Bartolo, L; Irusta, S; Mendoza, G
2018 *Journal of Colloid and Interface Science* 531, pp 126-137
DOI: 10.1016/j.jcis.2018.07.029
IF: 6.361

167. Tuning the activity of Cu-containing rare earth oxide catalysts for CO oxidation reaction: Cooling while heating paradigm in microwave-assisted synthesis
AlKetbi, M; Polychronopoulou, K; Zedan, AF; Sebastian, V; Baker, MA; AlKhoori, A; Jaoude, MA; Alnuaimi, O; Hinder, SS; Tharalekshmy, A; Allaber, AS
2018 *Materials Research Bulletin* 108, pp 142-150
DOI: 10.1016/j.materresbull.2018.08.045
IF: 3.355

168. Homogeneous thin coatings of zeolitic imidazolate frameworks prepared on quartz crystal sensors for CO2 adsorption
Sarango, L; Benito, J; Gascon, I; Zornoza, B; Coronas, J
2018 *Microporous and Mesoporous Materials* 272, pp 44-52
DOI: 10.1016/j.micromeso.2018.06.018
IF: 4.182

169. High-temperature oxidation of CrAlYN coatings: Implications of the presence of Y and type of steel
Rojas, TC; Dominguez-Meister, S; Brizuela, M; Sanchez-Lopez, JC
2018 *Surface & Coatings Technology* 354, pp 203-213
DOI: 10.1016/j.surfcoat.2018.09.020
IF: 3.192

170. Enzyme structure and function protection from gastrointestinal degradation using enteric coatings
Gracia, R; Yus, C; Abian, O; Mendoza, G; Irusta, S; Sebastian, V; Andreu, V; Arruebo, M
2018 *International Journal of Biological Macromolecules* 119, pp 413-422
DOI: 10.1016/j.ijbiomac.2018.07.143
IF: 4.784

171. Tailoring the structural and magnetic properties of Co-Zn nanosized ferrites for hyperthermia applications
Gomez-Polo, C; Recarte, V; Cervera, L; Beato-Lopez, JJ; Lopez-Garcia, J; Rodriguez-Velamazan, JA; Ugarte, MD; Mendonca, EC; Duque, JGS
2018 *Journal of Magnetism and Magnetic Materials*, 465, pp 211-219
DOI: 10.1016/j.jmmm.2018.05.051
IF: 2.683

172. Effect of epitaxial strain and vacancies on the ferroelectric-like response of CaTiO3 thin films
Sarantopoulos, A; Ong, WL; Malen, JA; Rivadulla, F
2018 *Applied Physics Letters* 113 (18)
DOI: 10.1063/1.5053857
IF: 3.521

173. Laser-Assisted Production of Carbon-Encapsulated Pt-Co Alloy Nanoparticles for Preferential Oxidation of Carbon Monoxide
Martinez, G; Malumbres, A; Lopez, A; Mallada, R; Hueso, JL; Santamaria, J
2018 *Frontiers in Chemistry* 6
DOI: 10.3389/fchem.2018.00487
IF: 3.782

174. Unvealing GaN Polytypism in Distributed GaN/InAlN Bragg Reflectors Through HRTEM Image Simulation
Lopez-Conesa, L; Perez-Omil, JA; Gacevic, Z; Calleja, E; Estrade, S; Peiro, F
2018 *Physica Status Solidi A-Applications and Materials Science* 215 (19)
DOI: 10.1002/pssa.201800218
IF: 1.606

175. Ultrapermeable Thin Film ZIF-8/Polyamide Membrane for H-2/CO2 Separation at High Temperature without Using Sweep Gas
Sanchez-Lainez, J; Paseta, L; Navarro, M; Zornoza, B; Tellez, C; Coronas, J
2018 *Advanced Materials Interfaces* 5 (19)
DOI: 10.1002/admi.201800647
IF: 4.713

176. Coercivity enhancement in heavy rare earth-free NdFeB magnets by grain boundary diffusion process
Salazar, D; Martin-Cid, A; Madugundo, R; Barandiaran, JM; Hadjipanayis, GC
2018 *Applied Physics Letters* 113 (15)
DOI: 10.1063/1.5043389
IF: 3.521

177. Highly Bi-doped Cu thin films with large spin-mixing conductance
Ruiz-Gomez, S; Serrano, A; Guerrero, R; Munoz, M; Lucas, I; Foerster, M; Aballe, L; Marco, JF; Amado, M; McKenzie-Sell, L; di Bernardo, A; Robinson, JWA; Barrio, MAG; Mascaraque, A; Perez, L
2018 *Apl Materials* 6 (10)
DOI: 10.1063/1.5049944
IF: 4.296

178. Azolla-derived hierarchical nanoporous carbons: From environmental concerns to industrial opportunities
Emrooz, HBM; Maleki, M; Rahmani, A
2018 *Journal of The Taiwan Institute of Chemical Engineers* 91, pp 281-290
DOI: 10.1016/j.jtice.2018.05.027
IF: 3.834

179. Asymmetric polybenzimidazole membranes with thin selective skin layer containing ZIF-8 for H-2/CO2 separation at pre-combustion capture conditions
Sanchez-Lainez, J; Zornoza, B; Tellez, C; Coronas, J
2018 *Journal of Membrane Science* 563, pp 427-434
DOI: 10.1016/j.memsci.2018.06.009
IF: 7.015

180. Epitaxial La0.7Sr0.3MnO3 thin films on silicon with excellent magnetic and electric properties by combining physical and chemical methods
Vila-Fungueirino, JM; Gazquez, J; Magen, C; Saint-Girons, G; Bachelet, R; Carretero-Genevrier, A
2018 *Science and Technology of Advanced* 19 (1), pp 702-710
DOI: 10.1080/14686996.2018.1520590
IF: 3.585

181. Successful encapsulation of beta-glucosidase during the synthesis of siliceous mesostructured materials
Gascon, V; Marquez-Alvarez, C; Blanco, RM
2018 *Journal of Chemical Technology and Biotechnology* 93 (9), pp 2625-2634
DOI: 10.1002/jctb.5616
IF: 2.659

182. Reduced graphene oxide-coated magnetic-nanoparticles as sorbent for the determination of phthalates in environmental samples by micro-dispersive solid-phase extraction followed by ultra-high-performance liquid chromatography tandem mass spectrometry
Santana-Mayor, A; Socas-Rodriguez, B; Afonso, MD; Palenzuela-Lopez, JA; Rodriguez-Delgado, MA
2018 *Journal of Chromatography A* 1565, pp 36-47
DOI: 10.1016/j.chroma.2018.06.031
IF: 3.858

183. PEG-copolymer-coated iron oxide nanoparticles that avoid the reticuloendothelial system and act as kidney MRI contrast agents
Gomez-Vallejo, V; Puigivila, M; Plaza-Garcia, S; Szczupak, B; Pinol, R; Murillo, JL; Sorribas, V; Lou, G; Veintemillas, S; Ramos-Cabrer, P; Llop, J; Millan, A
2018 *Nanoscale* 10 (29), pp 14153-14164
DOI: 10.1039/c8nr03084g
IF: 6.970

184. Functionalization of Silver Nanowire Transparent Electrodes with Self-Assembled 2-Dimensional Tectomer Nanosheets
Jurewicz, I; Garriga, R; Large, MJ; Burn, J; Bardi, N; King, AAK; Velliou, EG; Watts, JF; Hinder, SJ; Munoz, E; Dalton, AB
2018 ACS *Applied Nano Materials* 1 (8), pp 3903-3912
DOI: 10.1021/acsanm.8b00689
IF: no Impact Factor assigned in 2018

185. Hybrid Noble-Metals/Metal-Oxide Bifunctional Nano-Heterostructure Displaying Outperforming Gas-Sensing and Photochromic Performances
Tobaldi, DM; Leonardi, SG; Movlaee, K; Lajaunie, L; Seabra, MP; Arena, R; Neri, G; Labrincha, JA
2018 *ACS Omega* 3 (8), pp 9846-9859
DOI: 10.1021/acsomega.8b01508
IF: 2.584

186. A Porphyrin Spin Qubit and Its 2D Framework Nanosheets
Urtizberea, A; Natividad, E; Alonso, PJ; Andres, MA; Gascon, I; Goldmann, M; Roubeau, O
2018 *Advanced Functional Materials* 28 (31)
DOI: 10.1002/adfm.201801695
IF: 15.621

187. CO-, Cu- and Fe-Doped Ni/Al2O3 Catalysts for the Catalytic Decomposition of Methane into Hydrogen and Carbon Nanofibers
Torres, D; Pinilla, JL; Suelves, I
2018 *Catalysts* 8 (8)
DOI: 10.3390/catal8080300
IF: 3.444

188. Synthesis of ZIF-93/11 Hybrid Nanoparticles via Post-Synthetic Modification of ZIF-93 and Their Use for H-2/CO2 Separation
Sanchez-Lainez, J; Zornoza, B; Orsi, AF; Lozinska, MM; Dawson, DM; Ashbrook, SE; Francis, SM; Wright, PA; Benoit, V; Llewellyn, PL; Tellez, C; Coronas, J
2018 *Chemistry-A European Journal* 24 (43), pp 11211-11219
DOI: 10.1002/chem.201802124
IF: 5.160

189. Enhanced gas separation performance of 6FDA-DAM based mixed matrix membranes by incorporating MOF UiO-66 and its derivatives
Ahmad, MZ; Navarro, M; Lhotka, M; Zornoza, B; Tellez, C; de Vos, WM; Benes, NE; Konnertz, NM; Visser, T; Semino, R; Maurin, G; Fila, V; Coronas, J
2018 *Journal of Membrane Science* 558, pp 64-77
DOI: 10.1016/j.memsci.2018.04.040
IF: 7.015

190. Polymer-Stabilized Percolation Membranes Based on Nanosized Zeolitic Imidazolate Frameworks for H-2/CO2 Separation
Sanchez-Lainez, J; Friebe, S; Zornoza, B; Mundstock, A; Strauss, I; Tellez, C; Caro, J; Coronas, J
2018 *ChemNanoMat* 4 (7), pp 698-703
DOI: 10.1002/cnma.201800126
IF: 3.379

191. Defect landscape and electrical properties in solution-derived LaNiO3 and NdNiO3 epitaxial thin films
Mundet, B; Jareno, J; Gazquez, J; Varela, M; Obradors, X; Puig, T
2018 *Physical Review Materials* 2 (6)
DOI: 10.1103/PhysRevMaterials.2.063607
IF: 2.926

192. Magnetic separation and high reusability of chloroperoxidase entrapped in multi polysaccharide micro-supports
Garcia-Embid, S; Di Renzo, F; De Matteis, L; Spreti, N; de la Fuente, JM
2018 *Applied Catalysis A-General* 560, pp 94-102
DOI: 10.1016/j.apcata.2018.04.029
IF: 4.630

193. Cationic poly(ester amide) dendrimers: alluring materials for biomedical applications
Lancelot, A; Gonzalez-Pastor, R; Claveria-Gimeno, R; Romero, P; Abian, O; Martin-Duque, P; Serrano, JL; Sierra, T
2018 *Journal of Materials Chemistry B* 6 (23), pp 3956-3968
DOI: 10.1039/c8tb00639c
IF: 5.047

194. Synthesis and characterization of CdS/MIL-125 (Ti) as a photocatalyst for water splitting
Rahmani, A; Emrooz, HBM; Abedi, S; Morsali, A
2018 *Materials Science in Semiconductor Processing* 80, pp 44-51
DOI: 10.1016/j.mssp.2018.02.013
IF: 2.722

195. Screening of Ni-Cu bimetallic catalysts for hydrogen and carbon nanofilaments production via catalytic decomposition of methane
Torres, D; Pinilla, JL; Suelves, I
2018 *Applied Catalysis A-General* 559, pp 10-19
DOI: 10.1016/j.apcata.2018.04.011
IF: 4.630

196. New active formulations against M. tuberculosis: Bedaquiline encapsulation in lipid nanoparticles and chitosan nanocapsules
De Matteis, L; Jary, D; Lucia, A; Garcia-Embid, S; Serrano-Sevilla, I; Perez, D; Ainsa, JA; Navarro, FP; de la Fuente, JM
2018 *Chemical Engineering Journal* 340, pp 181-191
DOI: 10.1016/j.cej.2017.12.110
IF: 8.355

197. Effect of the polymer architecture on the photoinduction of stable chiral organizations
Royes, J; Nogales, A; Ezquerra, TA; Oriol, L; Tejedor, RM; Pinol, M
2018 *Polymer* 143, pp 58-68
DOI: 10.1016/j.polymer.2018.03.064
IF: 3.771

198. Coaxial nanowires as plasmon-mediated remote nanosensors
Funes-Hernando, D; Pelaez-Fernandez, M; Winterauer, D; Mevellec, JY; Arenal, R; Batten, T; Humbert, B; Duvail, JL
2018 *Nanoscale* 10 (14), pp 6437-6444
DOI: 10.1039/c8nr00125a
IF: 6.970

199. Percolating Metallic Structures Templated on Laser-Deposited Carbon Nanofoams Derived from Graphene Oxide: Applications in Humidity Sensing
Nufer, S; Fantanas, D; Ogilviec, SP; Large, MJ; Winterauer, DJ; Salvage, JP; Meloni, M; King, AAK; Schellenberger, P; Shmeliov, A; Victor-Roman, S; Pelaez-Fernandez, M; Nicolosi, V; Arenal, R; Benito, AM; Maser, W; Brunton, A; Dalton, AB
2018 *ACS Applied Nano Materials* 1 (4), pp 1828-1835
DOI: 10.1021/acsanm.8b00246
IF: no Impact Factor assigned in 2018

200. Controlled deposition of MOFs by dip-coating in thin film nanocomposite membranes for organic solvent nanofiltration
Sarango, L; Paseta, L; Navarro, M; Zornoza, B; Coronas, J
2018 *Journal of Industrial and Engineering Chemistry* 59, pp 8-16
DOI: 10.1016/j.jiec.2017.09.053
IF: 4.978

201. Catalytic removal of chlorinated compounds over ordered mesoporous cobalt oxides synthesised by hard-templating
Gonzalez-Prior, J; Lopez-Fonseca, R; Gutierrez-Ortiz, JI; de Rivas, B
2018 *Applied Catalysis B-Environmental* 222 pp 9-17
DOI: 10.1016/j.apcatb.2017.09.050
IF: 14.229

202. Near infrared dye-labelled polymeric micro- and nanomaterials: in vivo imaging and evaluation of their local persistence
Mendoza, G; de Solorzano, IO; Pintre, I; Garcia-Salinas, S; Sebastian, V; Andreu, V; Gimeno, M; Arruebo, M
2018 *Nanoscale*, 10 (6), pp 2970-2982
DOI: 10.1039/c7nr07345c
IF: 6.970

203. Enhancement of CO2/CH4 separation performances of 6FDA-based co-polyimides mixed matrix membranes embedded with UiO-66 nanoparticles
Ahmad, MZ; Navarro, M; Lhotka, M; Zornoza, B; Tellez, C; Fila, V; Coronas, J
2018 *Separation and Purification Technology* 192, pp 465-474
DOI: 10.1016/j.seppur.2017.10.039
IF: 5.107

204. Core/Shell Nanoparticles of Non-Stoichiometric Zn-Mn and Zn-Co Ferrites as Thermosensitive Heat Sources for Magnetic Fluid Hyperthermia
Pilati, V; Gomes, RC; Gomide, G; Coppola, P; Silva, FG; Paula, FLO; Perzynski, R; Goya, GF; Aquino, R; Depeyrot, J
2018 *Journal of Physical Chemistry C*, 122 (5), pp 3028-3038
DOI: 10.1021/acs.jpcc.7b11014
IF: 4.309

205. Evolution and stabilization of subnanometric metal species in confined space by in situ TEM
Liu, LC; Zakharov, DN; Arenal, R; Concepcion, P; Stach, EA; Corma, A
2018 *Nature Communications* 9
DOI: 10.1038/s41467-018-03012-6
IF: 11.878

206. Probing the variability in oxidation states of magnetite nanoparticles by single-particle spectroscopy
Rodriguez, AF; Moya, C; Escoda-Torroella, M; Romero, A; Labarta, A; Batlle, X
2018 *Journal of Materials Chemistry C* 6 (4), pp 875-882
DOI: 10.1039/c7tc03010j
IF: 6.641

207. Insight into the reversible structural crystalline-state transformation from MIL-53(Al) to MIL-68(Al)
Perea-Cachero, A; Romero, E; Tellez, C; Coronas, J
2018 *Crystengcomm* 20 (4), pp 402-406
DOI: 10.1039/c7ce02034a
IF: 3.382

208. Thin-Film Nanocomposite Membrane with the Minimum Amount of MOF by the Langmuir-Schaefer Technique for Nanofiltration
Navarro, M; Benito, J; Paseta, L; Gascon, I; Coronas, J; Tellez, C
2018 *ACS Applied Materials & Interfaces* 10 (1), pp 1278-1287
DOI: 10.1021/acsami.7b17477
IF: 8.456

209. Highly efficient and selective extraction of uranium from aqueous solution using a magnetic device: succinyl-beta-cyclodextrin-APTES@maghemite nanoparticles
Helal, AS; Mazario, E; Mayoral, A; Decorse, P; Losno, R; Lion, C; Ammar, S; Hemadi, M
2018 *Environmental Science-Nano* 5 (1), pp 158-168
DOI: 10.1039/c7en00902j
IF: 7.704

210. Microfluidic devices as gas - Ionic liquid membrane contactors for CO2 removal from anaesthesia gases
Malankowska, M; Martins, CF; Rho, HS; Neves, LA; Tiggelaar, RM; Crespo, JG; Pina, MP; Mallada, R; Gardeniers, H; Coelhoso, IM
2018 *Journal of Membrane Science* 545, pp 107-115
DOI: 10.1016/j.memsci.2017.09.065
IF: 7.015

Patents

During 2017 and 2018 three patents were granted with the participation of the LMA:

Inventors : M. JAAFAR, J.M. DE TERESA, A. ASENJO, J. PABLO-NAVARRO, P. ARES, C. MAGEN, J. GOMEZ

Títle: Sistema para un Microscopio de Fuerzas Atómicas

Priority Country: España

Priority Date: Nov. 3rd 2017.

Application number: P201731292

Patent number: ES1641.1290

Patent holder: CSIC (70%), Universidad de Zaragoza (15%), Fundación ARAID (5%), Universidad Autónoma de Madrid (10%)

Countries extension: PCT/ES2018/070709 (submission date Nov. 5th 2018)

Inventors: J.M. DE TERESA, R. CORDOBA, S. STROHAUER, T. TORRES

Title: Procedimiento para depositar elementos sobre un sustrato de interés y dispositivo

Priority Country: España

Priority date: Jul. 25th 2018

Application number: P201830757

Patent holder: CSIC (60%) y Universidad de Zaragoza (40%)

Countries extension: PCT/ES2019/070526 (submission date July 25th 2019)

Inventors M. C. Artal Lahoz; P. Cea Mingueza; J. Cortes Cameros; M. Fenero Bisquer; I. Gascón Sabate; E. Martinez Solanas; S. Martín Solans; J. Sanz Naval.

Title: Method for coating a base element for a household appliance component and a household appliance component.

Priority Country: España

Priority date: Sep. 2017

Application number: P20170321

Patent holder: BSH HAUSGERÄTE GMBH (40%) - BSH ELECTRODOMESTICOS ESPAÑA, S.A. (40%) - UNIVERSIDAD DE ZARAGOZA (20%)

Highlights

Artificial chemical and magnetic structure at the domain walls of an epitaxial oxide

Strained oxide thin films oxides often present radically different physical properties than bulk materials. For instance, they often contain high density of ferroelastic domains to accommodate the epitaxial strain. This symmetry breaking can induce properties absent from the domains themselves, such as magnetic or ferroelectric order and other functionalities, as well as the formation of new structural and chemical phases. In this sense, domain walls can function as nanoscale chemical reactors.

In this work, a new 2D ferromagnetic phase is synthesized at the domain walls of the orthorhombic perovskite terbium manganite ($TbMnO_3$) thin films grown under epitaxial strain on strontium titanate ($SrTiO_3$). Aberration corrected STEM has enabled a comprehensive characterization of the structure and chemical composition of this novel ferromagnetic phase by means of atomically resolved High Angle Annular Dark Field (HAADF) imaging and Electron Energy Loss Spectroscopy (EELS). This new phase, yet to be created by standard chemical routes, is characterized by the selective substitution of alternate Tb atoms in the perovskite structure by Mn atoms in the B positions of the perovskite structure (ABO_3). The density of these 2D sheets can be tuned by changing the film thickness, and they can grow as densely as to represent up to 25 per cent of the film volume. The general concept of using domain walls of epitaxial oxides to promote the formation of unusual phases may be applicable to other materials systems, thus giving access to new classes of nanoscale materials for applications in nanoelectronics and spintronics.

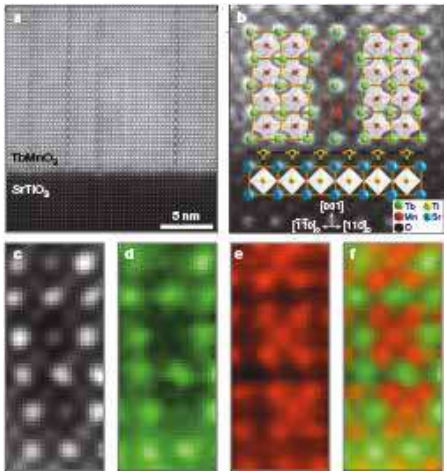

Figure caption. (a) HAADF-STEM image of the $TbMnO_3$–$SrTiO_3$ interface. b) Domain wall of $TbMnO_3$ close to the interface with the $SrTiO_3$ substrate, with the proposed atomic model superimposed. (c–f) STEM-EELS spectrum image of the domain wall; (c) HAADF signal, (d) Tb signal, (e) Mn signal, (f) color map of Tb (green) and Mn (red).

Reference:

Farokhipoor, S., Magén, C.Email Author, Venkatesan, S., Íñiguez, J, Daumont, C.J.M , Rubi, D., Snoeck, E., Mostovoy, M., De Graaf, C., Müller, A., Döblinger, M., Scheu, C., Noheda, B.
Artificial chemical and magnetic structure at the domain walls of an epitaxial oxide
2014, **Nature** 515, 379–383.

Highlights

Observation of magnetic dead layers in the surface of strained $La_{2/3}Ca_{1/3}MnO_3$ films

Most technological applications of spintronics (such as low power electronics or high density data storage) require the use of the chosen functional material in the form of thin film. These may present physical properties remarkably different from bulk due to scale reduction or the influence of a substrate. These factors need to be taken into account so that thin film specimens present the same or even optimized functional properties with respect to their bulk counterparts. An ideal benchmark to study these effects is single crystalline $La_{2/3}Ca_{1/3}MnO_3$ (LCMO), a colossal magnetoresistive spin-polarized ferromagnetic material which often presents a dramatic reduction or weakening of their magnetic and transport properties in thin films with due to the strain by epitaxy on a single crystalline substrate.

In this work, we show the first experimental images of the magnetization state of strained LCMO thin films obtained by electron holography demonstrating that epitaxial strain induces the segregation of a non-FM (***magnetically dead***) layer with antiferromagnetic (AFM) character at the top surface of a FM layer, the whole film being chemical and structurally homogeneous at room temperature. For different substrates and growth conditions the tetragonality of LCMO at room temperature, a critical tetragonal distorsion is found above which this phase coexistence takes place. Theoretical calculations prove that the increased tetragonality changes the energy balance of the FM and AFM ground states in strained LCMO, enabling the formation of magnetically inhomogeneous states. This work gives the key evidence that opens a new route to synthesize strain-induced exchanged-biased FM–AFM bilayers in single thin films, which could serve as building blocks of future spintronic devices.

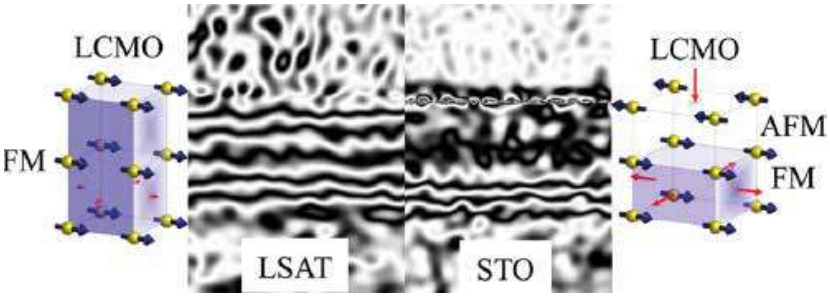

Figure caption. Magnetic flux lines of weakly strained LCMO films grown on LSAT (left) and tensile-strained LCMO film on STO (right). The strained LCMO on STO shows a non-ferromagnetic layer near the film surface segregated from the ferromagnetic layer near the substrate. The cartoons illustrate the type of lattice distortion induced and the predicted magnetic coupling in each case.

Reference:
Marín, L.; Rodríguez, L. A.; Magén, C.; Snoeck, E.; Arras, R.; Lucas, I.; Morellón, L.; Algarabel, P. A.; de Teresa, J. M.; Ibarra, M. R.
Observation of the Strain Induced Magnetic Phase Segregation in Manganite Thin Films
2015 **Nano Letters**, 15 (1), 492-497

Highlights

Purification of 3D FEBID Co nanowires

Text: Focused-electron-beam-induced deposition (FEBID) is considered the ultimate direct-write lithography technique for three-dimensional (3D) structures. However, it has not yet been possible to obtain 3D deposits by FEBID with the same purity and crystallinity of the corresponding bulk materials. In the present work, purified and crystalline 3D Co nanowires of diameter below 90 nm have been fabricated by ex situ high-vacuum annealing at 600 °C after FEBID growth. Advanced TEM techniques, in particular Off-Axis Electron Holography, have evidenced that the annealing process improves the magnetization of the nanowires up to virtually bulk, by inducing a purification and crystallization process that transforms the nanocrystalline 3D nanowires into pure (>95 % at. Co) crystalline nanowires. This achievement opens new pathways for applications of this synthetic method in the fabrication of either individual or arrays of 3D high-purity and crystalline Co nanowires for high-density memory and logic devices, nanosensors, and actuators, and could be a viable method to obtain other pure and crystalline 3D materials by FEBID.

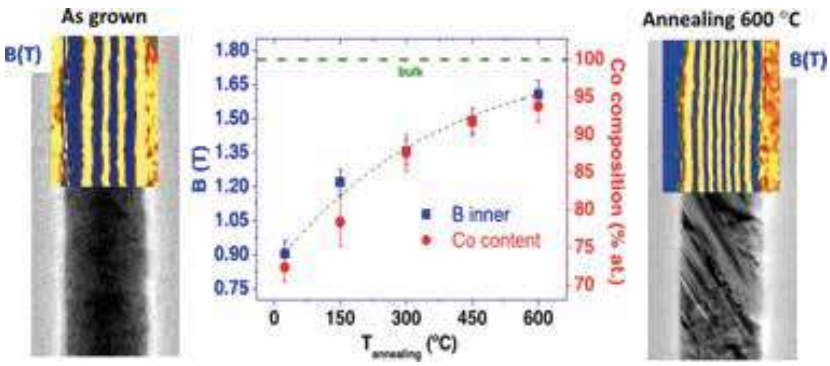

Figure caption. a-c) TEM images and magnetic flux lines determined by Electron Holography of the as grown, and 600ºC annealed nanowires. b) Evolution of the net magnetic induction and Co content of 3D Co nanowires as a function of the annealing temperature as determined by Off Axis Electron holography and quantitative Electron Energy Loss Spectroscopy (EELS).

Reference:
Pablo-Navarro J; Magén C. and De Teresa J.M.
Purified and Crystalline Three-Dimensional Electron-Beam- Induced Deposits: The Successful Case of Cobalt for High Performance Magnetic Nanowires
2018 **ACS Applied Nano Materials** 1, 38-46

Highlights

Polar states in epitaxially strained $Sr_{1-x}Ba_xMnO_3$ thin films

The perovskite $Sr_{1-x}Ba_xMnO_3$ (SBMO) system is an ideal candidate for tailoring the magnetoelectric properties of multiferroics through the accurate control of Ba content and epitaxial strain due to the strong coupling between polar instability, spin order, and lattice. In this work, we demonstrate the epitaxial growth of highly Ba-doped (x > 0.3) SBMO films grown on $TbScO_3$ (100), together with the onset of polar order on tensile strained films by aberration corrected Scanning Transmission Electron Microscopy (STEM) using Annular Bright Field (ABF) imaging, which we can correlate with the macroscopic dielectric behavior. ABF enables the simultaneous imaging of heavy and light atoms, which enable the visualization of the oxygen octahedra distortions in perovskite oxides as well as the off centering of the cations. In particular, polar films evidence a strong dependence of the capacitance as a function of temperature, which is a common feature of ferroelectric materials, and sharp anomalies at the magnetic (Neel) ordering temperature evidencing a strong magnetoelectric coupling.

a) b)

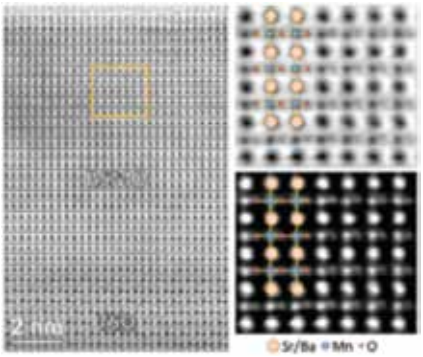

Figure caption. Annular Bright Field (ABF) STEM [110] cross sectional images of a) $Sr_{0.7}Ba_{0.3}MnO_3$ and b) $Sr_{0.6}Ba_{0.4}MnO_3$ films grown on $TbScO_3$ (100) evidencing the different displacements of the oxygen octahedra (strong in x = 0.3, weak in x = 0.4) as a function of the combined epitaxial strain and chemical doping on the parent $SrMnO_3$.

Reference:
Langenberg E., Maurel L., Marcano N., Guzmán R., Štrichovanec P., Prokscha T., Magén C., Algarabel P.A. and Pardo J.A.
Controlling the Electrical and Magnetoelectric Properties of Epitaxially Strained $Sr_{1-x}BaxMnO_3$ Thin Films.
2017 **Advanced Materials Interfaces** 4, 1601040

Highlights

TEM investigations of covalently functionalized transition metal dichalcogenides

Text: Exfoliated semiconducting MoS_2 and WS_2 were covalently functionalized with 1,2-dithiolane-modified carbon nanodots (CNDs). The newly synthesized CND-MoS2 and CND-WS2 hybrids were studied by transmission electron microscopy (TEM) imaging and spectroscopy (electron energy loss (EELS) and X-ray energy dispersive (EDS)). The present study highlights the importance of TMD-derived donor-acceptor hybrids in light energy harvesting and optoelectronic applications. Furthermore, the fundamental information obtained from the current results will benefit design strategies and impact the development of additional TMD-based hybrid materials to efficiently manage and perform in electron-transfer processes.

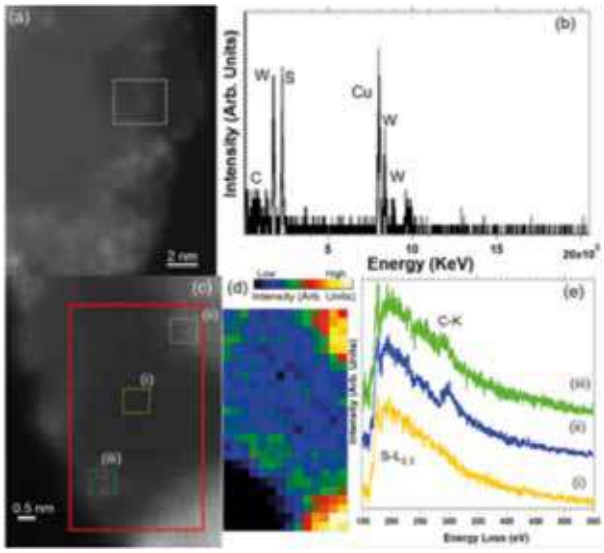

Figure caption: Representative HRSTEM-ADF images for (a, d) CND-WS_2. (b) EDS acquired on the squared white area in (a). In the red regions of (c) spectra images of SR-EELS were recorded. (d) Carbon elemental maps extracted from the integrated intensity of the C-K edge of the two EELS spectra image recorded in the red area in (c). (e) Three spectra from the sum of 16 (4 × 4) EEL spectra extracted from the EELS SPIM of (c), showing the S-$L_{2,3}$ and C-K (in this case only in (ii) and (iii)) edges. The C-K edge (~284 eV) is observed in (ii) and (iii). The S-$L_{2,3}$ edge is visible in the three spectra ((i)–(iii)).

Reference:
Vallan L., Canton-Vitoria R., Gobeze H., Jang Y., Arenal R., Benito A., Maser W., D'Souza F., Tagmatarchi N.,
Interfacing TMDS with carbon nan-odots for managing photoinduced energy and charge-transfer processes
2018 **Journal of the American Chemical Society**, 140, 13488-13496

Highlights

Generation of subnanometric platinum with high stability during transformation of two-dimensional into three-dimensional zeolite - STEM HAADF analyses

It has been reported a new strategy for the generation of single Pt atoms and Pt clusters with exceptional high thermal stability in purely siliceous MCM-22 during the transformation of a two-dimensional (2D) into a 3D zeolite. These structures, and in particular the incorporation of Pt species in the form of single-atoms or small clusters, have been investigated by high-resolution STEM high-angle annular dark field (HAADF) imaging analyses. These studies have shown that these Pt species were confined in the zeolite cups (created from the 2D to 3D transformation).

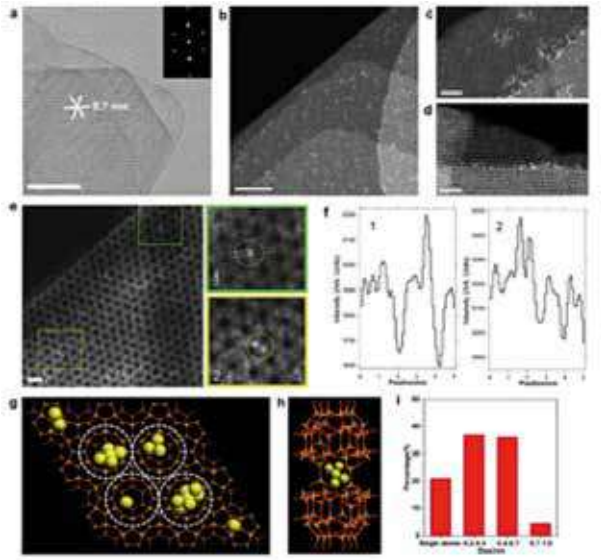

Figure caption. Atomic structures of Pt@MCM-22. a, TEM image of Pt@MCM-22. The insert is the corresponding FFT diffractogram of the TEM image. Scale bar, 50 nm. b, HAADF-STEM image of Pt@MCM-22. Scale bar, 20 nm. c and d, Atomic structures of Pt clusters confined in MCM-22. Scale bar, 5 nm. e, HAADF-HRSTEM image of Pt@MCM-22, where two zooms have been done in the square regions (marked in green (#1) and yellow (#2)). In these two areas, several single atoms have been highlighted. Scale bar, 2 nm. f. Corresponding intensity profiles obtained on the two zoomed areas. g, Schematic illustration of Pt@MCM-22 in a "top-down" view along the c axis. Pt clusters and individual Pt atoms are located in the surface cups, cavities and 12-MR supercages. h, Schematic illustration of Pt_5 cluster in supercages of MCM-22. i, Size distribution of subnanometric Pt species in Pt@MCM-22 sample.

Reference:

Liu L., Diaz U., Arenal R., Agostini G., Concepcion P., Corma A.,
Generation of Pt single atoms and clusters with exceptional high stability during transformation of two-dimensional into three-dimensional zeolite
2017 **Nature Materials** 16, 132-138

Highlights

Calcium cobalt oxide misfit nanotubes, STEM (HAADF & EELS) studies

We reported a comprehensive structural, compositional and theoretical study of the formation of a new phase of cobalt-oxide-based misfit nanotubes . For achieving this, we have developed systematic and advanced analyses combining high-resolution (scanning) transmission electron microscopy (including image simulations), spatially-resolved electron energy-loss spectroscopy (SR-EELS) and electron diffraction. We also proposed a formation mechanism for these nanotubes that could also apply more generally to realizing other oxide-based MLC nanotubes. These NTs, based on layered $Ca_3Co_4O_9$, are very promising thermoelectric (TE) material due to its high TE performance, remarkable thermal and chemical stability at elevated temperatures, and its reduced toxicity.

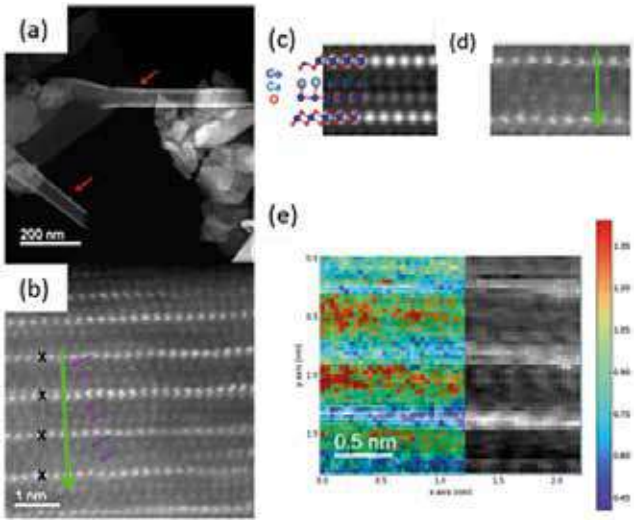

Figure caption: (a) Low-Magnification STEM HAADF micrograph of the products coming from the hydrothermal synthesis of $Ca_3Co_4O_9$. The red arrows draw attention to the tubular nanostructures. (b) HR-STEM HAADF micrograph of a nanotube, highlighting the 0.86 nm-periodicity of the bright layers. (c) Simulated HR-STEM HAADF micrograph superposed with the relaxed atomic structure of $CaCoO_2$-CoO_2 used as input. (d) Experimental STEM HAADF image. (e) Superposition of the Ca/Co ratio map obtained from SR-EELS (left) and the HR-STEM ADF micrograph (right) acquired at the same time.

Reference:

Panchakarla L., Lajaunie L., Ramasubramaniam A., Arenal R., Tenne R.
Nanotubes from oxide-based misfit family: the case of calcium cobalt oxide
2016 **ACS Nano** 10, 6248

Highlights

STA-20: An ABC-6 Zeotype Structure Prepared by Co-Templating and Solved via a Hypothetical Structure Database and STEM-ADF Imaging

A microporous silicoaluminophosphate with a novel topology type, STA-20, has been prepared via a dual templating method. Its structure has been solved and confirmed using a multitechnique approach that included the use of a hypothetical zeolite database to obtain a candidate starting structure, followed by scanning transmission electron microscopy with annular dark field imaging at atomic level and Rietveld refinement. STA-20 is a member of the ABC-6 family of zeotype structures. The structure has trigonal symmetry, ***P***-31***c***, with a = 13.15497(18) Å and c = 30.5833(4) Å in the calcined form. It has a 12-layer stacking sequence of 6-rings (6Rs), AABAABAACAAC(A), which contains single and double 6R units. In addition to d6r, can, and gme cages, STA-20 possesses the longest cage observed in an ordered ABC-6 material, giving a 3D-connected pore system limited by 8R windows. Solving the structure as well as determining the stacking sequence was possible thanks to the atomic-resolution data that allowed to identify all the Si, Al and P atoms.

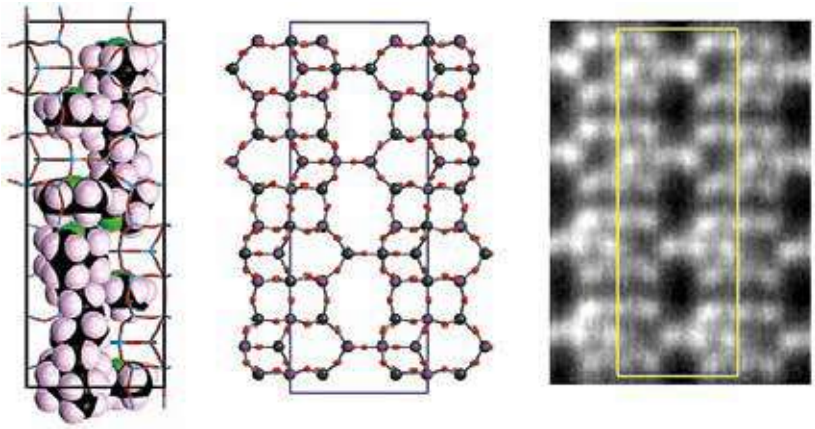

Figure caption: Left: Model proposed containing a single unit cell with the zeolite template inside the pores. Middle: Structural solution, after removing the organic part, the blue rectangle shows a single unit cell. Right: C_s-corrected STEM-HAADF micrograph at atomic level of the zeolite framework. The single unit cell is denoted by the yellow rectangle.

Reference:

Turrina A., Garcia R., Watts A. E., Greer H. F., Bradley J., W. Zhou W., Cox P. A., Shannon M. D, Mayoral., A., Casci J.L., Wright P.A.
STA-20: An ABC-6 Zeotype Structure Prepared by Co-Templating and Solved via a Hypothetical Structure Database and STEM-ADF Imaging
2017 **Chemistry of Materials**, 29, 2180–2190

Highlights

Cs-corrected STEM imaging of both pure and Ag-supported metal-organic framework MIL-100(Fe)

Metal-organic frameworks (MOFs) are a family of porous solids combining organic and inorganic moieties with tunable porosity. Their particular structural parameters have converted MOFs into suitable compounds for gas storage or drug delivery. However, despite the excellent crystallinity they tend to exhibit their analysis through transmission electron microscopy is extraordinarily complicated due to the high instability under the electron beam irradiation. This work presents ultra-high-resolution Cs-corrected STEM data achieved by paying special attention to the electron beam current. In addition, MIL-100(Fe) was reacted with $AgNO_3$ through a solid-state reaction technique, which has resulted into the formation of metal nanoparticles on the surface. The incorporation of Ag into the porous network was also investigated.

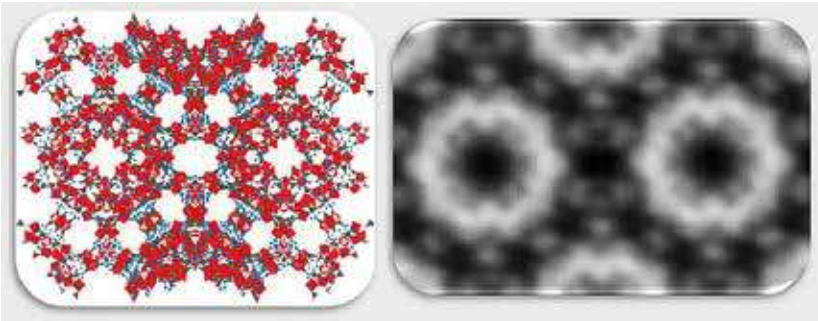

Figure caption: Left: Model of Mil-100 along the [110] orientation where the metals are appear as red polyhedral. Right: C_s-corrected STEM-ADF image displaying exactly the same units, confirming a perfect agreement between the theoretical model and the experimental data.

Reference(s):
Mayoral A., Mahugo R., Sánchez-Sánchez M., Díaz I.
Cs-Corrected STEM Imaging of both Pure and Silver-Supported Metal-Organic Framework MIL-100(Fe)
2017 **Chem Cat Chem** 9, 3497

Highlights

All-Carbon Electrode Molecular Electronic Devices Based on Langmuir–Blodgett Monolayers

Nascent molecular electronic devices, based on monolayer Langmuir–Blodgett films sandwiched between two carbonaceous electrodes, have been prepared. Tightly packed monolayers of 4-((4-((4-ethynylphenyl)ethynyl)phenyl)ethynyl)benzoic acid, compound **1**, are deposited onto a highly oriented pyrolytic graphite electrode. An amorphous carbon top contact electrode is formed on top of the monolayer from a naphthalene precursor using the focused electron beam induced deposition technique. This allows the deposition of a carbon top-contact electrode with well-defined shape, thickness, and precise positioning on the film with nm resolution. These results represent a substantial step toward the realization of integrated molecular electronic devices based on monolayers and carbon electrodes.

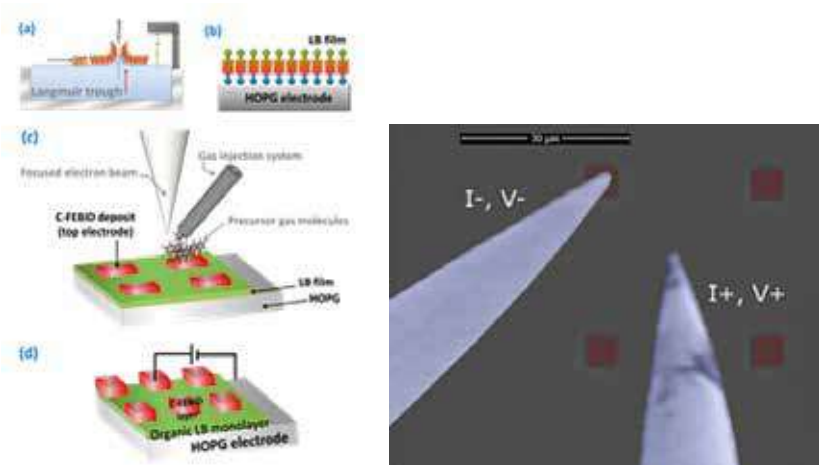

Figure caption: Left panel: Sketch of the fabrication process of all-carbon electrode molecular electronic devices by carbon FEBID deposition onto a monolayer LB film. a) Langmuir film at the air–water interface a scheme of the transference process onto HOPG by withdrawal of the electrode from the water subphase. b) Monolayer LB film deposited onto an HOPG electrode. c) FEBID is an additive lithography technique where the precursor (naphthalene, C10H8) is delivered onto the surface by a nearby gas injection system. As the focused beam is scanned, it dissociates locally the precursor gas molecules, creating a deposit with the same shape of the beam scan. d) 3D view of all-carbon electrode molecular electronic devices. Right panel: Artificially colored SEM image of a monolayer LB film of **1** *grown on HOPG, containing four all-carbon electrode devices, with red regions indicating the four carbon top electrodes and blue regions indicating the in situ electrical microprobes.*

Reference:

Sangiao, S.; Martin, S.; Gonzalez-Orive, A.; Magen, C.; Low, P. J.; de Teresa, J. M.; Cea, P.
All-Carbon Electrode Molecular Electronic Devices Based on Langmuir-Blodgett Monolayers
2017 **Small,** 2017, 13, 1603207

Highlights

Fabrication of the smallest superconducting hollow nanowire

The fabrication and characterization of 3D superconducting crystalline WC hollow nanowires with diameters down to 32 nm and aspect ratio above 200 have been successfully achieved. The method is based on using highly-focused beam of He^+ ions to decompose precursor molecules of $W(CO)_6$. The growth of a vertical WC nanowire occurs around the ion beam spot, mainly due to the interaction of secondary electrons with the adsorbed precursor molecules, whereas a hole at the center of the nanowire is formed due to the He^+ beam milling effect on the growing material. The achieved small nanowire diameter is due to the use of a very small He^+ beam spot (<1 nm). The nanowires exhibit 1.5 times higher superconducting critical temperatures (6.4 K) as well as 1.5 times higher upper critical magnetic fields (≈14 T) when compared to nanowires grown by an analogous technique based on Ga^+ focused ion beam. This study could pave the way for the development of complex 3D nanosuperconductors, which could be implemented in future electronic components.

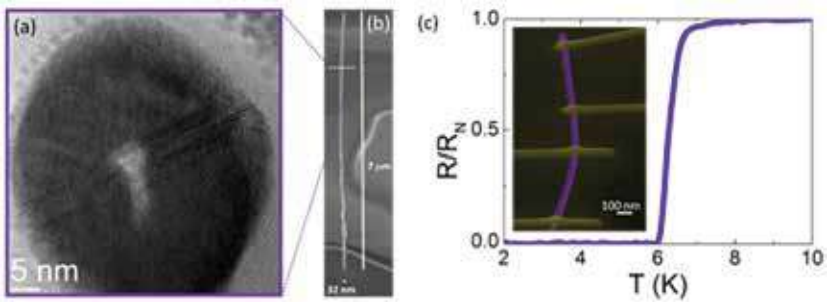

Figure caption: (a) HRTEM image of the cross-sectional view of the hollow NW indicated in (b). (b) SEM image of a vertical hollow NW grown by He^+ FIBID. (c) Normalized resistance for a NW versus T. Inset shows an SEM image (coloured) of a NW connected by four contacts. Adapted with permission from (R. Córdoba, A. Ibarra, D. Mailly, and J. M. De Teresa, Vertical Growth of Superconducting Crystalline Hollow Nanowires by He^+ Focused Ion Beam Induced Deposition, Nano Lett., 2018, 18 (2), pp 1379–1386). Copyright (2018) American Chemical Society.

Reference:
Córdoba R., Ibarra A., Mailly D., De Teresa J.M.,
Vertical Growth of Superconducting Crystalline Hollow Nanowires by He+ Focused Ion Beam Induced Deposition
2018 **Nano Letters** 18 (2), pp 1379-13869

Highlights

New active formulations against *M. tuberculosis*

In the last years, the increase in antimicrobial resistance, together with a lack of new drugs for the treatment of bacterial infections resistant to classical antibiotics are of growing concern. Moreover, some of current therapies induce severe side effects and are often difficult to administer. In 2012 the FDA approved the use of bedaquiline, a new drug designed specifically to treat multi-drug resistant tuberculosis (MDR-TB). Despite its effectiveness, unfortunately bedaquiline side effects can be so dangerous that at present it is to be prescribed only when no other treatment options are available. The development of effective and safe nanotechnology-based methods can be particularly relevant to increase antimicrobial concentration at the site of infection, to reduce doses in the general circulation, which in turn reduces adverse effects. In this work bedaquiline was encapsulated in two types of nanocarriers, lipid nanoparticles and chitosan-based nanocapsules with high encapsulation efficiency and drug loading values. The efficacy of the drug-encapsulating nanocarriers has been demonstrated ***in vitro*** against ***Mycobacterium tuberculosis***, together with the excellent compatibility of both carriers with animal cells. The obtained results open the way for ***in vivo*** studies of the optimized nanocarriers for reducing the administered doses of a quite dangerous antibiotic as bedaquiline, tuning the antibiotic biodistribution and so decreasing its adverse effects, finally allowing its use in a higher number of patients.

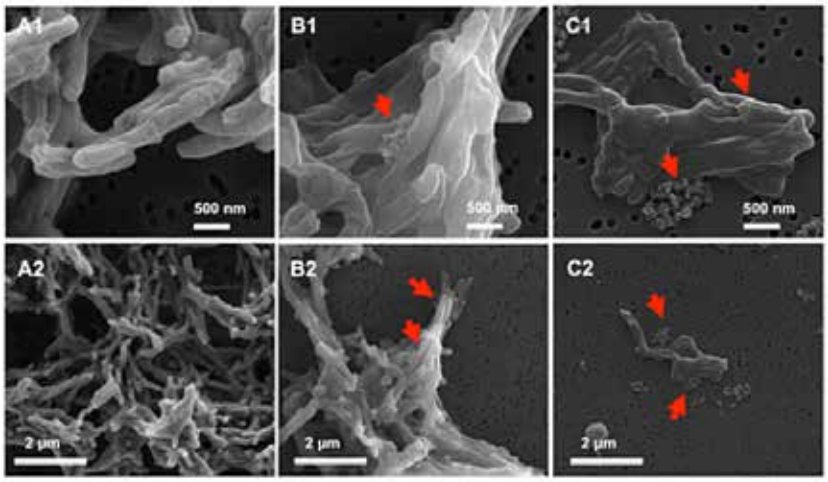

*Figure caption: SEM images of **M. tuberculosis** H37Rv untreated (A1 and A2), incubated with CS-NC (B1 and B2) and with PEG-CS-NC (C1 and C2). The presence of chitosan nanocapsules close to the bacterial cells is indicated by the arrows.*

Reference:
de Matteis L., Jary D., Lucia A., Gacía-Embid S.,. Serrano-Sevilla I, Pérez D., Ainsa J.A., Navarro F.P., de la Fuente J.M..
New active formulations against M. tuberculosis: Bedaquiline encapsulation in lipid nanoparticles and chitosan nanocapsules
2018 **Chemical Engineering Jounal** 340, 181-191.

Highlights

Magnetic hyperthermia enhances cell toxicity with respect to exogenous heating

This *in vitro* study compared the effect of hyperthermia in response to the application of exogenous heating (EHT) sources with the corresponding effect produced by magnetic hyperthermia (MHT). Human neuroblastoma SH-SY5Y cells were loaded with magnetic nanoparticles (MNPs) and packed into dense pellets to generate an environment that is crudely similar to that expected in solid micro-tumors, and the above-mentioned protocols were applied to these cells. An analysis of TEM and SEM-FIB Dual Beam images of the cells after the EHT and MHT treatments showed the enhanced effectiveness observed with MHT is associated with local cell destruction triggered by the magnetic nano-heaters.

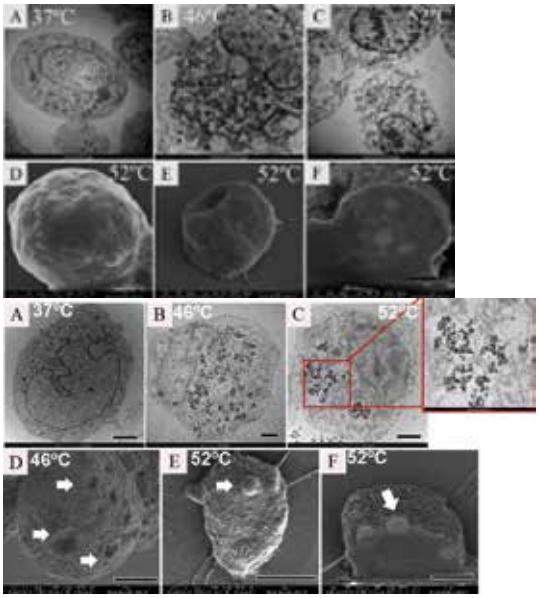

Figure caption: (Left panel) TEM and FIB-SEM micrographs of SH-SY5Y cells subjected to MHT for 30 min. A) Control cell (AMF, no particles). After MHT at 46 ºC (B) and 52 ºC (C), the PEI-MNPs (100 mg/mL) were still easily identifiable within the cytoplasm inside membranous structures. Dual-beam FIB-SEM images after MHT at 46 ºC (D) show drastic changes in cellular roughness and numerous holes (arrows) and apoptotic blebs on the cytoplasmic membrane (E) and the cytoplasm (F). The scale bars are 2 mm, except in (F) (5 mm). (Right panel) TEM and FIB-SEM micrographs of SH-SY5Y cells A) Control cell (AMF, no particles). After MHT at 46 ºC (B) and 52 ºC (C), the PEI-MNPs were still easily identifiable within the cytoplasm inside membranous structures. Dual-beam FIB-SEM images after MHT at 46 ºC (D) show drastic changes in cellular roughness and numerous holes (arrows) and apoptotic blebs on the cytoplasmic membrane (E) and the cytoplasm (F). The scale bars are 2 mm, except in (F) (5 mm).

Reference:

Sanz B., Calatayud M.P., Torres T.E., Fanarraga M.L., Ibarra M.R. and Goya G.F.
Magnetic hyperthermia enhances cell toxicity with respect to exogenous heating
2017 **Biomaterials** 114, 62–70

Highlights

Tuning shape, composition and magnetization of 3D Co NWs grown by FEBID

The control of the growth parameters in Focused Electron Beam Induced Deposition (FEBID), especially the electron beam current and the precursor flux, allows the tuning of the diameter, composition and magnetization of 3D Co NWs. A sharp transition between two growth modes, coined as ***radial*** and ***linear***, has been unveiled in single NWs, resulting in individual nanostructures with two different diameters. The capacity to dissipate the heat caused by the electron beam is reduced as the NW grows progressively further away from the substrate. At a certain height, there is an overheating which could result in a change of the growth mode, from linear to radial (see Figure). In the radial-growth mode, NWs exhibit large diameters (>120 nm), >85% at. Co content and a high magnetization, not far from the bulk value, 1.8 T. In the lineal-growth mode, with smaller diameters (<80 nm), the Co content diminishes for the decreasing diameter. For a diameter of 80 nm, NWs can attain Co content of 80% at. and show magnetization around half the bulk value. When the diameter is 60 nm, the Co content is 45% at. and the magnetization is around 1/4 of the bulk value. The existence of single NWs with two diameters seems useful for studies of magnetic domain-wall propagation, providing pinning sites at the location of the transition.

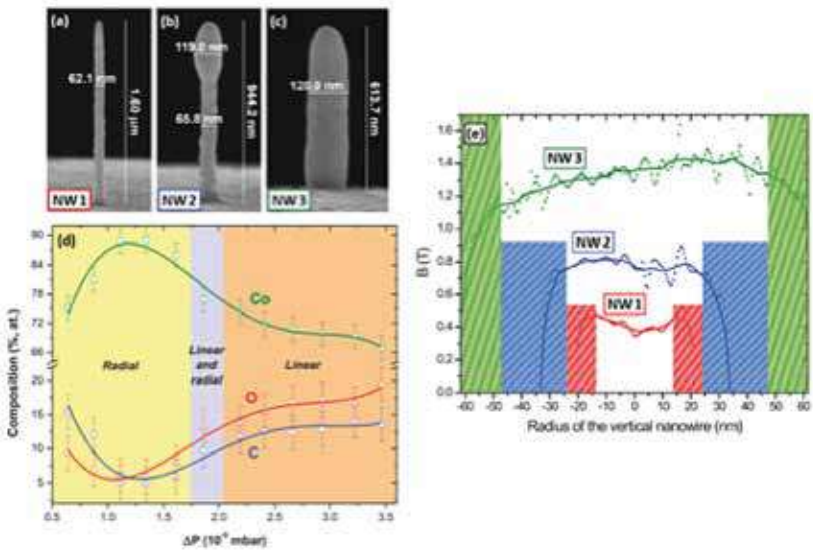

Figure caption: SEM images of Co NWs grown at ΔP of (a) 7.3 × 10^{-6} mbar, (b) 6.4 × 10^{-6} mbar and (c) 5.1 × 10^{-6} mbar. The transition from linear to radial growth mode with decreasing precursor flux is noticed. (d) NW composition as a function of ΔP. (e) Profiles of the magnetic induction along the short axis of nanowires NW1, NW2 (in the linear region) and NW3.

Reference:

Pablo-Navarro J., Sanz-Hernández D., Magén C., Fernández-Pacheco A. and De Teresa. J. M.
Tuning shape, composition and magnetization of 3D Co NWs grown by FEBID
2017 **Journal of Physics D Applied Physics**, 50, 18

Highlights

NanoSQUID Magnetometry on Individual As-grown and Annealed Co Nanowires at Variable Temperature

In this work, we present a detailed study of the magnetic properties of individual cobalt nanowires annealed at different temperatures by means of nanoSQUID magnetometry. This is possible thanks to the broad field and temperature operation range of YBCO nanoSQUID sensors. For these studies, we use a FEI Helios Nanolab dual-beam system allowing sensor patterning by means of focused ion beam milling, nanowires growing through focused electron beam induced deposition of cobalt and subsequent integration onto the nanoSQUIDs with nanometric resolution. This latter fact, together with the high spin-sensitivity of YBCO nanoSQUIDs, allows distinguishing minute magnetic signals produced by domain wall nucleation, pinning/depinning, or complete magnetization reversal. Magnetization measurements underscore the intrinsic structural and chemical differences between the nanowires. These point to significant changes in the crystalline structure and to the nucleation and subsequent vanishing of antiferromagnetic species within the nanowires annealed at different temperatures.

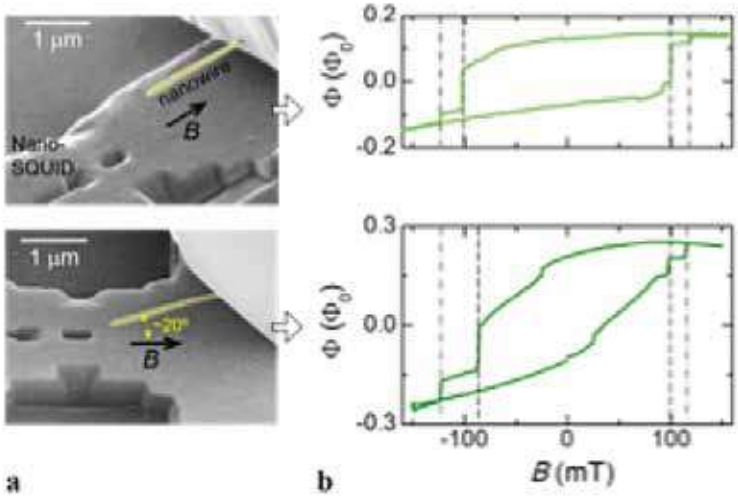

Figure caption: (a) SEM images of two different nanoSQUID devices where a Co nanowire is deposited (top) parallel to the direction of the externally applied magnetic field and (bottom) at an angle of 20 degrees. (b) Resulting experimental hysteresis loops measured with each device. The main switching events (dashed lines) take place at very similar magnetic fields proving the reproducibility of the growing, annealing and deposition processes. Differences in the shape of the hysteresis loops stem from the different angles between the easy axis of the nanowire and the externally applied magnetic field.

Reference:

Martínez-Pérez M.J., Pablo-Navarro J., Müller B., Kleiner R., Magén C., Koelle D., De Teresa J.M., Sesé J.
NanoSQUID Magnetometry on Individual As-grown and Annealed Co Nanowires at Variable Temperature
2018 **Nano Letters** 18 (12), pp 7674-7682

Highlights

Sub-20 nm patterning of epitaxial graphene

Sub-20 nm patterns have been fabricated by using oxidation scanning probe lithography (o-SPL) on epitaxial graphene. In order to perform TEM studies, cross-sectional lamellae of the patterned samples have been fabricated in the LMA Helios Nanolab 650 (FEI Company) by using the Ga ion column operated at 30 kV during the milling and initial thinning and at 5 kV during the final polishing. Morphology and atomic structure studies were performed in the LMA Titan Cubed TEM (FEI Company) equipped with an image-aberration corrector. In addition, compositional studies by STEM-HAADF were performed in the LMA Titan G2 STEM microscope (FEI Company), equipped with a probe corrector. Spectroscopic analysis by EELS and EDX confirm the presence of graphene oxide along the graphene lines patterned by o-SPL of aobut 17 nm in width and 1-2 nm in depth and the absence of any oxygen signal outside the nanopatterned areas. These results pave the way for future research on design of high-performance graphene devices.

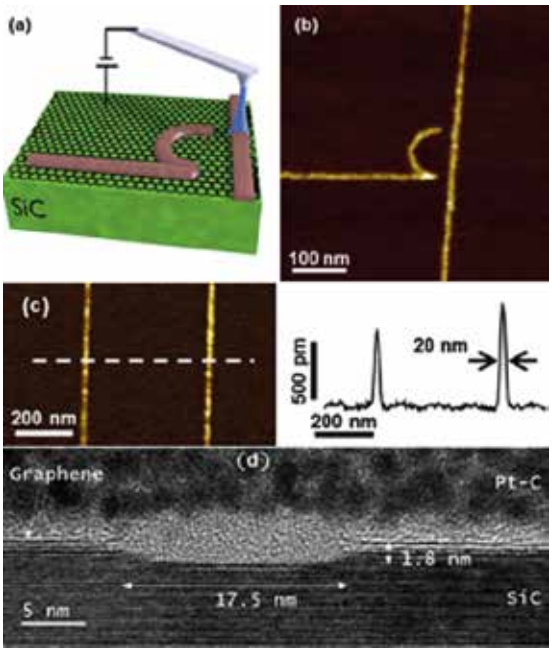

Figure caption: (a) Scheme of o-SPL patterning on a graphene layer formed on SiC. (b) o-SPL pattern on graphene. The narrowest section between the o-SPL patterns is of 18 nm. (c) AFM topology image of two parallel lines fabricated on graphene. The right panel shows the cross-section along the dashed line marked in the AFM image. HRTEM image of one of the lines shown in (c).

Reference:
Dago A. I., Sangiao S., Fernández-Pacheco R., De Teresa J. M. and García R.
Sub-20 nm patterning of epitaxial graphene
2018 **Carbon** 129, 281–285

Highlights

Chemical Disorder in Topological Insulators: A Route to Magnetism Tolerant Topological Surface States

Instrument: JT-STM. The chemical inhomogeneity in ternary three-dimensional topological insulators preserves the topological spin texture of their surface states against a net surface magnetization. The spin texture is that of a Dirac cone with helical spin structure in the reciprocal space, which gives rise to spin-polarized and dissipation-less charge currents. Thanks to the nontrivial topology of the bulk electronic structure, this spin texture is robust against most types of surface defects. However, magnetic perturbations break the time-reversal symmetry, enabling magnetic scattering and loss of spin coherence of the charge carriers. This intrinsic incompatibility precludes the design of magnetoelectronic devices based on the coupling between magnetic materials and topological surface states. We demonstrate that the magnetization coming from individual Co atoms deposited on the surface can disrupt the spin coherence of the carriers in the archetypal topological insulator Bi2Te3, while in Bi2Se2Te the spin texture remains unperturbed. This is concluded from the observation of elastic backscattering events in quasiparticle interference patterns obtained by scanning tunneling spectroscopy. The mechanism responsible for the protection is investigated by energy resolved spectroscopy and ab initio calculations, and it is ascribed to the distorted adsorption geometry of localized magnetic moments due to Se–Te disorder, which suppresses the Co hybridization with the surface states.

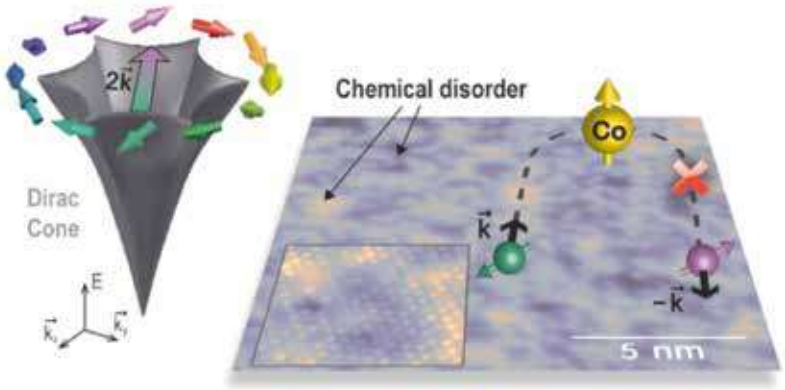

Reference:
Martínez-Velarte, M. C.; Kretz, B.; Moro-Lagares, M.; Aguirre, M. H.; Riedemann, T. M.; Lograsso, T. A.; Morellón, L.; Ibarra, M. R.; Garcia-Lekue, A.; Serrate, D.
Chemical Disorder in Topological Insulators: A Route to Magnetism Tolerant Topological Surface States
2017 **Nano Letters**, 17, 4047.

Highlights

Electric polarization switching in an atomically thin binary rock salt structure"

Instrument: LT-qPlus. Inducing and controlling electric dipoles is hindered in the ultrathin limit by the finite screening length of surface charges at metal–insulator junctions1–3, although this effect can be circumvented by specially designed interfaces. Heterostructures of insulating materials hold great promise, as confirmed by perovskite oxide superlattices with compositional substitution to artificially break the structural inversion symmetry. Bringing this concept to the ultrathin limit would substantially broaden the range of materials and functionalities that could be exploited in novel nanoscale device designs. Here, we report that non-zero electric polarization can be induced and reversed in a hysteretic manner in bilayers made of ultrathin insulators whose electric polarization cannot be switched individually. In particular, we explore the interface between ionic rock salt alkali halides such as NaCl or KBr and polar insulating Cu2N terminating bulk copper. The strong compositional asymmetry between the polar Cu2N and the vacuum gap breaks inversion symmetry in the alkali halide layer, inducing out-of-plane dipoles that are stabilized in one orientation (self-poling). The dipole orientation can be reversed by a critical electric field, producing sharp switching of the tunnel current passing through the junction.

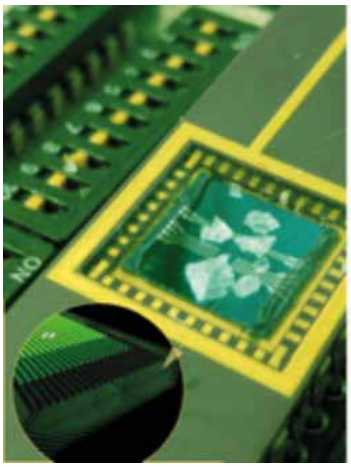

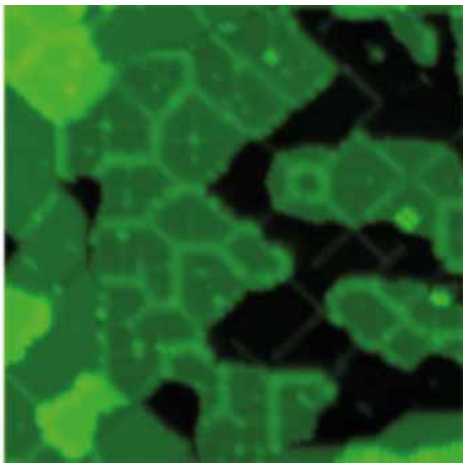

Reference:
Martinez-Castro, J., Piantek, M., Schubert, S., Persson, M., Serrate, D., Hirjibehedin, C.F.
Electric polarization switching in an atomically thin binary rock salt structure
2018 **Nature Nanotechnology**, 13, 19.

Highlights

Reversible Monolayer–Bilayer Transition in Supported Phospholipid LB Films under the Presence of Water: Morphological and Nanomechanical Behavior

Instrument: Veeco Multimode AFM. Mixed monolayer Langmuir–Blodgett (LB) films of 1,2-dipalmitoyl-sn-glycero-3-phosphocholine (DPPC) and cholesterol (Chol) in the 1:1 ratio have been prepared onto solid mica substrates. Upon immersion in water or in an aqueous HEPES solution (pH 7.4) the monolayer LB films were spontaneously converted into well-organized bilayers leaving free mica areas. The process has been demonstrated to be reversible upon removal of the aqueous solution, resulting in remarkably free of defects monolayers that are homogeneously distributed onto the mica. In addition, the nanomechanical properties exhibited by the as-formed bilayers have been determined by means of AFM breakthrough force studies. The bilayers formed by immersion of the monolayer in an aqueous media exhibit nanomechanical properties and stability under compression analogous to those of DPPC:Chol supported bilayers obtained by other methods previously described in the literature. Consequently, the hydration of a monolayer LB film has been revealed as an easy method to produce well-ordered bilayers that mimic the cell membrane and that could be used as model cell membranes. AFM image: The LB mixed monolayer of DPPC+cholesterol is stablished as a model system to study the behavior of cell membranes.

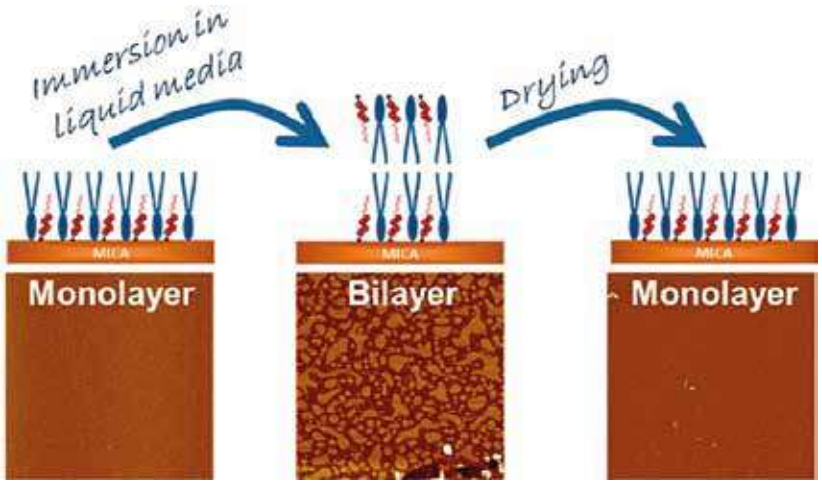

Reference:
Ruiz-Rincón, S., González-Orive, A., de la Fuente, J.M., Cea, P.
Reversible Monolayer–Bilayer Transition in Supported Phospholipid LB Films under the Presence of Water: Morphological and Nanomechanical Behavior
2017 **Langmuir**, 33, 30, 7538-7547

Highlights

Unconventional Single-Molecule Conductance Behavior for a New Heterocyclic Anchoring Group: Pyrazolyl

Instrument Veeco Multimode. Electrical conductance across a molecular junction is strongly determined by the anchoring group of the molecule. Here we highlight the unusual behavior of 1,4-bis(1H-pyrazol-4-ylethynyl)benzene that exhibits unconventional junction current versus junction-stretching distance curves, which are peak-shaped and feature two conducting states of 2.3 × 10-4 G0 and 3.4 × 10-4 G0. A combination of theory and experiments is used to understand the conductance of single-molecule junctions featuring this new anchoring group, i.e., pyrazolyl. These results demonstrate that the pyrazolyl moiety changes its protonation state and contact binding during junction evolution and that it also binds in either end-on or facial geometries with gold contacts. The pyrazolyl moiety holds general interest as a contacting group, because this linkage leads to a strong double anchoring of the molecule to the gold electrode, resulting in enhanced conductance values.

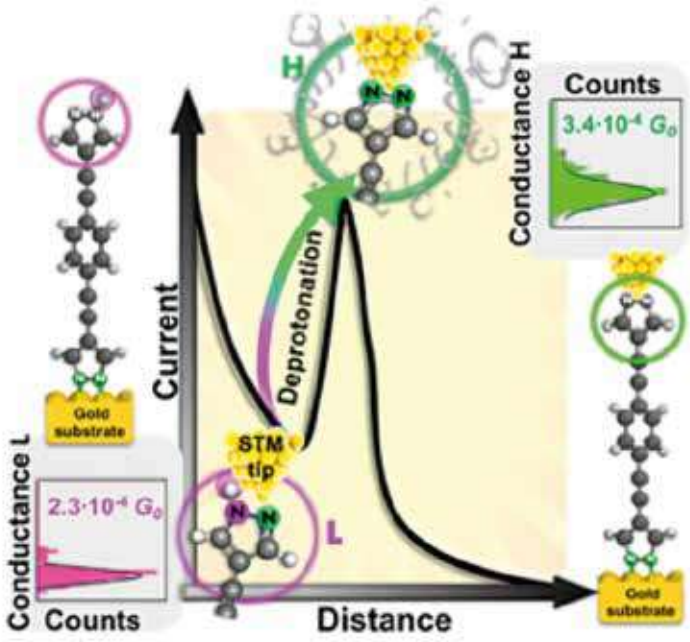

Reference:
Herrer, I.L.; Ismael, A.K. ; Milán, D.C. ; Vezzoli, A. ; Martín, S.; González-Orive, A. ; Grace, I. ; Lambert, C. ; Serrano, J.L. Nichols, R.J.; Cea, P. J.
Unconventional Single-Molecule Conductance Behavior for a New Heterocyclic Anchoring Group: Pyrazolyl
2018 **Phys. Chem. Lett.**, 9, 18, 5364-5372

Highlights

Molecular basis for the integration of environmental signals by FurB from Anabaena sp. PCC 7120

Instrument**:** Veeco Multimode AFM. Ferric uptake regulator proteins are among the most important families of transcriptional regulators in prokaryotes. In the cyanobacterium Anabaena PCC 7120, FurB (Zur, Zinc uptake regulator) controls zinc and redox homeostasis through the repression of target genes in a zinc-dependent manner. In vitro, non-specific binding of FurB to DNA elicits protection against oxidative damage and avoids cleavage by deoxyribonuclease I. We provide evidence of the influence of redox environment in the interaction of FurB with regulatory zinc and its consequences in FurB–DNA-binding affinity. Calorimetry studies showed that, in addition to one structural Zn(II), FurB is able to bind two additional Zn(II) per monomer and demonstrated the implication of cysteine C93 in regulatory Zn(II) coordination. The interaction of FurB with the second regulatory zinc occurred only under reducing conditions. While non-specific FurB–DNA interaction is Zn(II)-independent, the optimal binding of FurB to target promoters required loading of two regulatory zinc ions. Those results combined with site-directed mutagenesis and gel-shift assays evidenced that the redox state of cysteine C93 conditions the binding of the second regulatory Zn(II) and, in turn, modulates the affinity for a specific DNA target. The AFM image bellow shows specific DNA binding (A) causing the repression of genes, and no binding at all (B)

Reference:
Sein-Echaluce V. C., Pallarés M. C, Lostao A., et al.
Molecular basis for the integration of environmental signals by FurB from Anabaena sp. PCC 7120
2018 **Biochemical Journal**, 475, 151–168

Highlights

The FAD synthetase from the human pathogen Streptococcus pneumoniae: a bifunctional enzyme exhibiting activity-dependent redox requirements

Instrument: Nanotec AFM. Prokaryotic bifunctional FAD synthetases (FADSs) catalyze the biosynthesis of FMN and FAD, whereas in eukaryotes two enzymes are required for the same purpose. FMN and FAD are key cofactors to maintain the flavoproteome homeostasis in all type of organisms. Here we shed light to the properties of the hitherto unstudied bacterial FADS from the human pathogen Streptococcus pneumoniae (SpnFADS). Collectively, our results add interesting mechanistic differences among the few prokaryotic bifunctional FADSs already characterized, which might reflect the adaptation of the enzyme to relatively different environments. In a health point of view, differences among FADS family members provide us with a framework to design selective compounds targeting these enzymes for the treatment of diverse infectious diseases. The image displays AFM topographies of SpnFADS assemblies, dimer on the same plane (B), dimer with an overlapping on a monomer (C), trimer (E), and tetramer (F)

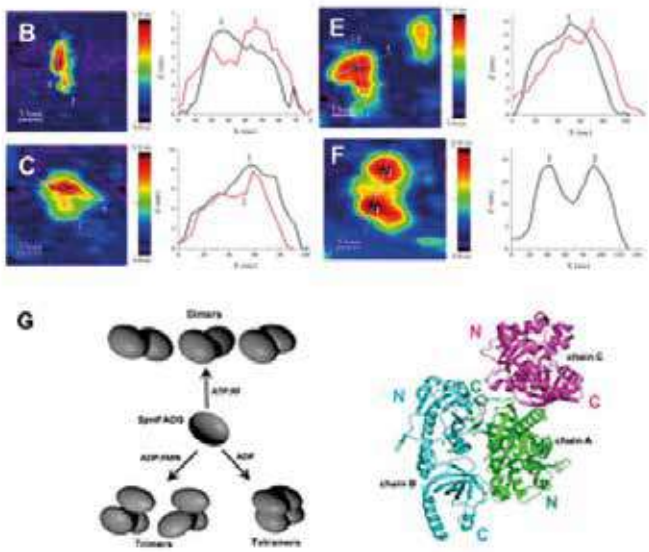

Reference:
Sebastián, M., Lira-Navarrete, E., Serrano, A., Marcuello, C., Velázquez-Campoy, A., Lostao, A., Hurtado-Guerrero, R., Medina, M., Martínez-Júlvez, M.
The FAD synthetase from the human pathogen Streptococcus pneumoniae: a bifunctional enzyme exhibiting activity-dependent redox requirements
2017 **Scientific Reports**, 7, 7609

Highlights

Reversible magnetic switching of high-spin molecules on a giant Rashba surface

Instrument: JT-STM. The quantum mechanical screening of a spin via conduction electrons depends sensitively on the environment seen by the magnetic impurity. A high degree of responsiveness can be obtained with metal complexes, as the embedding of a metal ion into an organic molecule prevents intercalation or alloying and allows for a good control by an appropriate choice of the ligands. There are prospects of reaching "on demand" control of the spin state of single molecules. Hitherto one route was to rely on "switchable" molecules with intrinsic bistabilities triggered by external stimuli, such as temperature or light, or on the controlled dosing of chemicals to form reversible bonds. However, these methods constrain the functionality to switchable molecules or depend on access to atoms or molecules. Here, we present a way to induce bistability also in a planar molecule by making use of the environment. We found that the particular "habitat" offered by an antiphase boundary of the Rashba system BiAg2 stabilizes a second structure for manganese phthalocyanine molecules, in which the central Mn ion moves out of the molecular plane. This corresponds to the formation of a large magnetic moment and a concomitant change of the ground state with respect to the conventional adsorption site. The reversible spin switch found here shows how we can rearrange electronic levels or lift orbital degeneracies. via the substrate

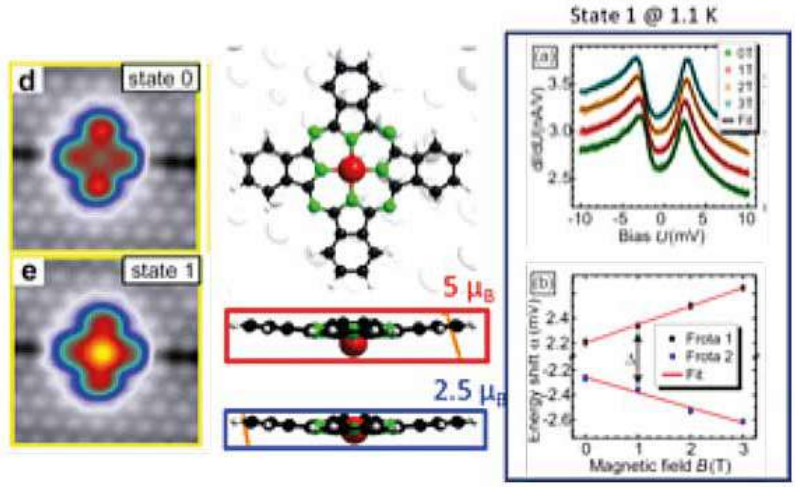

Reference:

Kügel J., Karolak M., Krönlein A., Serrate D., Bode M., and Sangiovanni G.
Reversible magnetic switching of high-spin molecules on a giant Rashba surface
2018 **npj Quantum Materials** 3, 53.

Organization of scientific events

LMA Scientific Meetings

A series of topical colloquia and seminars on the three scientific areas (TEM, Dual Beam and SPM).) devoted to informing local researchers about the capabilities of our infraestructures and to promote inderdisciplinar work. These seminars included both local speakers and external ones, including both national and international world wide recognized scientists.

Dr. Raúl Arenal

Institute of Nanoscience of Aragon

November 24, 2017

Prof. Richard Nichols

University of Liverpool (UK)

March 22, 2018

Dr. Diego Peña

University of Santiago de Compostela

February 2, 2018

Dr. Martino Poggio

University of Basel (Switzerland)

May 8, 2018

ELECMI International Workshop

The aim of the ELECMI International Workshop is to be an excellence international forum for the promotion of Advanced Microscopies, strengthening of already existing collaborations and laying the foundations for new ones. To achieve these objectives, representative scientists working at the forefront of materials fabrication and characterization present their latest results and reflections on the future of Electron Microscopy and associated techniques in the framework of this annual workshop. The venue for this International Workshops was the Laboratory of Advanced Microscopies (LMA) located in the city of Zaragoza both in the first (2017) and second (2018) editions.

1st ELECMI International Workshop June 2017

2nd ELECMI International Workshop June 2018

After the large success of the 1st ELECMI International Workshop, the LMA organized the second workshop in this series (in 2019 has taken placed the third one).

XI Conference "Fuerzas y Túnel 2018"

This biennial conference is addressed to the Spanish scientific community working on topics that encompass the use of scanning probe microscopies (SPM). It aims at scientists who share an interest in the applications, the use, the development and the theoretical description of technology based in scanning probes. SPM techniques are nowadays central in many fields of nanoscience, with applications that range from solid state physics to material sciences, surface chemistry and biology.

FyT2018 was the XI edition of this conference series that already enjoys two decades of tradition and successful sharing of ideas.

A wide range of scientific topics were covered in dedicated sessions to atomic force microscopy, scanning tunneling microscopy and theory of local probes techniques covering a wide range of applications from soft matter physics and biophysics to surface science in vacuum.

7th Spanish Workshop in Nanolithography

Nanolito is the Spanish Network of Nanolithography (www.unizar.es/nanolito). It is an initiative sponsored by the Spanish Ministry of Economy and Competitiveness and has as an objective to promote knowledge transfer among the different partners involved in nanolithography. The aim of this workshop is to strengthen the research in this field, sharing and exchanging the knowledge of different teams.

As previous Nanolito workshops, this meeting provided a conductive setting for technological discussions and sharing of ideas to encourage interregional scientific cooperation and to explore avenues for partnerships and commercialization.

Seminars given by industry in collaboration with the LMA

Obducat Seminars: It is a world-leading supplier of lithography solutions for manufacturing and replication of advanced micro and nanoscale structures. Obducat has choosen the LMA as the center of reference for presentation of its most advanced instruments in the field.


OBDUCAT SCIENTIFIC SEMINAR

1st, December. 2017. 12:30H –14:00H
Aula Room (Free Access)
INA (Institute of Nanoscience of Aragon)

Content:

- Description, explanation and examples of Nanoimprint Technology
- Description of Spinning Technics, Coater, Developer, Stripping, Etching, Lift Off
- Other Lithography products
- PVD systems (Sputtering and Evaporator), Vacuum Technics, Thermal Processes, Small equipment such as Vapor HF Etcher, UV led Upgrade for Mask Aligner

Obducat is a world-leading supplier of lithography solutions for manufacturing and replication of advanced micro and nanoscale structures


OBDUCAT SCIENTIFIC SEMINAR

7th, June. 2018. 12:30H - 14:00H.
Aula Room (Free Access)
INA (Institute of Nanoscience of Aragon)

Content:

- Description, explanation and examples of Nanoimprint Technology
- Description of Spinning Technics, Coater, Developer, Stripping, Etching, Lift Off
- Other Lithography products
- PVD systems (Sputtering and Evaporator), Vacuum Technics, Thermal Processes, Small equipment such as Vapor HF Etcher, UV led Upgrade for Mask Aligner

Obducat is a world-leading supplier of lithography solutions for manufacturing and replication of advanced micro and nanoscale structures

Asylum Research: Technology Leader in Atomic Force Microscopy that has presented the last advances in the field of Atomic Force Microscopies.


ULTIMOS AVANCES EN LA MICROSCOPIA DE FUERZA ATOMICA (AFM)

Seminario

Organizado por:

Visibility actions

Presentation of the Laboratory of Advanced Microscopies in business and industry forums

TRANSFIERE 2017 and 2018

It is the biggest professional and multisectoral forum of Spanish Innovation, in which participants can:

> Establish B2B contacts

> Transfer scientific knowledge and lines of technological research

> Show their innovative products and services

> Get to know the technological needs of Public Administration

> Seek funding for innovative projects

Venue: Trade Fairs and Congress Center of Malaga (Spain)

The LMA has participated both in the 2017 and 2018 editions of Transfiere.

Transfiere
14-15 feb 2018

ELECMI (LMA + CNME) completed its presence at the event with an information stand to promote the ELECMI available facilities.

National Nano-Safety Meeting

Presentation of the national facility "Singular Scientific and Technical Infraestructure" (ICTS) and the Laboratory of Advances Microscopies (LMA) to the participants in the National Nano-safety Meeting on 31st may 2017.

Venue: The Institute of Nanoscience of Aragon (Zaragoza)

CDTI-LMA ELECMI: ICTS facilities provided to the Industry

The Laboratory of Advanced Microscopies, the Nanoscience Institute of Aragon (LMA-INA) and the Centre for the Development of Industrial Technology (CDTI), organized the seminar "CDTI-LMA ELECMI", focused on the facilities provided by the ICTS to the industry.

Microscopy at the frontiers of science 2017

The main goals of the "MICROSCOPY AT THE FRONTIERS OF SCIENCE 2017" was to present and discuss the state of art and the potential of Microscopy and Microanalysis techniques in research areas such as materials and life sciences, biomaterials, geology, heritage and archaeology, forensic sciences and industrial quality and innovation. The LMA and ELECMI facilities were officially presented to the electron microscopy community in this conferencence through a talk of the ELECMI coordinator. Zaragoza. September 5th – 8th 2017

Seminar "Industrial Applications of the Nanotechnology"

The Nanoscience Institute of Aragón (INA) organized this meeting with the attendance of academic and industrial sectors. It took place on 19th December 2017 in Zaragoza. The objetive of this seminar was:

- to describe the last action lines carried out by the industry related to the application of nanotechnology.
- to introduce to the Industrial Community the services offered by the Laboratory of Advanced Microscopies.

Visits to the facilities

With the objective of increasing the interest of society in general in Science, giving visibility and stressing the value of the daily work of researchers, the INA stands for the realization of guided tours and open days in its installations, in which the Laboratory of Advanced Microscopies acquires special importance to seize the interest of its visitors. The most significant visits received throughout 2017 and 2018 are listed below:

- Former members of Aragón Parliament Association, 15th February, 2017.
- Aragón Exterior Delegation, 13th January, 2017.
- The University of Experiencie (University of Zaragoza), 1st June, 2017.
- Visit International Science Week, 1st and 2nd July, 2017.
- Nanjing Tech University (China), 27th November,2017.
- Hubei University (China), 3rd November, 2017.

Training actions

We understand that this is another way to promote our facilities to future scientists, to contribute to train highly qualified professionals and to increase the internationalisation of the University of Zaragoza (all Erasmus Mundus students and many of the students of the Nanomat come from abroad). During 2017 and 2018, the LMA made available its facilities and technical staff to the students in the following actions:

Training course for companies: Micro and Nano Materials and Surfaces Characterization

This training course was the the third of a series devited to the promotion of the use of characterizacion techniques in the industry. The event provided an excellent opportunity to show the most advanced facilities of LMA in the fields of nanofabrication and characterization, making participants aware of the potential of these instruments for the day-to-day work in the field of advanced materials. There were 23 participants involved. They came from 16 private companies which belong to several branches of industry as diverse as dyes and pigments industry, telecommunications, chemistry or biotechnology.

Master in nanostructured materials for Nanotechnology Applications (Nanomat)

This official and international course is multidisciplinary and aims to provide students with fundamental knowledge, practical experience, and skills in the fabrication and characterization of nanostructured materials and devices with applications in key areas of nanochemistry, nanophysics, and nanobiomedicine. More than 50% of the ECTS credits in this master are practical ones and many of these practicals and demonstrations are done at the LMA.

Erasmus Mundus Masters course in Engineering of membranes

The Master in Membrane Engineering EM3E offers an advanced education programme related to membrane science and engineering at the interface between material science and chemical engineering and focused on specific applicative fields. It involves 6 Higher Education Institutions of 5 European countries. As in Nanomat many of the practical classes are given at the LMA, where the students are trained in the most advanced nanofabrication and characterization techniques in materials sciences.

Master degree in Physics and Physical Technologies

The Master in Physics and Physical Technologies aims to provide a rigorous and advanced academic and professional training, adapted to the needs of society in various fields of Physics and Physical Technologies. Also the LMA opens its doors to students from this master.

Basic course on Transmission Electron Microscopy

The objective of the course was to provide users with the training required to operate the instrument as an autonomous user and to be able to interpret the obtained results. For this reason, the course was primarily aimed at those researchers who have a continuing need of this very versatile tool. The course was structured in a theoretical section and a very practical one, performed in laboratory.

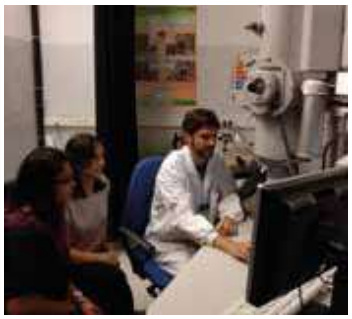

LMA and the industry

LMA and the industry

Along 2017 and 2018, the Advanced Microscopy Laboratory has offered the expertise of its researchers and technical staff to provide service to several private companies in order to help them to solve production problems and advance in their R&D programs. These companies benefited from the transfer of our technical expertise and scientific knowledge in highly advanced characterization and nanofabrication techniques. These companies belong to different branches of industry including electronics and microelectronics, biotechnology, white goods industry, telecommunications, chemistry, logistics or automotive industry. A list of several private companies both from Spain and abroad which have benefited from these services is provided below.

Company	**Industrial activity**	**Geographical Area**
Abalonyx AS	Innovative materials	International
Arcelor-Mittal S.A.	Steel industry	National
Atria Innovación S.L.	Research and development	Local
BeoNchip S.L.	Biotechnology	Local
Bionanoplus S.L.	Biotechnology	National
BSH Electrodomesticos España S.A.	White goods industry	National
Fersa Innova S.L.	Biotechnology	Local
Graphene Nanotech S.L.	Electronics and microlectronics	Local
Graphene-Tech S.L.	Electronics and microlectronics	Local
Henkel Ibérica S.A.	Adhesive Technologies	National
Jhonson Matthey	Sustainable Technologies	International
Laboratorios Argenol S.L.	Pharmaceutical	Local
Mann-Hummel Ibérica S.A.U.	Automotive industry	National
Microliquid S.L.	Electronics and microlectronics	National
Nanoimmnotech S.L.	Biotechnology	National
Nanopow	Biotechnology	International
Nurel S.A.	Chemistry	Local
Pavimentos de Tudela S.L.	Building materials	National
Quantum Designed Materials	Chemistry	International
Repsol Technology	Hydrocarbon	International
SMR Automotive Systems SAU	Automotive industry	International


LABORATORIOS
ARGENOL

Abalonyx
Innovative materials

Fersa
Bearings

B/S/H/

ATRIA
INNOVATION

BIONANOPLUS
Drug Delivery Technologies

NanoPow

BEOnChip

ArcelorMittal

nanoimmunotech
global solutions in nanobiotechnology

JM Johnson Matthey
Inspiring science, enhancing life

Henkel

Valeo

NUREL

GPNT
Graphene
& Nanotechnologies

MANN+
HUMMEL

microLIQUID
experts in microfluidics

QDM
TECH

pvt

REPSOL

smr

LMA

LABORATORIO
DE MICROSCOPÍAS
AVANZADAS

GOBIERNO DE ESPAÑA
MINISTERIO DE CIENCIA, INNOVACIÓN Y UNIVERSIDADES

Universidad Zaragoza
1542

GOBIERNO DE ARAGON